Targeting Host Cell Processing Glucosidase Activity as a Potential Strategy for Reducing Viral Replication

A Thesis Submitted to the Board of Faculty of Biological Sciences
University of Oxford
In Partial Fulfilment of the requirements for Degree of Doctor of Philosophy

Marvin J.-R. Lee

Glycobiology Institute
Department of Biochemistry
University of Oxford

Targeting host cell processing glucosidase activity as a potential strategy for reducing viral replication

Marvin J.-R. Lee

Lincoln College, D.Phil Thesis, Michaelmas Term 2011

ABSTRACT

The anti-viral efficacy of N-butyl-deoxynojirimycin (*N*B-DNJ, Miglustat, Zavesca) against a broad spectrum of viruses including bovine viral diarrhoea virus (BVDV), hepatitis C virus (HCV) and human immunodeficiency virus (HIV) is attributed to the disruption of viral envelope glycoprotein formation through the inhibition of the host ER alpha(α)-glucosidase activity. The DNJ-derived compound, N-(6'-4"-azido-2"-nitrophenylamino) hexyl-1-deoxynojirimycin (NAP-DNJ) is a more potent ER α-glucosidase inhibitor than *N*B-DNJ and together with the HCV surrogate model, BVDV, was used in this study to explore the relevance of ER α-glucosidase inhibition as a therapeutic target. The free oligosaccharide analysis (FOS) used in this study detected for the abundance of $Glc_1Man_5GlcNAc_1$ ($G_1M_5N_1$) and $Glc_3Man_5GlcNAc_1$ ($G_3M_5N_1$), indicative of α-glucosidases II and I inhibition respectively. The exclusive inhibition of α-glucosidase II was found to significantly reduce the virus titre of progeny virions as a result of viral protein misfolding and reduced heterodimerization and incorporation of envelope glycoproteins E1 and E2. A more pronounced reduction of viral infectivity required the perturbation of both α-glucosidases I and II. A modest library of DNJ-derived compounds was also synthesized and subjected to FOS analyses to compare their α-glucosidase inhibitory potential. NAP-DNJ was shown to be one of the more potent α-glucosidase inhibitors in both MDBK and HL60 cells. Relative to *N*B-DNJ and N-9-methoxynonyl-DNJ, NAP-DNJ was also found evoke significantly higher levels of mono- and tri-glucosylated species *in vivo*. The findings of this study provide key insights into the replicative cycle of BVDV and other flaviviruses and have significant implications for the future development of DNJ derivatives as anti-viral compounds.

FOREWORD

So this is it, the light at the end of the tunnel. 1,460 days of sweat, blood and tears, beckoning the rest of my body to keep up with the pace of my clawing fingers as I inched towards this finale, I am finally a step away from this revered milestone.

I would like to express my gratitude towards all who have lent me their helping hands in one way or the other, including everyone in the Butters lab, Raymond, Ian Wilson, the Glycobiology Institute, the Scripps Research Institute and A*STAR, Singapore.

Heartfelt thanks to Terry, my supervisor, for his tested patience, nurturing mentorship and dedicated guidance towards me these past four years, without whom I might never get the chance to pen these words. His capacity to tolerate my occasional overbearing exuberance and precipitous mood troughs is tantamount to the colossal universe.

I thank lab darling Katy and God-sent Omodele for their listening ears, for always being there and for their sage advice. You will be sorely missed.

I thank Gorgeous Gabi for her courage to share with me her fascinating school day anecdotes and for her stunning ability to fish out reagents from the most obscure corners of the lab.

Many thanks to Lynda for her dedication and motherly affection towards all of us in the lab. Gladys, our lovely cleaning lady, who never fails to brighten up my mornings with her ear-to-ear grin and her endearing compliments. Dom and Nikolay, for adding colours to my life and to all the students who had survived their days and continued to preserve their ingenuity under my supervision – Jake, Sebastian, Jessica, Marie and Nick. Thank you.

To the invaluable friendships forged, I will always hold our fond memories close to my heart – Sani, Jenny, Lukasz, Johannes, amigos espanoles, people… and more.

If Science were an enraged bull, I would have been the tenacious matador, flailing atop, who had time and again fallen and remounted. Some in the spectator stand applaud, lauding the undying effort, cheering on the worn out soul, whilst others watched on, only to anticipate the looming ultimatum.

Thanks to those who had challenged my pride, my sanity, my intellect and my lifestyle, for making me the stronger person that I am today, to be able to stand up fearless to the trials and tribulations ahead and for reminding me that life is not always a bed of roses.

The DPhil pursuit has not only been a rewarding experience and a staggering eye-opener, but also a gruelling odyssey at times. I am proud to have embarked on this academic marathon and experienced the spire chase. I wished I had broken the tape in record time, but I cannot deny that I am almost exhausted as the finishing line finally came into view.

Last but not least, special thanks to mom, dad, Adrian, Amos, Geetha, Jenny, Sani and all my loved ones. You are the greatest gifts to my life.

Marvin

CONTENTS

WORD COUNT

Abstract – 241 words
Main text – 21 610 words

ACRONYMS AND ABBREVIATIONS

Alb-IFN, Albumin-IFN

ALT, Alanine aminotransferase

BSA, Bovine serum albumin

BVDV, Bovine viral diarrhea virus

cccDNA, Covalently closed circular DNA

CC_{50}, 50% cytotoxic concentration

CGT, Ceramide glucosyltransferase

CHO, Chinese hamster ovary

CIFN, Consensus IFN

CN-Br, Cyanogen-bromide

ConA, Concanavalin A

DAAs, Directly acting anti-virals

DAPI, 4',6-diamidino-2-phenylindole

DNJ, Deoxynojirimycin

DV, Dengue virus

EBOV, Ebola Zaire virus

EC_{50}, 50% effective concentration

EDEM, ER degradation-enhancing α-mannosidase-like protein

ENGase, Endo-β-N- acetylglucosaminidase

ERAD, Endoplasmic reticulum associated degradation

FFU, Fluorescent focus units

FITC, Fluorescein isothiocyanate

FOS, Free oligosaccharides

GAA, Acid α-glucosidase

GAPDH, Glyceraldehyde 3-phosphate dehydrogenase

HBV, Hepatitis B virus

HCV, Hepatitis C virus

HCVpp, HCV pseudotyped particles

HIV, Human immunodeficiency virus

HRP, Horse-radish peroxidase

IFN, Interferon

ISGs, IFN-stimulated genes

IgG, Immunoglobulin G

IRES, Internal ribosome entry site

IRE1, Inositol-requiring enzyme 1

MARV, Marburg virus

MDBK, Mardin-Darby bovine kidney

MOI, Multiplicity of infection

MTS, 3-(4,5-dimethylthiazol-2-yl)-5-(3-carboxymethoxyphenyl)-2-(4-sulfophenyl)-2*H*-tetrazolium)

NADL, National Animal Disease Laboratory

NAP-DNJ, N-(6'-(4"-Azido-2"-nitrophenylamino)hexyl)-1-deoxynojirimycin 1

*N*B-DNJ, *N*-butyl-deoxynojirimycin

*N*N-DGJ, *N*-nonyl-deoxygalactonojirimycin

*N*N-DNJ, *N*-nonyl-deoxynojirimycin

NP-HPLC, Normal-phase-high performance liquid chromatography

PBS, Phosphate-buffered saline

PEG, Polyethylene glycol

p.i., Post-infection

PKR, Protein kinase R

PNGase, Peptide N-glycanase

RdRps, RNA-dependent RNA polymerases

RT-PCR, Reverse transcriptase-polymerase chain reaction

RVR, Rapid viral response

SDS-PAGE, Sodium dodecyl sulfate-polyacrylamide gel electrophoresis

SOC, Standard of care

STAT1/2, Signal transducer and activator of transcription proteins 1 and 2

SVR, Sustained virological response

t.l.c., Thin layer chromatography

UGGT, UDP-Glc:glycoprotein glucosyltransferase

WNV, West Nile virus

XBP1, X-box binding protein1

2-AA, 2-anthranillic acid

ACKNOWLEDGMENTS

Marie Gallesio is thanked for the production of all the data pertaining to the compound UV4 in Chapter 3.

CHAPTER 1
GENERAL INTRODUCTION

1.1 INTRODUCTION

Since the discovery of the Hepatitis C Virus (HCV) in 1989, alpha-interferon (IFN-α) and pegylated IFN-α/ ribavirin combination therapy have been the only approved therapies for HCV infection. Nonetheless, such a synergistic strategy has only been successful with 50% of infected patients, and serious side effects are evident, including gastrointestinal malabsorption and weight loss (*1*). The rapid emergence of resistant viral strains continues to present a challenge to the development of effective anti-viral compounds, spurring investigations into the different phases in the replication, morphogenesis and infection cycle of the virus in order to accurately target the virus at its most vulnerable stage with an effective drug or a combinatory cocktail of anti-viral compounds. Various anti-viral strategies targeted at either viral or cellular processes or both, have been studied in viruses such as the human immunodeficiency virus (HIV), HCV, hepatitis B virus (HBV) and dengue virus (DV).

1.1.1 HCV life cycle and potential targets for anti-viral intervention

HCV is a positive, single-stranded RNA virus that contains a 9.6 kb genome. After entry of the viral genome into the host-cell cytoplasm, the virus undergoes an uncoating process to expose the viral genome to host-cell translation machinery, where the viral genome is then translated in preparation for viral replication. In order to gain entry into the mammalian host cell, the virion has to establish attachment and fusion before viral entry and this process is governed by the two surface envelope glycoproteins and their glycan structures.

The two envelope glycoproteins, E1 and E2 of the HCV virion envelope are type I transmembrane glycoproteins, which form non-covalent heterodimers essential for viral entry and fusion (*2*), (*3*). E1 and E2 are highly glycosylated, containing up to 5 and 11 glycosylation sites, respectively. During the early steps of infection, interaction of E2 with one or several components of the receptor complex, such as glycosaminoglycans (4), (*5*), CD81 (*6*), scavenger receptor class B1 (*7*), claudin-1 (*8*), brings about viral attachment, fusion and internalization. HCV entry into cells has been shown to be pH dependent and related to clathrin-mediated endocytosis (*9*), (*10*), (*11*), (*12*), (*13*). Entry is followed by a fusion step within an acidic endosomal compartment (*11*), (*12*). The identity of the HCV fusion peptide remains controversial. E1 appeared as a good candidate because sequence analysis suggested the presence of a fusion peptide in its ectodomain (*14*), (*15*).

There is a wide spectrum of anti-HCV therapeutic approaches, including the perturbation of HCV internal ribosome entry site (IRES) function, HCV polyprotein translation and disruption of NS3/4A serine proteinases and RNA-dependent RNA polymerases (RdRps) using small molecule inhibitors, termed directly acting anti-virals (DAAs).

1.1.1 DAAs

DAAs have largely been used as supplements to existing current standard of care (SOC) therapy, with limited success in early clinical trials of HCV-specific NS3-4A serine protease- and NS5B RNA polymerase-inhibitors (*16*), (*17*), (*18*), (*19*), (*20*), (*21*), (*22*). The structures of some of these DAAs are shown in Table 1. The proteolytic activity of NS3-4A serine protease in the production of mature virions and its involvement in the

host immune evasion through the suppression of interferon regulatory factor 3 (IRF-3) has presented itself as a promising dual therapeutic target (*23*), (*24*). High throughput screening programmes have led to the discovery of first generation protease inhibitors telaprevir and boceprevir, currently in the final stages of clinical trials (*16*), (*25*), (*26*). Unfortunately, these linear ketoamids continue to exhibit some level of cross-resistance mutations (*27*), (*28*). Efforts are underway to produce the second generation of protease inhibitors that are more potent, with a lower susceptibility to cross resistance mutations.

Type of DAA	**DAA**	**Structure**	**Viral target (s)**
Non-nucleoside inhibitors	Telaprevir	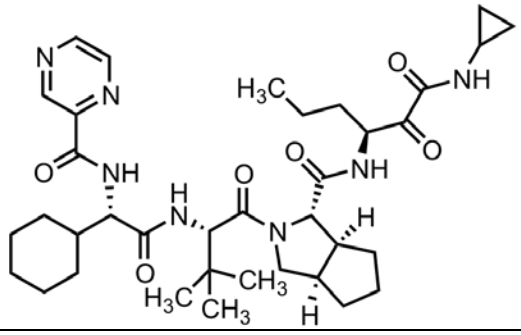	HCV
	Boceprevir	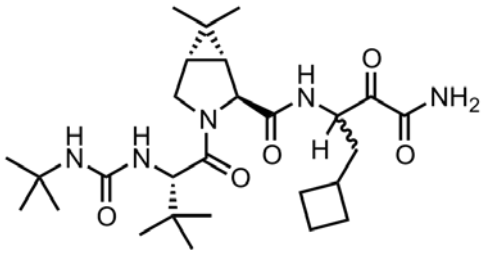	HCV
Nucleoside inhibitors	Adefovir disoproxil	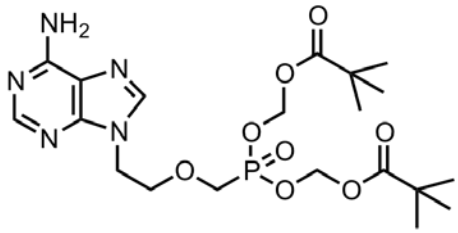	HBV
	Tenofovir disoproxil (Viread®)	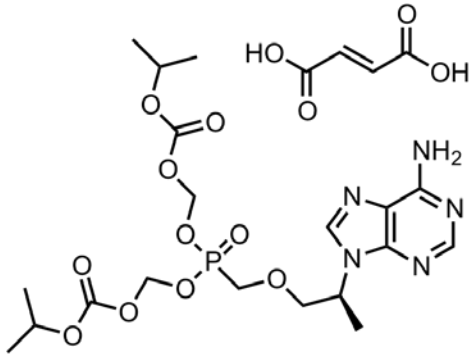	HIV

Lamivudine (Zeffix®)	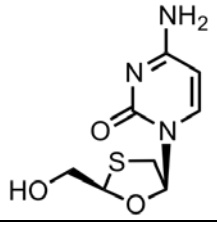	HBV, HIV
Emtricitabine (Emtriva®)	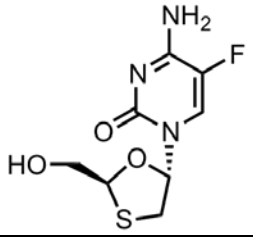	
Telbivudine (Tyzeka®, Sebivo®)	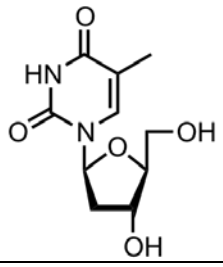	
Entecavir (Baraclude®)	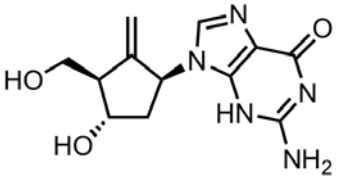	

Table 1 Summary of leading DAAs.

Relative to non-nucleoside polymerase inhibitors and protease inhibitors, nucleoside inhibitors have been shown to pose a higher barrier against the development of resistant HCV (*29*). In fact, there is the also the added advantage of targeting all four DV serotypes when using nucleoside analogues against RdRps (*30*). However, due to their polar nature, nucleoside inhibitors often exhibit poor passive diffusion and therefore low or variable bioavailability in animal studies, making the development of nucleoside inhibitors challenging (*31*). Aliphatic acids or amino acids often have to be conjugated to the alcohol groups on the ribose or acyclic ribose to circumvent this problem (*32*).

Nucleoside inhibitors usually remained inactive as pro-drugs until they have been converted to the triphosphate forms by host kinases, often a rate-limiting step (*33*), (*34*).

Nucleotide phosphonates such as Adefovir Disoproxil and Tenofovir Disoproxil for the treatment of HBV and HIV respectively, approved by FDA, circumvent the need for conversion. However, the problem of mitochondrial toxicity still remains, especially when targeting DNA viruses, such as HBV, resulting in the inhibition of the mitochondrial polymerase gamma (*35*).

The use of an approved oral nucleoside analogue, lamivudine (Zeffix®), licensed since 1998, is limited due to the development of resistance in the YMDD motif in up to 70% of patients after 5 years (*36*), (*37*), (*38*). Mutations of this motif found in the polymerases have rendered nucleoside inhibitors such as lamivudine, emtricitabine (Emtriva®), telbivudine (Tyzeka®, Sebivo®) and entecavir (Baraclude®) ineffective against HBV and HIV (*39*). Lamivudine exhibits potent suppressive action on HBV replication. However, it is incapable of eliminating covalently closed circular DNA (cccDNA) and is limited by the development of resistance in patients (*40*), (*41*). Adefovir is an acyclic phosphonate that is effective against lamivudine- and telbivudine- resistant mutations, although it is relatively weak in its anti-viral action as a monotherapy, resulting in the gradual development of resistance in 29% of HBeAg-negative patients by year 5 (*42*). On the other hand, Tenofovir (Viread®), a nucleotide analogue of adefovir, has exhibited excellent safety profile, with an oral dose of 300mg a day licensed for the treatment of HIV (*43*). Although no evidence of tenofovir resistance was found in HBeAg-positive and –negative patients after 2 years, nephrotoxicity and hypophosphatemia had developed in 4% of patients after 6 years of tenofovir use (*44*).

The rapid emergence of resistance against nucleoside inhibitors has therefore led to the exploration of combination therapy, which involves additional or synergistic efficacy.

Cumulative HBeAg seroconversion rate was significantly higher in adefovir add-on lamivudine combination therapy relative to adefovir monotherapy in the lamivudine-resistant chronic HBV patients (*45*). Long-term use of adefovir should be monitored since a significantly higher incidence and severity of renal dysfunction has been found in older patients, patients with renal insufficiency at baseline or those with hypertension or diabetes (*46*). Further to this, rapid reductions in serum HBV DNA level and normalization of alanine aminotransferase (ALT) levels were seen by 4 weeks in patients receiving adefovir dipivoxil (Hepsera®)/lamivudine (*47*).

Anti-viral treatment in the case of both HBeAg-positive and –negative patients should aim at long-term suppression of HBV DNA, which will eventually lead to HBsAg seroconversion. Therefore, other combination therapies also involve coupling anti-viral activity with immune modulation, such as lamivudine with IFN or adefovir with pegylated-IFN-α2a (*48*).

The current SOC for HCV patients is the combination of pegylated (Peg) IFN-α and the nucleoside analogue ribavirin. Both forms of pegylated IFN-α, PegIFN-α2a (Pegasys®, Roche, Basel, Switzerland) or PegIFN-α2b (PegIntron®, Merck & Co./Shering-Plough, Kenilworth, New Jersey, USA), have been found to demonstrate better pharmacokinetic performance than the standard IFN formulation (*49*). The addition of ribavirin increased the sustained virological response (SVR) rates to 41-43% from 10-20% with recombinant IFN-α monotherapy in mice (*50*), (*51*), (*52*). However, pegylated IFN-α-based therapies have also been impeded by the development of adverse side effects and psychiatric symptoms (*53*), (*54*), (*55*), leading to either dose-reduction or the premature cessation of therapy in up to 32% of patients, causing suboptimal SVR rates (*56*), (*57*), (*58*).

Erythropoietic agents have been prescribed to overcome hematological abnormalities and decrease in neutrophil count in patients receiving the pegylated IFN-α and ribavirin combination therapy (*59*), (*60*).

1.1.3 Combination therapy

The future for HCV therapy appears to be the combination of DAA(s) with the current IFN-α/ ribavirin regimen. Figure 1.1 shows the evolution of HCV therapy since 1996.

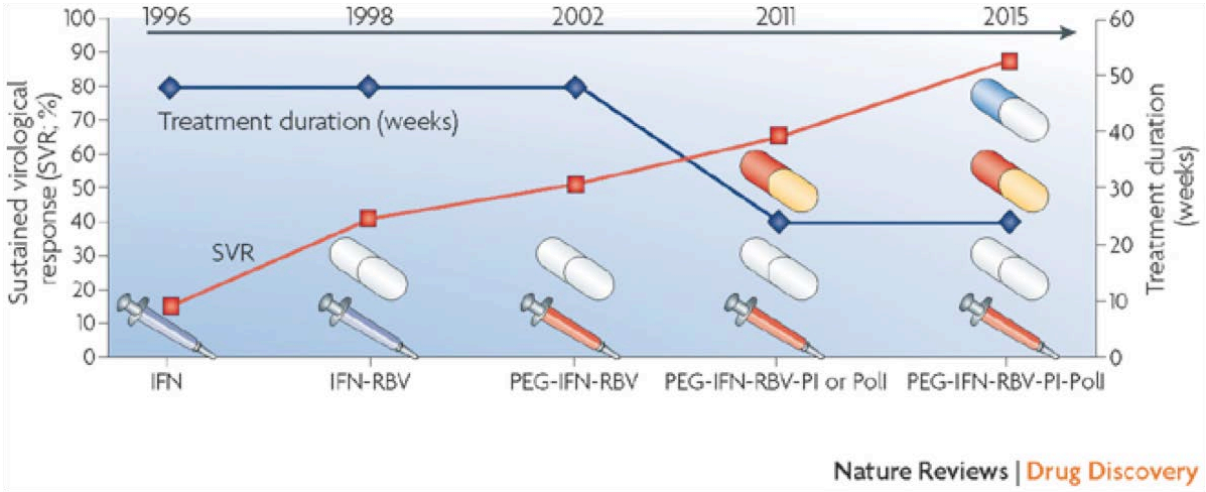

Figure 1.1 The evolution of HCV therapy. Figure adapted from (*61*)**.**

The inception of triple therapy with pegylated IFN-α, ribavirin plus a DAA, such as viral protease and polymerase inhibitors, has been shown to improve the rapid viral response (RVR) rates while lowering the development of viral resistance in HCV-1 naïve patients (*62*). This approach poses an alternative to the current SOC for HCV-1 patients. However, the safety profiles and tolerability of combination therapy require further improvements since more side effects due to IFN therapy, such as alopecia and weight loss, are anticipated (*63*). Phase II studies have shown that ribavirin continues to be

essential for the first generation of protease inhibitors such as telaprevir and boceprevir, to achieve higher sustained virological response (SVR) rates and lower relapse rates in patients (*64*), whilst phase II and III studies have further highlighted the importance of keeping pegylated IFN-α as the backbone of both drugs (*65*), (*66*).

To date, none of the new IFN molecules, including consensus IFN (CIFN), albumin-IFN (Alb-IFN), PegIFN-λ1 or IFN-ω, has shown any improvement in efficacy or reduction in side effects relative to PegIFN-α (*67*), (*68*).

Circulating IFN-α binds to IFN cell-surface-receptor subunits, leading to their dimerization resulting in the activation of the receptor-associated Janus-activated kinase 1 and tyrosine kinase 2 (*69*), (*70*). The signal transducer and activator of transcription proteins 1 and 2 (STAT1/2) are then phosphorylated by the activated kinases and the STAT1/2 complex is then translocated to the cell nucleus, where it combines with IFN-regulatory factor 9 to form a complex that binds to IFN-stimulated response elements on cellular DNA, leading to the expression of the multiple IFN-stimulated genes (ISGs). Hundreds of genes are induced by type-1 IFN, many of which are related to anti-viral activity, as shown by microarray analyses (*71*).

Ribavirin leads to the upregulation of several ISGs and enhanced STAT1 binding to DNA, increasing the anti-viral activity of endogenously produced IFN. It has also been shown that IL-8 is down regulated by ribavirin therapy (*72*). Therefore, ribavirin is active against HCV by its ability to augment or stabilize the intracellular mediators of IFN activity against HCV.

Compared to the IFN-α/ ribavirin combination therapy used to treat HCV inflicted patients, iminosugars such as *N*7-oxadecyl-DNJ (*N*7-DNJ) exhibited much less cytotoxicity in the persistently infected surrogate BVDV/MDBK model (*73*). The host-driven anti-viral mechanism of iminosugars also avoids problems faced with currently used drugs associated with emergence of viral escape mutants (*73*). Viral glycoprotein folding is largely dependent on the conservation of the asparagine residues at N-glycosylation sites (*74*). Therefore the use of iminosugars to target these glycosylation sites lowers the likelihood of emergence of CRT/CNX-independent drug-resistant mutants, avoiding the drug resistance problems faced in the development of the seasonal flu vaccines (*75*).

The emergence of adaptive mutations in DAA therapy has been the primary problem that results in the incomplete suppression of viral replication, leading to the exploration of other therapeutic interventions, including the perturbation of the N-glycosylation pathway of the mammalian hosts that some viruses rely on for critical protein processing.

1.1.4 N-linked glycosylation

During protein synthesis, the nascent polypeptide is translocated via the Sec61 translocon into the ER lumen, where an oligosaccharide precursor $G_3M_9N_2$ is transferred en bloc from its dolichol precursor onto the Asn residue on the consensus sequence Asn-X-Ser/Thr, where X can be any amino acid except proline. This reaction is catalyzed by oligosaccharyltransferase (OST) (*76*, *77*), shown in Figure 1.2.

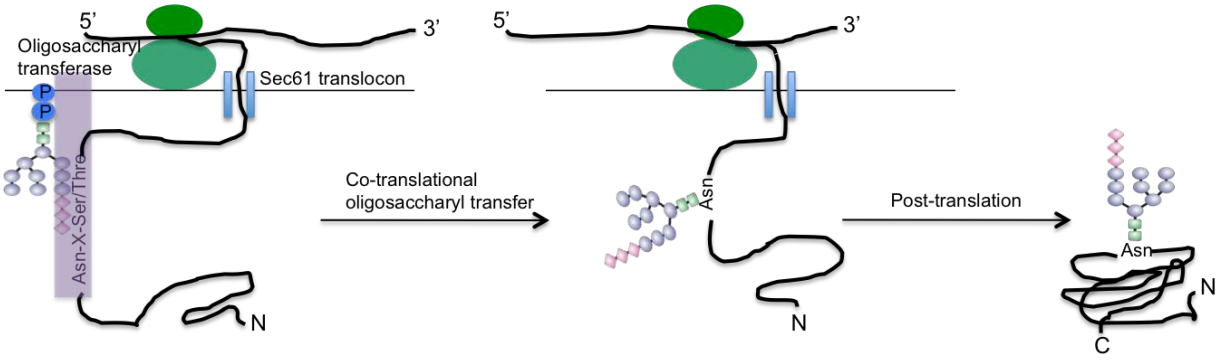

Figure 1.2 Transfer of oligosaccharide prevursor ($G_3M_9N_2$) to protein in the ER.

The glycan chain subsequently undergoes a series of glucose trimming reactions catalyzed by ER localized enzymes α-glucosidases I and II (*78-80*). This step-wise removal of glucose residues begins with the rapid cleavage of the terminal α-1,2-linked glucose residue by membrane bound α-glucosidase I, followed by the action of soluble ER luminal α-glucosidase II on the α-1,3 linked glucose unit, yielding a mono-glucosylated glycoform of the polypeptide (*81*). The ER lectin chaperone, calnexin, then associates with this glycoform, providing a docking site for the protein disulphide isomerase ERp57 (*82*), which is responsible for catalyzing the formation of disulphide bonds within the polypeptide, allowing it to assume its native conformation (*83*). The removal of the final glucose residue by α-glucosidase II is a rate-limiting step (*84*), following which the calnexin-glycoprotein complex dissociates, and proceeds into the Golgi for further processing. The UDP-Glc:glycoprotein glucosyltransferase (UGGT) recognizes any protein that has not been correctly folded and re-glucosylates it before directing it for calnexin re-association (*85*). This cycle perpetuates until the glycoprotein assumes its correct conformation, otherwise it gets targeted for endoplasmic reticulum associated degradation (ERAD).

ERp57 loses its association with a misfolded glycoprotein rapidly whilst the opposite is true for calnexin (*86*). Figure 1.3 illustrates the calnexin quality control pathway and the fate of glycans associated with native and misfolded proteins.

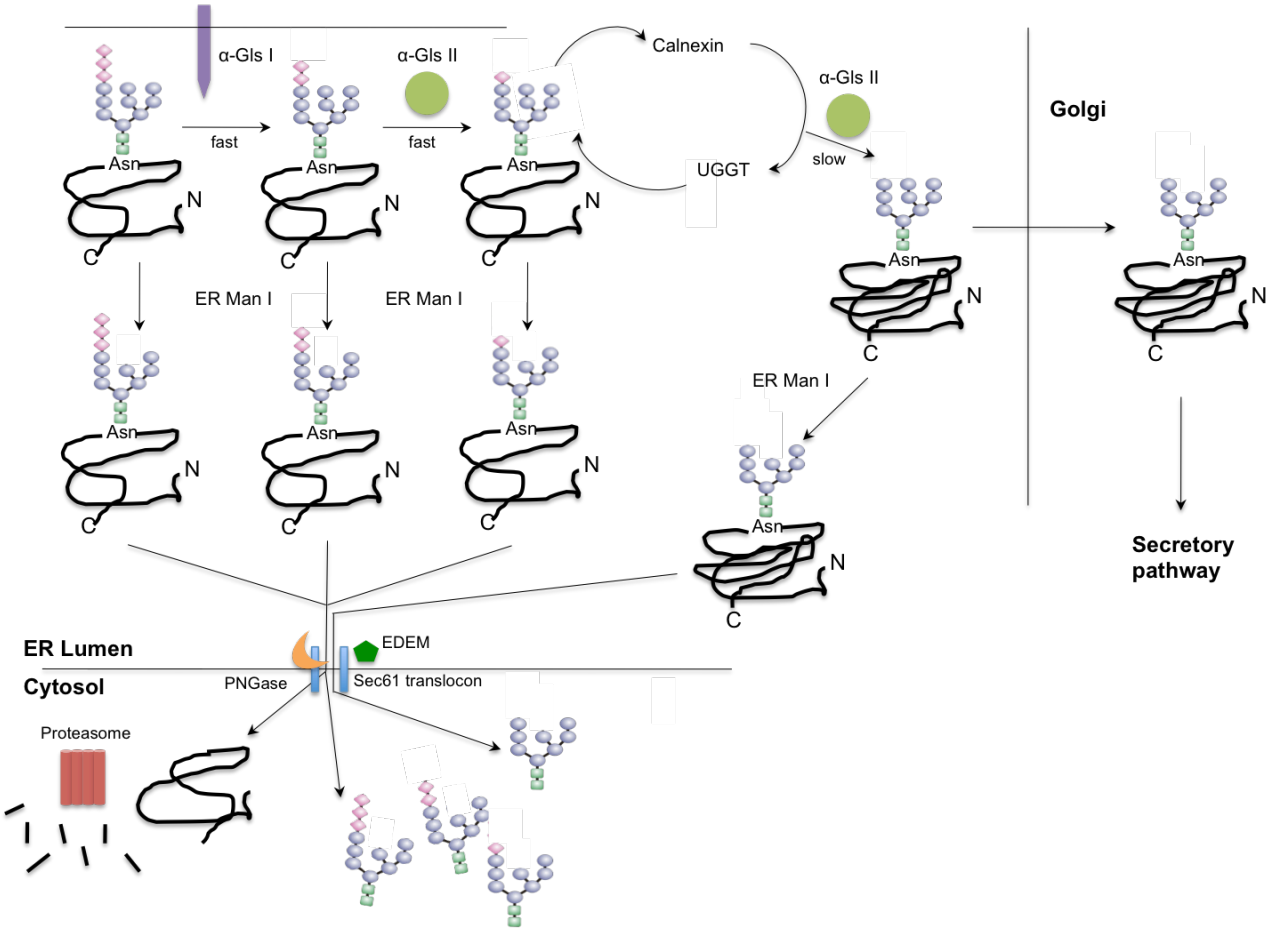

Figure 1.3 The calnexin pathway and the fate of glycans associated with native and misfolded proteins in the ER.

The misfolded glycoprotein is acted on by a cytosolic peptide N-glycanase (PNGase), which may or may not be in direct interaction with the Sec61 translocon, separating the oligosaccharide component from the protein component of the glycoprotein (*87*), (*88*), producing free oligosaccharides (FOS). The selective protein export from the ER to the cytosol followed by proteasomal degradation is termed ER-associated degradation (ERAD). Endo-β-N- acetylglucosaminidase (ENGase) (*89*) and cytosolic α-mannosidase

(*90*) subsequently act on cytosolic FOS, trimming them down to a $Man_5GlcNAc_1$ species that is targeted to the lysosome for further degradation. Glucosylated FOS are not able to access the lysosome for degradation (*91*).

ERAD results in the retro-translocation of misfolded proteins into the cytosol, followed by polyubiquitylation and proteasomal degradation (*92*). Initiation of the ERAD pathway occurs following the oligomerization and auto-phosphorylation of an ER-stress-sensor, inositol-requiring enzyme 1 (IRE1). Activation of ER degradation-enhancing α-mannosidase-like protein (EDEM) is subsequently triggered by the removal of an intron from X-box binding protein1 (XBP1) mRNA by activated IRE1. EDEMs are responsible for delivering misfolded glycoproteins to the ERAD pathway. EDEM1 (*93*), EDEM2 (*94*), EDEM3 (*95*) and ER mannosidase I all belong to the glycoside hydrolase 47 family. EDEM1 and EDEM3 for instance, were found to bind with SEL1L, resulting in the increased ubiquitylation of HCV envelope proteins, targeting unassembled glycoproteins for proteasomal degradation, highlighting the crucial role of the ERAD pathway in the life cycle of specific viruses (*96*). Under stress conditions, EDEM1 is upregulated, significantly enhancing terminal α-1,2-linked mannose removal from *N*-glycans exposed by folding-defective polypeptides, generating Man_8 isomer A (Figure 1.4) and impose interruption on folding attempts in the calnexin chaperone system (*97*), (*98*).

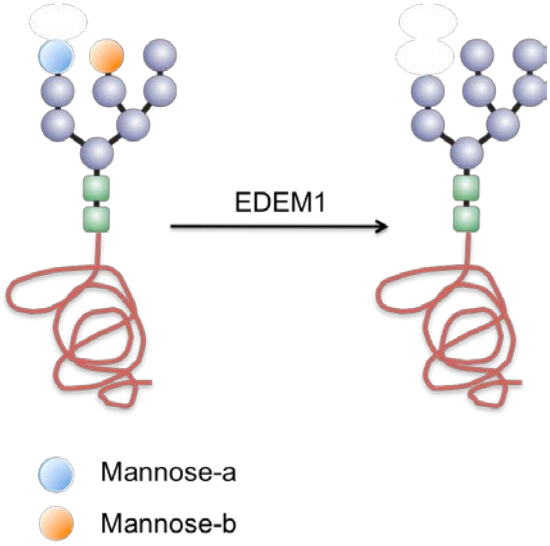

Figure 1.4 Production of Man_8 isomer A as an ERAD precursor through the removal of mannose-a residue by EDEM1.

It was previously thought that M_8B, generated through the removal of a single mannose-b residue from M_9, was the marker oligosaccharide that targeted the glycoprotein to ERAD (*99*). However, studies have found that the M_8-bearing glycoproteins remain in the calnexin cycle in the ER (*100*) and can be further processed later in the Golgi. The removal of the mannose-a residue has been identified to be important step prior to ERAD (*98*). The properly folded protein then gets channelled downstream to the Golgi for further processing of complex type carbohydrates and transported along the secretory pathway (*98*).

1.1.5 Iminosugars

1.1.5.1 Iminosugars as ER α-glucosidase inibitors

Iminosugars are monosaccharide mimics, with the ring oxygen atom replaced with a nitrogen atom (*101*). Deoxynojirimycin (DNJ) is the 1-deoxy analogue of its unstable parent compound nojirimycin and occurs naturally in the mulberry plants, *Streptomyces* and *Bacillus.* This unmetabolizable glucose analogue has no hydroxyl group at the C1 position of the pyranose ring. Iminosugars with such six-membered rings bear close structural resemblance to the substrates of carbohydrate processing enzymes such as α-glucosidases I and II within the ER. Protonation of the imino sugar nitrogen allows the inhibitor to mimic the charge on the proposed oxocarbonium ion transition state formed during hydrolysis, conferring upon the inhibitor the ability to reversibly compete with the glucose substrates for the active binding sites of the α-glucosidases. Consequently, the hindered trimming of glucose residues on the glycoproteins results in the accumulation of hyperglucosylated N-linked oligosaccharides that may fail to interact with the ER chaperones calnexin and calreticulin, both of which are involved in the protein folding quality control (*102*). Endo-α(1,2)mannosidase in the Golgi may process some of these hyperglucosylated proteins, therefore circumventing the block in N-linked oligosaccharide processing due to glucosidase inhibition (*103*), (*104*).

The large increase in the amount of glucosylated high-mannose containing oligosaccharides present on glycoproteins following α-glucosidase inhibition in the presence of iminosugars and the entry of misfolded glycoproteins into the ERAD pathway therefore led to an increase in glucosylated FOS (*105*). Measuring the amount of

FOS produced was found to be a quantitative approach in comparing the differing α-glucosidase inhibitory potency between iminosugars (*106*), (*107*).

1.1.5.2 Iminosugars as anti-viral compounds

Some, but not all glycoproteins, require the glucose trimming activity of ER α-glucosidases to remove the terminal glucose residues from the high-mannose N-linked glycans attached to nascent glycoproteins, in order to enter the calnexin/calreticulin-mediated protein folding pathway for correct folding. Due to the extreme dependency of HCV on calnexin for folding and assembly of their glycoproteins, the virus appears to be particularly sensitive to ER α-glucosidase inhibition compared with host proteins (*108*). The use of ER α-glucosidase inhibitors at a low level therefore serves to disrupt the proper folding of certain viral envelope glycoproteins, without affecting host cell viability (*1*). Even though most cellular proteins are dependent on the α-glucosidase-mediated folding pathway, certain cell lines deficient in α-glucosidase expression are still viable (*109*).

Many members of the Flaviviridae that use calnexin pathways and acquire envelopes by budding through the ER membrane, such as bovine viral diarrhea virus (BVDV) (*110*), DV (*111*), (*112*), West Nile virus (WNV), Japanese encephalitis virus, and HCV (*113*), (*114*), were reported to be relatively more sensitive to α-glucosidase inhibition compared to other viruses.

1.1.5.3 Suppression of α-glucosidase activity by iminosugars demonstrates potent anti-viral capability

Other studies have also confirmed the detrimental influence of iminosugars on viral protein folding. The N-linked glycosylation of the HIV envelope glycoprotein gp120 was altered in *N*B-DNJ treated chinese hamster ovary (CHO) cells, leading to conformational changes in the V1 and V2 loops of gp120 folding (*115*). Castanospermine, an α-glucosidase inhibitor, induced aberrant folding in the measles virus fusion protein, compromising its binding with conformational-dependent monoclonal antibodies (*116*). Misfolding of HCV glycoproteins E1 and E2 and the misassembly of HCV pre-budding complexes following *N*B-DNJ or *N*N-DNJ treatment resulted in a reduction in the incorporation of E1-E2 complexes into infectious HCV pseudotyped particles (HCVpp) produced in HEK-293T cells (*117*). Alterations in glycosylation pattern on the surface of the HIV Env protein in the presence of 1-deoxynojirimycin modified the immunoreactivity of regions involved in interactions of Env with co-receptor CXCR4 (V1, V2, C2, and V3), hindering membrane fusion (*118*).

However, side effects resulting from the inhibition of target enzymes ER α-glucosidases limit the extent of this therapeutic approach. The decrease in enzymatic activity of sucrase isomaltase in the presence of iminosugars such as N-(6'-(4"-Azido-2"-nitrophenylamino)hexyl)-1-deoxynojirimycin 1 (NAP-DNJ) (Unpublished data, DS Alonzi), could potentially lead to disruption in the metabolization of sucrose. The concentration of compound, in this case NAP-DNJ, required to inhibit the enzymatic activity (IC_{50}) of sucrase isomaltase by 50% was found to be 2.32μM ± 0.23 (Unpublished data, DS Alonzi). DNJ compounds such as *N-cis*-13-octadecenyl-DNJ, *N*-

butyl-DNJ (*N*B-DNJ) and *N*-nonyl-DNJ (*N*N-DNJ) were reported to inhibit ceramide glucosyltransferase (CGT), which catalyses the first step in the glucosphingolipid (GSL) biosynthetic pathway (*119*), (*120*). An N-alkylated side chain of at least three carbon atoms is required for inhibition of CGT (*121*) and *N*B-DNJ has been identified with the potential to treat GSL lysosomal storage diseases (*119*). The concentration of iminosugar administered that effectively translates to potential therapeutic dose in man is variable (5–500μM). A previous study have shown that the oral dosing of 300 mg *N*B-DNJ/day in patients (steady state concentration 6μM) (*122*) was necessary to achieve partial reduction of CGT activity in cells (5μM) in a type I Gaucher trial (*121*).

*N*B-DNJ has also been reported to impair spermatogenesis in mice, leading to reversible male infertility (*123*). Glycogen accumulation was also found to occur in the livers of *N*B-DNJ-treated mice after a 12-hr fast, likely due to α-1,6-glucosidase and/or acid α-glucosidase (GAA) inhibition (*124*). Furthermore, the folding and assembly of some host proteins could also be compromised in the presence of prolonged ER glucosidase inhibition, leading to altered cellular physiology, such as apoptosis or cellular transformation as a result of sustained unfolded protein response (*108*).

Nevertheless, the use of ER α-glucosidase inhibitors at a low level serves to disrupt the proper folding of certain viral envelope glycoproteins that accumulate and assemble in the ER, without affecting host cell viability (*1*). Even though most cellular proteins are dependent on the α-glucosidase-mediated folding pathway, certain cell lines deficient in α-glucosidase expression are still viable (*125*).

1.1.5.4 Anti-viral mechanism of iminosugars

Several hypotheses that explain the selective impact of iminosugar α-glucosidase inhibitors on viral N-glycosylation have been described (*126*). The envelope glycoprotein complex of most ER budding viruses, such as HBV, requires the correct inter-polypetide oligomer interactions (*127*) and the generation of a large number of defective oligomers in the presence of an α-glucosidase inhibitor perturbs the native structure of the envelope glycoprotein complex, imposing a detrimental impact on the larger population of viral proteins, known as the amplification effect (*126*). As a result, this also affects the interactions between the viral particles and their complementary cellular receptors, compromising viral infectivity and viral entry (*126*), (*128*). This amplification effect has a more significant impact on ER budding viruses than the plasma membrane budding viruses whilst host cell proteins retain their abilities to carry out their functions in spite of local or minor folding errors. Further to compromising virion production, some DNJ derivatives have also been reported to inhibit viral entry during BVDV and HCV infections (*111*), (*112*).

1.1.6 Bovine viral diarrhoea virus

The genus *Pestivirus* of the family *Flaviviridae* comprises several members including the bovine viral diarrhoea virus (BVDV), classical swine fever virus and bovine border disease virus (*129*) and these viruses infect ruminants and related species in the order Artyodactyla, such as swine (*130*), (*131*), (*132*).

BVDV is an important veterinary pathogen that results in major annual losses in the cattle industry, that range between 10 and 40 million $ per million calvings on a national level in the USA (*133*). The production losses due to BVDV infections include reduced milk production, reduced reproductive performance, growth retardation, increased occurrence of other diseases, early culling and increased mortality among young stock (*133*). The spread and maintenance of two types of BVDV infection have been identified, acute or transient and persistent (*134*), (*135*). Most infections established are acute and self-limiting, and viral clearance is relatively rapid. However, persistent infections caused by the non-cytopathic BVDV strain, can sporadically lead to a fatal pathology called mucosal disease, usually passed on from pregnant animals early in gestation via transplacental transmission to the foetus, resulting in the birth of a persistently infected immunotolerant calf and making them the main reservoir of BVDV (*136*). Severe diarrhoea and sometimes with haemorrhagic complications in cattle are characteristic of severe acute infections by BVDV (*137*), (*138*), (*139*).

The genome of the typical non-cytopathic BVDV strain is 12.5kb in length and is made up of a 59 non-translated region, a single open reading frame that encodes for all viral polypeptides and a non-polyadenylated 39 non-translated region (*140*). The initiation of

BVDV RNA translation occurs via an internal ribosome entry mechanism mediated by the 5' untranslated region of the viral RNA (*141*). The 5' and 3' boundaries of the IRES of the cytopathic National Animal Disease Laboratory (NADL) strain have been mapped and it has been suggested that the IRES extends into the coding of the BVDV polyprotein (*142*). The single large open reading frame encodes a polyprotein of approximately 3,900 amino acids (*143*), (*140*) produced through the translation of uncapped BVDV mRNA via internal initiation and cleaved into 12 functional polypeptides (Npro-C-Erns-E1-E2/p7-NS2-NS3-NS4A-NS4B-NS5A-NS5B) by both host and viral proteases (*140*), (*144*), (*145*), (*146*), illustrated in Figure 1.5.

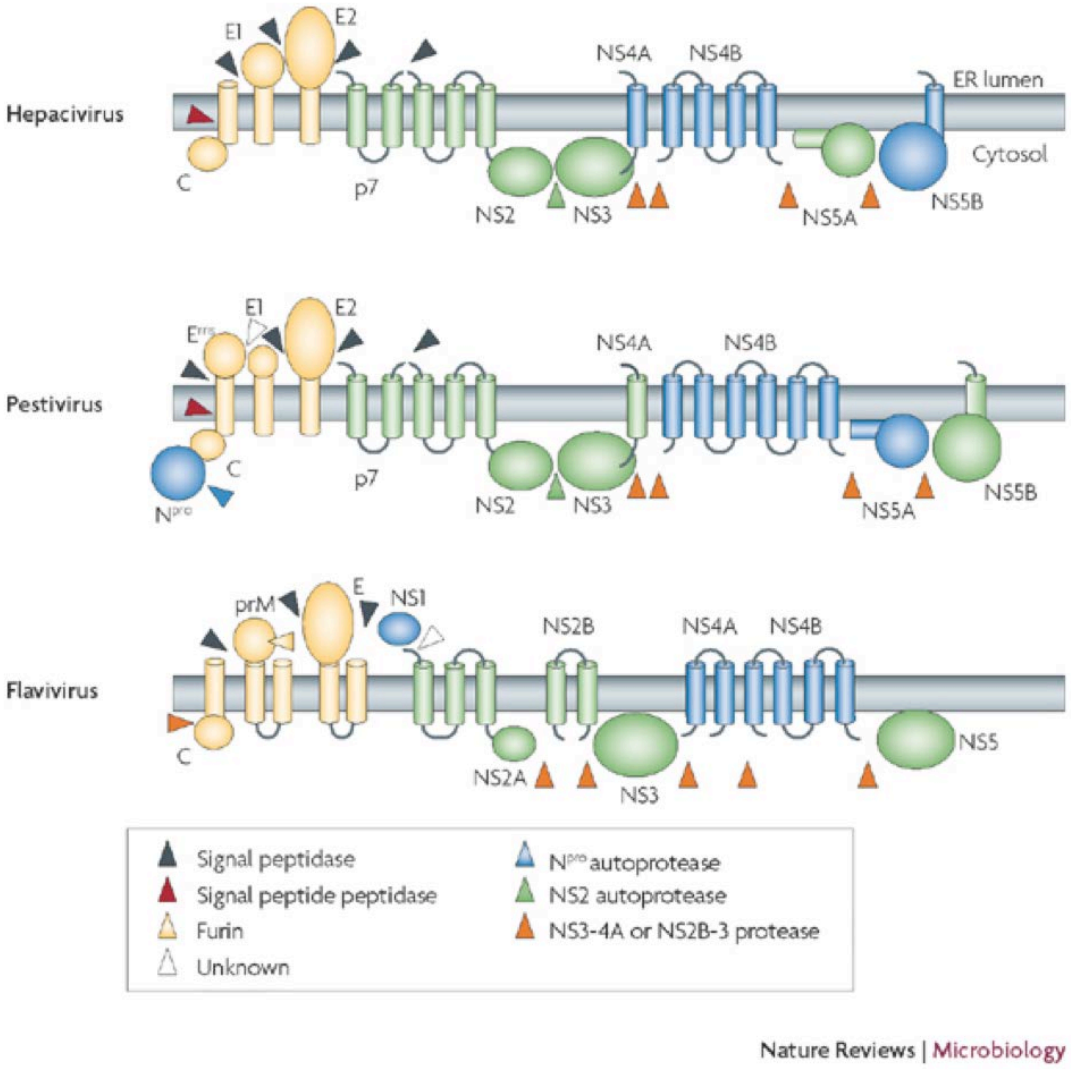

Figure 1.5 The proposed topologies of viral proteins of pestivirus such as BVDV, relative to those of hepacivirus and flavivirus. Structural proteins are shown in yellow and non-structural proteins are shown in green (required for infectious virus production) or blue (have not been implicated in infectious virus production). C, core protein (or capsid protein in flaviviruses); N^{pro}, amino-terminal protease. Figure adapted from (*147*)**.**

The BVDV-encoded serine protease processes the non-structural components of the polyprotein at four sites (3/4A, 4A/4B, 4B/5A, and 5A/5B) (*148*), (*149*), (*145*). The NS3 region contains the catalytic domain of this enzyme and together with the NS4A protein

as a co-factor, mediates the cleavage of at least two sites (4B/5A and 5A/5B) (*145*). Cleavage at the NS2/NS3 junction determines the difference between the cytopathic and non-cytopathic virus strain, with cleavage seen at the NS2/NS3 junction only in the former strain, giving a discrete NS3 protein with the cytopathic strain and the uncleaved NS2/NS3 in both strains (*150*), (*151*). The production of the NS3 protein is mediated by RNA recombinational events, including duplication and rearrangement of sequences, insertion of cellular sequences and large in-frame deletions (*140*), involving the insertion of a 270-base portion of a bovine mRNA, called cIns, of unknown function, that results in an in-frame insertion of 90 amino acid residues (Jiv90) potentiating the partial cleavage at the NS2/NS3 junction (*152*). Not only has cIns been found to induce cytopathogenicity in the NADL strain, but it is also responsible for NADL RNA replication (*136*). The cytopathic phenotype is also characterized by a loss of control of genome replication and a reduced ability of the infected cell to prevent a type I interferon (IFN) response to double-stranded RNA (dsRNA) (*153*), (*154*), (*155*), (*156*).

Signal peptidases encoded by host cell mediates the downstream cleavages that produce the structural components of BVDV such as C, Erns, E1, and E2 are mediated by (*148*), (*149*), (*145*). Both E^{rns} and E2 of pestiviruses induce neutralizing antibodies in infected animals (*157*), (*158*) and elicit protective immunity (*159*), (*160*), (*161*), (*162*). The E^{rns} protein was found to play a role in the infectivity of BVDV virions and also shown to bind dsRNA, interfering with the type I IFN response of cells to dsRNA (*163*). E2 has also been found to be a determinant of cell culture tropism in ruminant pestiviruses (*164*).

Until the availability of functional molecular HCV clones (*165*), BVDV remained a popular model system from which potential anti-HCV drugs can be investigated for its

mechanism of action (*166*), (*167*). There are a number of molecular and virological features shared between both viruses, including seemingly comparable virion maturation, assembly and egress mechanisms. HCV and BVDV are small, enveloped viruses with positive single-stranded RNA genomes of approximately 9.6K and 12.5K nucleotides respectively. Both ER-budding viruses produce a polypeptide precursor, transcribed from a single large open reading frame, which is subsequently co- and post-translationally processed into functionally homologous structural and non-structural proteins. BVDV exhibits cytopathic and plaque-forming properties in cell cultures, allowing rapid and quantitative analysis of viral replication and growth (*136*), (*168*), (*145*).

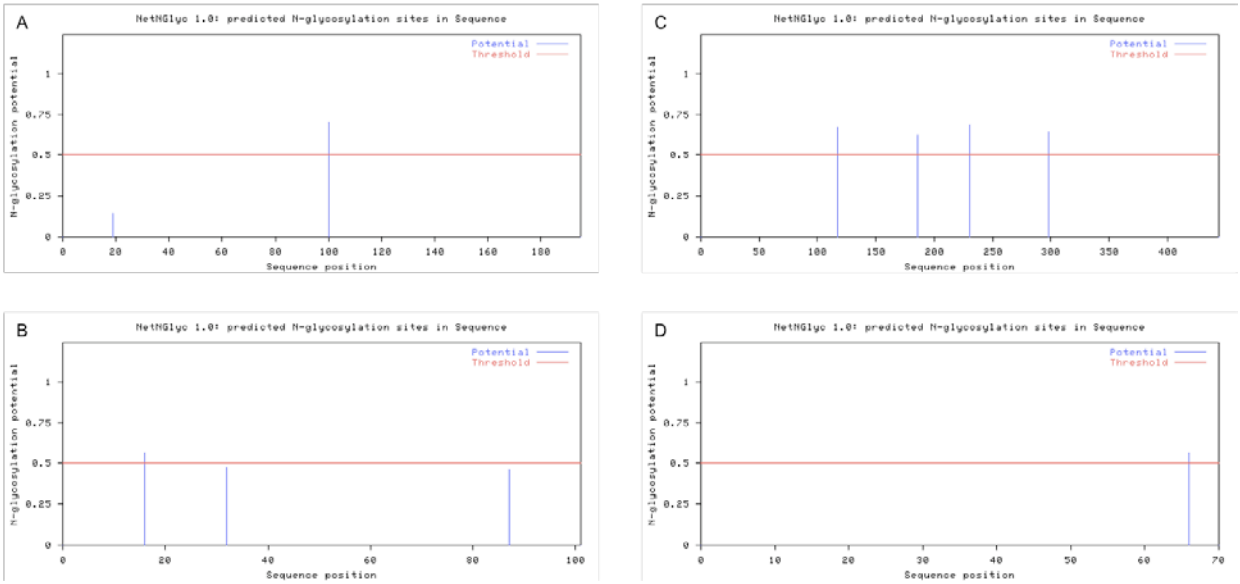

Figure 1.6 Potential N-glycosylation sites of the surface envelope glycoproteins BVDV E1 (A), and HCV E1 (B), as well as BVDV E2 (C) and HCV E2 (D).

The BVDV NADL strain used in this study is a cytopathic strain that encodes three envelope glycoproteins, Erns, E1, and E2, which carry eight, two, and four potential N-glycosylation sites, respectively (*146*). E1 and E2 envelope glycoproteins associate with each other to form a dimer either via non-covalent interactions in the case of HCV (*169*) or through covalent bonds in BVDV (*170*), (*157*). Figure 1.6 illustrates the potential N-

glycosylation sites of the surface envelope glycoproteins of both BVDV and HCV, based on the protein sequence of each glycoprotein.

The E1E2 heterodimer has been proposed to be the functional complex expressed on the surfaces of mature virions, responsible for viral attachment to host cell receptors, the fusion process, as well as viral entry. *N*B-DNJ has been shown to have a dose-dependent antiviral effect against BVDV, whereby the interaction of the BVDV envelope glycoproteins E1 and E2 with calnexin is prevented, leading to misfolding of the envelope glycoproteins and the inefficient formation of E1-E2 heterodimers (*171*). In a separate study, it has been shown that glucosidase inhibition, mediated through a calnexin-dependent pathway, was responsible for interfering with the replication and/or morphogenesis of HBV and BVDV (*126*). However, *N*B-DNJ was unable to disrupt viral protein folding pathways fully at physiologically significant concentrations highlighting the need to generate more potent glucosidase inhibitors.

1.2 Project aims

The aim of this project is to elucidate the anti-viral mechanism of iminosugars, specifically as a result of targeting ER α-glucosidases I and II, in treating filoviral diseases primarily using NAP-DNJ as a subject of study in BVDV, the prototype representative of the pestivirus genus in the *Flaviviridae* family.

Chapter 2 gives an overview of the structure-activity study of a modest library of DNJ-derived compounds, modified from the backbone of *N*B-DNJ. This study compared the inhibitory potency of different iminosugars against α-glucosidases I and II in cells using FOS analyses and gave an insight to the unique inhibitory properties of NAP-DNJ, making it the suitable candidate for use to investigate the anti-viral mechanism of iminosugars.

Chapter 3 provides a deeper understanding of the anti-viral mechanism of NAP-DNJ in BVDV and through a series of *in cellulo* analyses, clearly identified the roles that each α-glucosidase plays in the life cycle of the virus, bearing far-reaching implications for other pestiviruses in the *Flaviviridae* family. The detailed correlation between α-glucosidase inhibition and anti-viral activity was drawn in this chapter, highlighting the importance of interfering with the chaperone-mediated protein-folding pathway in the mammalian ER as a relevant therapeutic strategy.

Chapter 4 describes the isolation and purification of the BVDV E2 glycoprotein to better understand the changes in its glycan composition following NAP-DNJ treatment.

Chapter 5 explores the *in vivo* inhibitory potency of NAP-DNJ against α-glucosidase activity.

Chapter 6 summarises the final conclusions drawn from this project and highlights possible future directions for this study.

1.3 REFERENCES

1. Dwek, R. a, Butters, T. D., Platt, F. M., and Zitzmann, N. (2002) Targeting Glycosylation As a Therapeutic Approach, *Nature Reviews Drug Discovery 1*, 65-75.
2. Bartosch, B., Dubuisson, J., and Cosset, F.-L. (2003) Infectious hepatitis C virus pseudo-particles containing functional E1-E2 envelope protein complexes., *The Journal of experimental medicine 197*, 633-42.
3. Nielsen, S. U., Bassendine, M. F., Burt, A. D., Bevitt, D. J., and Toms, G. L. (2004) Characterization of the genome and structural proteins of hepatitis C virus resolved from infected human liver., *The Journal of general virology 85*, 1497-507.
4. Barth, H., Schafer, C., Adah, M. I., Zhang, F., Linhardt, R. J., Toyoda, H., Kinoshita-Toyoda, A., Toida, T., Van Kuppevelt, T. H., Depla, E., Von Weizsacker, F., Blum, H. E., and Baumert, T. F. (2003) Cellular binding of hepatitis C virus envelope glycoprotein E2 requires cell surface heparan sulfate., *The Journal of biological chemistry 278*, 41003-12.
5. Barth, H., Schnober, E. K., Zhang, F., Linhardt, R. J., Depla, E., Boson, B., Cosset, F.-L., Patel, A. H., Blum, H. E., and Baumert, T. F. (2006) Viral and cellular determinants of the hepatitis C virus envelope-heparan sulfate interaction., *Journal of virology 80*, 10579-90.
6. Cormier, E. G., Tsamis, F., Kajumo, F., Durso, R. J., Gardner, J. P., and Dragic, T. (2004) CD81 is an entry coreceptor for hepatitis C virus., *Proceedings of the National Academy of Sciences of the United States of America 101*, 7270-4.
7. Barth, H., Cerino, R., Arcuri, M., Hoffmann, M., Schürmann, P., Adah, M. I., Gissler, B., Zhao, X., Ghisetti, V., Lavezzo, B., Blum, H. E., Weizsäcker, F. von, Vitelli, A., Scarselli, E., and Baumert, T. F. (2005) Scavenger receptor class B type I and hepatitis C virus infection of primary tupaia hepatocytes., *Journal of virology 79*, 5774-85.
8. Evans, M. J., Hahn, T. von, Tscherne, D. M., Syder, A. J., Panis, M., Wölk, B., Hatziioannou, T., McKeating, J. A., Bieniasz, P. D., and Rice, C. M. (2007) Claudin-1 is a hepatitis C virus co-receptor required for a late step in entry., *Nature 446*, 801-5.

9. Bartosch, B., Vitelli, A., Granier, C., Goujon, C., Dubuisson, J., Pascale, S., Scarselli, E., Cortese, R., Nicosia, A., and Cosset, F.-L. (2003) Cell entry of hepatitis C virus requires a set of co-receptors that include the CD81 tetraspanin and the SR-B1 scavenger receptor., *The Journal of biological chemistry 278*, 41624-30.
10. Hsu, M., Zhang, J., Flint, M., Logvinoff, C., Cheng-Mayer, C., Rice, C. M., and McKeating, J. A. (2003) Hepatitis C virus glycoproteins mediate pH-dependent cell entry of pseudotyped retroviral particles., *Proceedings of the National Academy of Sciences of the United States of America 100*, 7271-6.
11. Tscherne, D. M., Jones, C. T., Evans, M. J., Lindenbach, B. D., McKeating, J. A., and Rice, C. M. (2006) Time- and temperature-dependent activation of hepatitis C virus for low-pH-triggered entry., *Journal of virology 80*, 1734-41.
12. Blanchard, E., Belouzard, S., Goueslain, L., Wakita, T., Dubuisson, J., Wychowski, C., and Rouillé, Y. (2006) Hepatitis C virus entry depends on clathrin-mediated endocytosis., *Journal of virology 80*, 6964-72.
13. Koutsoudakis, G., Kaul, A., Steinmann, E., Kallis, S., Lohmann, V., Pietschmann, T., and Bartenschlager, R. (2006) Characterization of the early steps of hepatitis C virus infection by using luciferase reporter viruses., *Journal of virology 80*, 5308-20.
14. Flint, M., and McKeating, J. A. The role of the hepatitis C virus glycoproteins in infection., *Reviews in medical virology 10*, 101-17.
15. Rosa, D., Campagnoli, S., Moretto, C., Guenzi, E., Cousens, L., Chin, M., Dong, C., Weiner, A. J., Lau, J. Y., Choo, Q. L., Chien, D., Pileri, P., Houghton, M., and Abrignani, S. (1996) A quantitative test to estimate neutralizing antibodies to the hepatitis C virus: cytofluorimetric assessment of envelope glycoprotein 2 binding to target cells., *Proceedings of the National Academy of Sciences of the United States of America 93*, 1759-63.
16. Forestier, N., Reesink, H. W., Weegink, C. J., McNair, L., Kieffer, T. L., Chu, H.-M., Purdy, S., Jansen, P. L. M., and Zeuzem, S. (2007) Antiviral activity of telaprevir (VX-950) and peginterferon alfa-2a in patients with hepatitis C., *Hepatology (Baltimore, Md.) 46*, 640-8.
17. Lawitz, E., Rodriguez-Torres, M., Muir, A. J., Kieffer, T. L., McNair, L., Khunvichai, A., and McHutchison, J. G. (2008) Antiviral effects and safety of

telaprevir, peginterferon alfa-2a, and ribavirin for 28 days in hepatitis C patients., *Journal of hepatology 49*, 163-9.

18. Durantel, D. (2009) Celgosivir, an alpha-glucosidase I inhibitor for the potential treatment of HCV infection., *Current opinion in investigational drugs (London, England : 2000) 10*, 860-70.
19. McHutchison, J. G., Everson, G. T., Gordon, S. C., Jacobson, I. M., Sulkowski, M., Kauffman, R., McNair, L., Alam, J., and Muir, A. J. (2009) Telaprevir with peginterferon and ribavirin for chronic HCV genotype 1 infection., *The New England journal of medicine 360*, 1827-38.
20. Kwo, P. Y., Lawitz, E. J., McCone, J., Schiff, E. R., Vierling, J. M., Pound, D., Davis, M. N., Galati, J. S., Gordon, S. C., Ravendhran, N., Rossaro, L., Anderson, F. H., Jacobson, I. M., Rubin, R., Koury, K., Pedicone, L. D., Brass, C. a, Chaudhri, E., and Albrecht, J. K. (2010) Efficacy of boceprevir, an NS3 protease inhibitor, in combination with peginterferon alfa-2b and ribavirin in treatment-naive patients with genotype 1 hepatitis C infection (SPRINT-1): an open-label, randomised, multicentre phase 2 trial., *Lancet 376*, 705-16.
21. Thompson, a J. V., and McHutchison, J. G. (2009) Antiviral resistance and specifically targeted therapy for HCV (STAT-C), *Journal of Viral Hepatitis 16*, 377-387.
22. Asselah, T., Benhamou, Y., and Marcellin, P. (2009) Protease and polymerase inhibitors for the treatment of hepatitis C., *Liver international : official journal of the International Association for the Study of the Liver 29 Suppl 1*, 57-67.
23. Li, K., Foy, E., Ferreon, J. C., Nakamura, M., Ferreon, A. C. M., Ikeda, M., Ray, S. C., Gale, M., and Lemon, S. M. (2005) Immune evasion by hepatitis C virus NS3/4A protease-mediated cleavage of the Toll-like receptor 3 adaptor protein TRIF., *Proceedings of the National Academy of Sciences of the United States of America 102*, 2992-7.
24. Meylan, E., Curran, J., Hofmann, K., Moradpour, D., Binder, M., Bartenschlager, R., and Tschopp, J. (2005) Cardif is an adaptor protein in the RIG-I antiviral pathway and is targeted by hepatitis C virus., *Nature 437*, 1167-72.
25. Lin, C., Gates, C. a, Rao, B. G., Brennan, D. L., Fulghum, J. R., Luong, Y.-P., Frantz, J. D., Lin, K., Ma, S., Wei, Y.-Y., Perni, R. B., and Kwong, A. D. (2005) In vitro studies of cross-resistance mutations against two hepatitis C virus serine

protease inhibitors, VX-950 and BILN 2061., *The Journal of biological chemistry 280*, 36784-91.

26. Tong, X., Chase, R., Skelton, A., Chen, T., Wright-Minogue, J., and Malcolm, B. a. (2006) Identification and analysis of fitness of resistance mutations against the HCV protease inhibitor SCH 503034., *Antiviral research 70*, 28-38.
27. Roberts, S. K., Cooksley, G., Dore, G. J., Robson, R., Shaw, D., Berns, H., Hill, G., Klumpp, K., Najera, I., and Washington, C. (2008) Robust antiviral activity of R1626, a novel nucleoside analog: a randomized, placebo-controlled study in patients with chronic hepatitis C., *Hepatology (Baltimore, Md.) 48*, 398-406.
28. Klinik, M., and Kiel, U. (2009) Original article Safety , pharmacokinetics and antiviral effect of BILB 1941 , a novel hepatitis C virus RNA polymerase inhibitor , after 5 days oral treatment, *Antiviral Therapy* 23-32.
29. McCown, M., Diamond, M. S., and Pekosz, A. (2003) The utility of siRNA transcripts produced by RNA polymerase i in down regulating viral gene expression and replication of negative- and positive-strand RNA viruses., *Virology 313*, 514-24.
30. Migliaccio, G., Tomassini, J. E., Carroll, S. S., Tomei, L., Altamura, S., Bhat, B., Bartholomew, L., Bosserman, M. R., Ceccacci, A., Colwell, L. F., Cortese, R., De Francesco, R., Eldrup, A. B., Getty, K. L., Hou, X. S., LaFemina, R. L., Ludmerer, S. W., MacCoss, M., McMasters, D. R., Stahlhut, M. W., Olsen, D. B., Hazuda, D. J., and Flores, O. a. (2003) Characterization of resistance to non-obligate chain-terminating ribonucleoside analogs that inhibit hepatitis C virus replication in vitro., *The Journal of biological chemistry 278*, 49164-70.
31. Pastor-Anglada, M., Cano-Soldado, P., Molina-Arcas, M., Lostao, M. P., Larráyoz, I., Martínez-Picado, J., and Casado, F. J. (2005) Cell entry and export of nucleoside analogues., *Virus research 107*, 151-64.
32. Kroschewski, H., Lim, S. P., Butcher, R. E., Yap, T. L., Lescar, J., Wright, P. J., Vasudevan, S. G., and Davidson, A. D. (2008) Mutagenesis of the dengue virus type 2 NS5 methyltransferase domain., *The Journal of biological chemistry 283*, 19410-21.
33. Perrone, P., Daverio, F., Valente, R., Rajyaguru, S., Martin, J. a, Lévêque, V., Le Pogam, S., Najera, I., Klumpp, K., Smith, D. B., and McGuigan, C. (2007) First example of phosphoramidate approach applied to a 4'-substituted purine nucleoside (4'-azidoadenosine): conversion of an inactive nucleoside to a

submicromolar compound versus hepatitis C virus., *Journal of medicinal chemistry 50*, 5463-70.

34. Perrone, P., Luoni, G. M., Kelleher, M. R., Daverio, F., Angell, A., Mulready, S., Congiatu, C., Rajyaguru, S., Martin, J. a, Levêque, V., Le Pogam, S., Najera, I., Klumpp, K., Smith, D. B., and McGuigan, C. (2007) Application of the phosphoramidate ProTide approach to 4'-azidouridine confers sub-micromolar potency versus hepatitis C virus on an inactive nucleoside., *Journal of medicinal chemistry 50*, 1840-9.
35. Côté, H. C. F., Brumme, Z. L., Craib, K. J. P., Alexander, C. S., Wynhoven, B., Ting, L., Wong, H., Harris, M., Harrigan, P. R., O'Shaughnessy, M. V., and Montaner, J. S. G. (2002) Changes in mitochondrial DNA as a marker of nucleoside toxicity in HIV-infected patients., *The New England journal of medicine 346*, 811-20.
36. Tillmann, H. L., and McHutchison, J. G. (2008) Telbivudine versus lamivudine in patients with chronic hepatitis B., *The New England journal of medicine 358*, 1517; author reply 1517-8.
37. Lai, C.-L., Shouval, D., Lok, A. S., Chang, T.-T., Cheinquer, H., Goodman, Z., DeHertogh, D., Wilber, R., Zink, R. C., Cross, A., Colonno, R., and Fernandes, L. (2006) Entecavir versus lamivudine for patients with HBeAg-negative chronic hepatitis B., *The New England journal of medicine 354*, 1011-20.
38. Marcellin, P., Lau, G. K. K., Bonino, F., Farci, P., Hadziyannis, S., Jin, R., Lu, Z.-M., Piratvisuth, T., Germanidis, G., Yurdaydin, C., Diago, M., Gurel, S., Lai, M.-Y., Button, P., and Pluck, N. (2004) Peginterferon alfa-2a alone, lamivudine alone, and the two in combination in patients with HBeAg-negative chronic hepatitis B., *The New England journal of medicine 351*, 1206-17.
39. Ghany, M. G., and Doo, E. C. (2009) Antiviral resistance and hepatitis B therapy., *Hepatology (Baltimore, Md.) 49*, S174-84.
40. Leung, N., Hospital, W., Chinese, T., and Kong, H. (2002) ADVANCES IN LIVER DISEASE : HEPATITIS B Treatment of chronic hepatitis B : Case selection and duration, *Journal of Gastroenterology and Hepatology*.
41. Yuen, M.-F., and Lai, C.-L. (2011) Treatment of chronic hepatitis B: Evolution over two decades., *Journal of gastroenterology and hepatology 26 Suppl 1*, 138-43.

42. Hadziyannis, S. J., Tassopoulos, N. C., Heathcote, E. J., Chang, T.-T., Kitis, G., Rizzetto, M., Marcellin, P., Lim, S. G., Goodman, Z., Ma, J., Brosgart, C. L., Borroto-Esoda, K., Arterburn, S., and Chuck, S. L. (2006) Long-term therapy with adefovir dipivoxil for HBeAg-negative chronic hepatitis B for up to 5 years., *Gastroenterology 131*, 1743-51.

43. Takkenberg, R. B., Weegink, C. J., Zaaijer, H. L., and Reesink, H. W. (2009) New developments in antiviral therapy for chronic hepatitis B., *Vox sanguinis* 481-494.

44. Cassetti, I., Madruga, J. V. R., Suleiman, J. M. a H., Etzel, A., Zhong, L., Cheng, A. K., and Enejosa, J. (2007) The safety and efficacy of tenofovir DF in combination with lamivudine and efavirenz through 6 years in antiretroviral-naïve HIV-1-infected patients., *HIV clinical trials 8*, 164-72.

45. Kim, H. J., Park, J. H., Park, D. I., Cho, Y. K., Sohn, C. I., Jeon, W. K., and Kim, B. I. (2010) Rescue therapy for lamivudine-resistant chronic hepatitis B: comparison between entecavir 1.0 mg monotherapy, adefovir monotherapy and adefovir add-on lamivudine combination therapy., *Journal of gastroenterology and hepatology 25*, 1374-80.

46. Ha, N. B., Ha, N. B., Garcia, R. T., Trinh, H. N., Vu, A. a, Nguyen, H. a, Nguyen, K. K., Levitt, B. S., and Nguyen, M. H. (2009) Renal dysfunction in chronic hepatitis B patients treated with adefovir dipivoxil., *Hepatology (Baltimore, Md.) 50*, 727-34.

47. Peters, M. (2004) Adefovir dipivoxil alone or in combination with lamivudine in patients with lamivudine-resistant chronic hepatitis B, *Gastroenterology 126*, 91-101.

48. Shepherd, J., Jones, J., Takeda, a, Davidson, P., and Price, a. (2006) Adefovir dipivoxil and pegylated interferon alfa-2a for the treatment of chronic hepatitis B: a systematic review and economic evaluation., *Health technology assessment (Winchester, England) 10*, iii-iv, xi-xiv, 1-183.

49. Aghemo, A., Rumi, M. G., and Colombo, M. (2010) Pegylated interferons alpha2a and alpha2b in the treatment of chronic hepatitis C., *Nature reviews. Gastroenterology & hepatology*, Nature Publishing Group *7*, 485-94.

50. Carithers, R. L., and Emerson, S. S. (1997) Therapy of hepatitis C: meta-analysis of interferon alfa-2b trials., *Hepatology (Baltimore, Md.) 26*, 83S-88S.

51. Poynard, T., Marcellin, P., Lee, S. S., Niederau, C., Minuk, G. S., Ideo, G., Bain, V., Heathcote, J., Zeuzem, S., Trepo, C., and Albrecht, J. (1998) Randomised trial

of interferon alpha2b plus ribavirin for 48 weeks or for 24 weeks versus interferon alpha2b plus placebo for 48 weeks for treatment of chronic infection with hepatitis C virus. International Hepatitis Interventional Therapy Group (IHIT), *Lancet 352*, 1426-32.

52. McHutchison, J. G., Gordon, S. C., Schiff, E. R., Shiffman, M. L., Lee, W. M., Rustgi, V. K., Goodman, Z. D., Ling, M. H., Cort, S., and Albrecht, J. K. (1998) Interferon alfa-2b alone or in combination with ribavirin as initial treatment for chronic hepatitis C. Hepatitis Interventional Therapy Group., *The New England journal of medicine 339*, 1485-92.
53. Mac Nicholas, R., and Norris, S. (2010) Review article: optimizing SVR and management of the haematological side effects of peginterferon/ribavirin antiviral therapy for HCV - the role of epoetin, G-CSF and novel agents., *Alimentary pharmacology & therapeutics 31*, 929-37.
54. Dienstag, J. L., and McHutchison, J. G. (2006) American Gastroenterological Association technical review on the management of hepatitis C., *Gastroenterology 130*, 231-64; quiz 214-7.
55. Ghany, M. G., Strader, D. B., Thomas, D. L., and Seeff, L. B. (2009) Diagnosis, management, and treatment of hepatitis C: an update., *Hepatology (Baltimore, Md.) 49*, 1335-74.
56. Hadziyannis, S. J., Sette, H., Morgan, T. R., Balan, V., Diago, M., Marcellin, P., Ramadori, G., Bodenheimer, H., Bernstein, D., Rizzetto, M., Zeuzem, S., Pockros, P. J., Lin, A., and Ackrill, A. M. (2004) Peginterferon-alpha2a and ribavirin combination therapy in chronic hepatitis C: a randomized study of treatment duration and ribavirin dose., *Annals of internal medicine 140*, 346-55.
57. Rumi, M. G., Aghemo, A., Prati, G. M., D'Ambrosio, R., Donato, M. F., Soffredini, R., Del Ninno, E., Russo, A., and Colombo, M. (2010) Randomized study of peginterferon-alpha2a plus ribavirin vs peginterferon-alpha2b plus ribavirin in chronic hepatitis C., *Gastroenterology*, Elsevier Inc. *138*, 108-15.
58. Fried, MW; Shiffman, ML; Reddy, K. et al. (2011) PEGINTERFERON ALFA - 2a PLUS RIBAV IRIN FOR H EPATITIS C PEGINTERFERON ALFA-2a PLUS RIBAVIRIN FOR CHRONIC HEPATITIS C VIRUS INFECTION, *English Journal 347*, 975-982.
59. Cooper, C. L., Al-Bedwawi, S., Lee, C., and Garber, G. (2006) Rate of infectious complications during interferon-based therapy for hepatitis C is not related to

neutropenia., *Clinical infectious diseases : an official publication of the Infectious Diseases Society of America 42*, 1674-8.

60. Chapko, M. K., and Dominitz, J. a. (2006) Cost-effectiveness of growth factors during hepatitis C anti-viral therapy., *Alimentary pharmacology & therapeutics 24*, 1067-77.
61. Melnikova, I. (2008) Hepatitis C therapies, *Nature Reviews Drug Discovery 7*, 799-800.
62. Zeuzem, S., Sulkowski, M. S., Lawitz, E. J., Rustgi, V. K., Rodriguez-Torres, M., Bacon, B. R., Grigorescu, M., Tice, A. D., Lurie, Y., Cianciara, J., Muir, A. J., Cronin, P. W., Pulkstenis, E., Subramanian, G. M., and McHutchison, J. G. (2010) Albinterferon Alfa-2b was not inferior to pegylated interferon-α in a randomized trial of patients with chronic hepatitis C virus genotype 1., *Gastroenterology*, Elsevier Inc. *139*, 1257-66.
63. Zeuzem, S., Sulkowski, M. S., Lawitz, E. J., Rustgi, V. K., Rodriguez-Torres, M., Bacon, B. R., Grigorescu, M., Tice, A. D., Lurie, Y., Cianciara, J., Muir, A. J., Cronin, P. W., Pulkstenis, E., Subramanian, G. M., and McHutchison, J. G. (2010) Albinterferon Alfa-2b was not inferior to pegylated interferon-α in a randomized trial of patients with chronic hepatitis C virus genotype 1., *Gastroenterology 139*, 1257-66.
64. Kwo, P. Y., Lawitz, E. J., McCone, J., Schiff, E. R., Vierling, J. M., Pound, D., Davis, M. N., Galati, J. S., Gordon, S. C., Ravendhran, N., Rossaro, L., Anderson, F. H., Jacobson, I. M., Rubin, R., Koury, K., Pedicone, L. D., Brass, C. a, Chaudhri, E., and Albrecht, J. K. (2010) Efficacy of boceprevir, an NS3 protease inhibitor, in combination with peginterferon alfa-2b and ribavirin in treatment-naive patients with genotype 1 hepatitis C infection (SPRINT-1): an open-label, randomised, multicentre phase 2 trial., *Lancet 376*, 705-16.
65. Hézode, C., Forestier, N., Dusheiko, G., Ferenci, P., Pol, S., Goeser, T., Bronowicki, J.-P., Bourlière, M., Gharakhanian, S., Bengtsson, L., McNair, L., George, S., Kieffer, T., Kwong, A., Kauffman, R. S., Alam, J., Pawlotsky, J.-M., and Zeuzem, S. (2009) Telaprevir and peginterferon with or without ribavirin for chronic HCV infection., *The New England journal of medicine 360*, 1839-50.
66. McHutchison, J. G., Manns, M. P., Muir, A. J., Terrault, N. a, Jacobson, I. M., Afdhal, N. H., Heathcote, E. J., Zeuzem, S., Reesink, H. W., Garg, J., Bsharat, M., George, S., Kauffman, R. S., Adda, N., and Di Bisceglie, A. M. (2010) Telaprevir

for previously treated chronic HCV infection., *The New England journal of medicine 362*, 1292-303.

67. Muir, A. J., Shiffman, M. L., Zaman, A., Yoffe, B., Torre, A. de la, Flamm, S., Gordon, S. C., Marotta, P., Vierling, J. M., Lopez-Talavera, J. C., Byrnes-Blake, K., Fontana, D., Freeman, J., Gray, T., Hausman, D., Hunder, N. N., and Lawitz, E. (2010) Phase 1b study of pegylated interferon lambda 1 with or without ribavirin in patients with chronic genotype 1 hepatitis C virus infection., *Hepatology (Baltimore, Md.) 52*, 822-32.
68. Rohloff, C. M., Alessi, T. R., Yang, B., Dahms, J., Carr, J. P., and Lautenbach, S. D. (2008) DUROS technology delivers peptides and proteins at consistent rate continuously for 3 to 12 months., *Journal of diabetes science and technology 2*, 461-7.
69. Gilmour, K. C., and Reich, N. C. (1995) Signal transduction and activation of gene transcription by interferons., *Gene expression 5*, 1-18.
70. Gale, M. (2003) Effector genes of interferon action against hepatitis C virus., *Hepatology (Baltimore, Md.) 37*, 975-8.
71. Veer, M. J. de, Holko, M., Frevel, M., Walker, E., Der, S., Paranjape, J. M., Silverman, R. H., and Williams, B. R. (2001) Functional classification of interferon-stimulated genes identified using microarrays., *Journal of leukocyte biology 69*, 912-20.
72. Fiedler, M. A., Wernke-Dollries, K., and Stark, J. M. (1996) Inhibition of viral replication reverses respiratory syncytial virus-induced NF-kappaB activation and interleukin-8 gene expression in A549 cells., *Journal of virology 70*, 9079-82.
73. Durantel, D., Carroue, S., Branza-nichita, N., Dwek, R. A., and Zitzmann, N. (2004) Effects of Interferon , Ribavirin , and Iminosugar Derivatives on Cells Persistently Infected with Noncytopathic Bovine Viral Diarrhea Virus, *Journal of virology 48*, 497-504.
74. Hebert, D. N., Zhang, J. X., Chen, W., Foellmer, B., and Helenius, A. (1997) The number and location of glycans on influenza hemagglutinin determine folding and association with calnexin and calreticulin., *The Journal of cell biology 139*, 613-23.
75. Russell, C. A., Jones, T. C., Barr, I. G., Cox, N. J., Garten, R. J., Gregory, V., Gust, I. D., Hampson, A. W., Hay, A. J., Hurt, A. C., Jong, J. C. de, Kelso, A., Klimov, A. I., Kageyama, T., Komadina, N., Lapedes, A. S., Lin, Y. P., Mosterin,

A., Obuchi, M., Odagiri, T., Osterhaus, A. D. M. E., Rimmelzwaan, G. F., Shaw, M. W., Skepner, E., Stohr, K., Tashiro, M., Fouchier, R. A. M., and Smith, D. J. (2008) Influenza vaccine strain selection and recent studies on the global migration of seasonal influenza viruses., *Vaccine 26 Suppl 4*, D31-4.

76. Silberstein, S., and Gilmore, R. (1996) Biochemistry, molecular biology, and genetics of the oligosaccharyltransferase., *The FASEB journal : official publication of the Federation of American Societies for Experimental Biology 10*, 849-58.
77. Yan, Q., and Lennarz, W. J. (1999) Oligosaccharyltransferase: a complex multisubunit enzyme of the endoplasmic reticulum., *Biochemical and biophysical research communications 266*, 684-9.
78. Shailubhai, K., Pukazhenthi, B. S., Saxena, E. S., Varma, G. M., and Vijay, I. K. (1991) Glucosidase I, a transmembrane endoplasmic reticular glycoprotein with a luminal catalytic domain., *The Journal of biological chemistry 266*, 16587-93.
79. Spiro, R. G. (2000) Glucose residues as key determinants in the biosynthesis and quality control of glycoproteins with N-linked oligosaccharides., *The Journal of biological chemistry 275*, 35657-60.
80. Trombetta, E. S., Simons, J. F., and Helenius, A. (1996) Endoplasmic reticulum glucosidase II is composed of a catalytic subunit, conserved from yeast to mammals, and a tightly bound noncatalytic HDEL-containing subunit., *The Journal of biological chemistry 271*, 27509-16.
81. Ware, F. E., Vassilakos, A., Peterson, P. A., Jackson, M. R., Lehrman, M. A., and Williams, D. B. (1995) The molecular chaperone calnexin binds Glc1Man9GlcNAc2 oligosaccharide as an initial step in recognizing unfolded glycoproteins., *The Journal of biological chemistry 270*, 4697-704.
82. Leach, M. R., Cohen-Doyle, M. F., Thomas, D. Y., and Williams, D. B. (2002) Localization of the lectin, ERp57 binding, and polypeptide binding sites of calnexin and calreticulin., *The Journal of biological chemistry 277*, 29686-97.
83. Lindquist, J. A., Hämmerling, G. J., and Trowsdale, J. (2001) ER60/ERp57 forms disulfide-bonded intermediates with MHC class I heavy chain., *The FASEB journal : official publication of the Federation of American Societies for Experimental Biology 15*, 1448-50.
84. Grinna, L. S., and Robbins, P. W. (1980) Substrate specificities of rat liver microsomal glucosidases which process glycoproteins., *The Journal of biological chemistry 255*, 2255-8.

85. Trombetta, S. E., and Parodi, A. J. (1992) Purification to apparent homogeneity and partial characterization of rat liver UDP-glucose:glycoprotein glucosyltransferase., *The Journal of biological chemistry 267*, 9236-40.
86. Frenkel, Z., Shenkman, M., Kondratyev, M., and Lederkremer, G. Z. (2004) Separate roles and different routing of calnexin and ERp57 in endoplasmic reticulum quality control revealed by interactions with asialoglycoprotein receptor chains., *Molecular biology of the cell 15*, 2133-42.
87. Li, G., Zhou, X., Zhao, G., Schindelin, H., and Lennarz, W. J. (2005) Multiple modes of interaction of the deglycosylation enzyme, mouse peptide N-glycanase, with the proteasome., *Proceedings of the National Academy of Sciences of the United States of America 102*, 15809-14.
88. Spiro, R. G. (2004) Role of N-linked polymannose oligosaccharides in targeting glycoproteins for endoplasmic reticulum-associated degradation., *Cellular and molecular life sciences : CMLS 61*, 1025-41.
89. Suzuki, T., Yano, K., Sugimoto, S., Kitajima, K., Lennarz, W. J., Inoue, S., Inoue, Y., and Emori, Y. (2002) Endo-beta-N-acetylglucosaminidase, an enzyme involved in processing of free oligosaccharides in the cytosol., *Proceedings of the National Academy of Sciences of the United States of America 99*, 9691-6.
90. Shoup, V. A., and Touster, O. (1976) Purification and characterization of the alpha-D-mannosidase of rat liver cytosol., *The Journal of biological chemistry 251*, 3845-52.
91. Saint-Pol, A., Codogno, P., and Moore, S. E. (1999) Cytosol-to-lysosome transport of free polymannose-type oligosaccharides. Kinetic and specificity studies using rat liver lysosomes., *The Journal of biological chemistry 274*, 13547-55.
92. Vembar, S. S., and Brodsky, J. L. (2008) One step at a time: endoplasmic reticulum-associated degradation., *Nature reviews. Molecular cell biology 9*, 944-57.
93. Helenius, A., and Aebi, M. (2004) Roles of N-linked glycans in the endoplasmic reticulum., *Annual review of biochemistry 73*, 1019-49.
94. Mast, S. W., Diekman, K., Karaveg, K., Davis, A., Sifers, R. N., and Moremen, K. W. (2005) Human EDEM2, a novel homolog of family 47 glycosidases, is involved in ER-associated degradation of glycoproteins., *Glycobiology 15*, 421-36.
95. Hirao, K., Natsuka, Y., Tamura, T., Wada, I., Morito, D., Natsuka, S., Romero, P., Sleno, B., Tremblay, L. O., Herscovics, A., Nagata, K., and Hosokawa, N. (2006)

EDEM3, a soluble EDEM homolog, enhances glycoprotein endoplasmic reticulum-associated degradation and mannose trimming., *The Journal of biological chemistry 281*, 9650-8.

96. Saeed, M., Suzuki, R., Watanabe, N., Masaki, T., Tomonaga, M., Muhammad, A., Kato, T., Matsuura, Y., Watanabe, H., Wakita, T., and Suzuki, T. (2011) Role of the ERAD pathway in degradation of hepatitis C virus envelope proteins and production of virus particles., *The Journal of biological chemistry*.
97. Olivari, S., Cali, T., Salo, K. E. H., Paganetti, P., Ruddock, L. W., and Molinari, M. (2006) EDEM1 regulates ER-associated degradation by accelerating de-mannosylation of folding-defective polypeptides and by inhibiting their covalent aggregation., *Biochemical and biophysical research communications 349*, 1278-84.
98. Ermonval, M., Kitzmüller, C., Mir, A. M., Cacan, R., and Ivessa, N. E. (2001) N-glycan structure of a short-lived variant of ribophorin I expressed in the MadIA214 glycosylation-defective cell line reveals the role of a mannosidase that is not ER mannosidase I in the process of glycoprotein degradation., *Glycobiology 11*, 565-76.
99. Lederkremer, G. Z., and Glickman, M. H. (2005) A window of opportunity: timing protein degradation by trimming of sugars and ubiquitins., *Trends in biochemical sciences 30*, 297-303.
100. Totani, K., Ihara, Y., Matsuo, I., and Ito, Y. (2006) Substrate specificity analysis of endoplasmic reticulum glucosidase II using synthetic high mannose-type glycans., *The Journal of biological chemistry 281*, 31502-8.
101. Winchester, B., and Fleet, G. W. (1992) Amino-sugar glycosidase inhibitors: versatile tools for glycobiologists., *Glycobiology 2*, 199-210.
102. Spiro, R. G., Zhu, Q., Bhoyroo, V., and Söling, H. D. (1996) Definition of the lectin-like properties of the molecular chaperone, calreticulin, and demonstration of its copurification with endomannosidase from rat liver Golgi., *The Journal of biological chemistry 271*, 11588-94.
103. Fujimoto, K., and Kornfeld, R. (1991) alpha-Glucosidase II-deficient cells use endo alpha-mannosidase as a bypass route for N-linked oligosaccharide processing., *The Journal of biological chemistry 266*, 3571-8.
104. Moore, S. E., and Spiro, R. G. (1990) Demonstration that Golgi endo-alpha-D-mannosidase provides a glucosidase-independent pathway for the formation of

complex N-linked oligosaccharides of glycoproteins., *The Journal of biological chemistry 265*, 13104-12.

105. Mellor, H. R., Neville, D. C. a, Harvey, D. J., Platt, F. M., Dwek, R. a, and Butters, T. D. (2004) Cellular effects of deoxynojirimycin analogues: inhibition of N-linked oligosaccharide processing and generation of free glucosylated oligosaccharides., *The Biochemical journal 381*, 867-75.
106. Alonzi, D. S., Dwek, R. a, and Butters, T. D. (2009) Improved cellular inhibitors for glycoprotein processing α-glucosidases: biological characterisation of alkyl- and arylalkyl-N-substituted deoxynojirimycins, *Tetrahedron: Asymmetry*, Elsevier Ltd *20*, 897-901.
107. Rawlings, A. J., Lomas, H., Pilling, A. W., Lee, M. J.-R., Alonzi, D. S., Rountree, J. S. S., Jenkinson, S. F., Fleet, G. W. J., Dwek, R. a, Jones, J. H., and Butters, T. D. (2009) Synthesis and biological characterisation of novel N-alkyl-deoxynojirimycin alpha-glucosidase inhibitors., *Chembiochem : a European journal of chemical biology 10*, 1101-5.
108. Durantel, D., Alotte, C., and Zoulim, F. (2007) Glucosidase inhibitors as antiviral agents for hepatitis B and C., *Current opinion in investigational drugs (London, England : 2000) 8*, 125-9.
109. Ora, A., and Helenius, A. (1995) Calnexin fails to associate with substrate proteins in glucosidase-deficient cell lines., *The Journal of biological chemistry 270*, 26060-2.
110. Jordan, R., Nikolaeva, O. V., Wang, L., Conyers, B., Mehta, A., Dwek, R. a, and Block, T. M. (2002) Inhibition of host ER glucosidase activity prevents Golgi processing of virion-associated bovine viral diarrhea virus E2 glycoproteins and reduces infectivity of secreted virions., *Virology 295*, 10-9.
111. Schul, W., Liu, W., Xu, H.-Y., Flamand, M., and Vasudevan, S. G. (2007) A dengue fever viremia model in mice shows reduction in viral replication and suppression of the inflammatory response after treatment with antiviral drugs., *The Journal of infectious diseases 195*, 665-74.
112. Whitby, K., Pierson, T. C., Geiss, B., Lane, K., Engle, M., Zhou, Y., Doms, R. W., and Diamond, M. S. (2005) Castanospermine , a Potent Inhibitor of Dengue Virus Infection In Vitro and In Vivo, *Journal of virology 79*, 8698-8706.

113. Steinmann, E., Whitfield, T., Kallis, S., Dwek, R. a, Zitzmann, N., Pietschmann, T., and Bartenschlager, R. (2007) Antiviral effects of amantadine and iminosugar derivatives against hepatitis C virus., *Hepatology (Baltimore, Md.) 46*, 330-8.
114. Zitzmann, N., Mehta, a S., Carrouée, S., Butters, T. D., Platt, F. M., McCauley, J., Blumberg, B. S., Dwek, R. a, and Block, T. M. (1999) Imino sugars inhibit the formation and secretion of bovine viral diarrhea virus, a pestivirus model of hepatitis C virus: implications for the development of broad spectrum anti-hepatitis virus agents., *Proceedings of the National Academy of Sciences of the United States of America 96*, 11878-82.
115. Fischer, P. B., Karlsson, G. B., Dwek, R. a, and Platt, F. M. (1996) N-butyldeoxynojirimycin-mediated inhibition of human immunodeficiency virus entry correlates with impaired gp120 shedding and gp41 exposure., *Journal of virology 70*, 7153-60.
116. Bolt, G., Pedersen, I. R., and Blixenkrone-Møller, M. (1999) Processing of N-linked oligosaccharides on the measles virus glycoproteins: importance for antigenicity and for production of infectious virus particles., *Virus research 61*, 43-51.
117. Chapel, C., Garcia, C., Bartosch, B., Roingeard, P., Zitzmann, N., Cosset, F.-L., Dubuisson, J., Dwek, R. a, Trépo, C., Zoulim, F., and Durantel, D. (2007) Reduction of the infectivity of hepatitis C virus pseudoparticles by incorporation of misfolded glycoproteins induced by glucosidase inhibitors., *The Journal of general virology 88*, 1133-43.
118. Papandréou, M.-J., Barbouche, R., Guieu, R., Kieny, M. P., and Fenouillet, E. (2002) The alpha-glucosidase inhibitor 1-deoxynojirimycin blocks human immunodeficiency virus envelope glycoprotein-mediated membrane fusion at the CXCR4 binding step., *Molecular pharmacology 61*, 186-93.
119. Andersson, U., Butters, T. D., Dwek, R. A., and Platt, F. M. (2000) N-butyldeoxygalactonojirimycin: a more selective inhibitor of glycosphingolipid biosynthesis than N-butyldeoxynojirimycin, in vitro and in vivo., *Biochemical pharmacology 59*, 821-9.
120. Mellor, H. R., Neville, D. C. a, Harvey, D. J., Platt, F. M., Dwek, R. a, and Butters, T. D. (2004) Cellular effects of deoxynojirimycin analogues: uptake, retention and inhibition of glycosphingolipid biosynthesis., *The Biochemical journal 381*, 861-6.

121. Platt, F. M., Neises, G. R., Dwek, R. A., and Butters, T. D. (1994) N-butyldeoxynojirimycin is a novel inhibitor of glycolipid biosynthesis., *The Journal of biological chemistry 269*, 8362-5.
122. Cox, T., Lachmann, R., Hollak, C., Aerts, J., Weely, S. van, Hrebícek, M., Platt, F., Butters, T., Dwek, R., Moyses, C., Gow, I., Elstein, D., and Zimran, A. (2000) Novel oral treatment of Gaucher's disease with N-butyldeoxynojirimycin (OGT 918) to decrease substrate biosynthesis., *Lancet 355*, 1481-5.
123. Spoel, A. C. van der, Jeyakumar, M., Butters, T. D., Charlton, H. M., Moore, H. D., Dwek, R. A., and Platt, F. M. (2002) Reversible infertility in male mice after oral administration of alkylated imino sugars: a nonhormonal approach to male contraception., *Proceedings of the National Academy of Sciences of the United States of America 99*, 17173-8.
124. Andersson, U., Reinkensmeier, G., Butters, T. D., Dwek, R. A., and Platt, F. M. (2004) Inhibition of glycogen breakdown by imino sugars in vitro and in vivo., *Biochemical pharmacology 67*, 697-705.
125. Helenius, a. (1995) Calnexin Fails to Associate with Substrate Proteins in Glucosidase-deficient Cell Lines, *Journal of Biological Chemistry 270*, 26060-26062.
126. Block, T. M., and Jordan, R. (2001) Iminosugars as possible broad spectrum anti hepatitis virus agents: the glucovirs and alkovirs., *Antiviral chemistry & chemotherapy 12*, 317-25.
127. Heermann, K. H., Goldmann, U., Schwartz, W., Seyffarth, T., Baumgarten, H., and Gerlich, W. H. (1984) Large surface proteins of hepatitis B virus containing the pre-s sequence., *Journal of virology 52*, 396-402.
128. Mehta, A., Rudd, P. M., Block, T. M., and Dwek, R. A. (1997) A strategy for anti-viral intervention: the use of alpha-glucosidase inhibitors to prevent chaperone-mediated folding of viral envelope glycoproteins., *Biochemical Society transactions 25*, 1188-93.
129. Murphy, F. A., Fauquet, C. M., Bishop, D. H. L., Ghabrial, S. A., Jarvis, A. W., Martelli, G. P., Mayo, M. A. & Summers, M. D. (1999) Virus Taxonomy: Sixth Report of the International Committee on Taxonomy of Viruses., Vienna & New York.
130. Avalos-Ramirez, R., Orlich, M., Thiel, H. J., and Becher, P. (2001) Evidence for the presence of two novel pestivirus species., *Virology 286*, 456-65.

131. Carlsson, U., and Belák, K. (1994) Border disease virus transmitted to sheep and cattle by a persistently infected ewe: epidemiology and control., *Acta veterinaria Scandinavica 35*, 79-88.
132. Nettleton, P. F., and Entrican, G. Ruminant pestiviruses., *The British veterinary journal 151*, 615-42.
133. Houe, H. (2003) Economic impact of BVDV infection in dairies., *Biologicals : journal of the International Association of Biological Standardization 31*, 137-43.
134. Baker, J. C. (1987) Bovine viral diarrhea virus: a review., *Journal of the American Veterinary Medical Association 190*, 1449-58.
135. Thiel, H.-J., P. G. W. Plagemann, and V. M. (1996) Pestiviruses. In *Fields Virology* (B. N. Fields, D. M. Knipe, and P. M. H., Ed.), p 1059–1073, Raven Press, New York.
136. Mendez, E., Ruggli, N., Collett, M. S., and Rice, C. M. (1998) Infectious bovine viral diarrhea virus (strain NADL) RNA from stable cDNA clones: a cellular insert determines NS3 production and viral cytopathogenicity., *Journal of virology 72*, 4737-45.
137. Perdrizet, J. A., Rebhun, W. C., Dubovi, E. J., and Donis, R. O. (1987) Bovine virus diarrhea--clinical syndromes in dairy herds., *The Cornell veterinarian 77*, 46-74.
138. Rebhun, W. C., French, T. W., Perdrizet, J. A., Dubovi, E. J., Dill, S. G., and Karcher, L. F. Thrombocytopenia associated with acute bovine virus diarrhea infection in cattle., *Journal of veterinary internal medicine / American College of Veterinary Internal Medicine 3*, 42-6.
139. Ridpath, J. F., Neill, J. D., Frey, M., and Landgraf, J. G. (2000) Phylogenetic, antigenic and clinical characterization of type 2 BVDV from North America., *Veterinary microbiology 77*, 145-55.
140. Meyers, G., and Thiel, H. J. (1996) Molecular characterization of pestiviruses., *Advances in virus research 47*, 53-118.
141. Poole, T. L., Wang, C., Popp, R. A., Potgieter, L. N., Siddiqui, A., and Collett, M. S. (1995) Pestivirus translation initiation occurs by internal ribosome entry., *Virology 206*, 750-4.
142. Chon, S. K., Perez, D. R., and Donis, R. O. (1998) Genetic analysis of the internal ribosome entry segment of bovine viral diarrhea virus., *Virology 251*, 370-82.

143. Colett, M. S., Larson, R., Gold, C., Strick, D., Anderson, D. K., and Purchio, A. F. (1988) Molecular cloning and nucleotide sequence of the pestivirus bovine viral diarrhea virus., *Virology 165*, 191-9.
144. Elbers, K., Tautz, N., Becher, P., Stoll, D., Rümenapf, T., and Thiel, H. J. (1996) Processing in the pestivirus E2-NS2 region: identification of proteins p7 and E2p7., *Journal of virology 70*, 4131-5.
145. Xu, J., Mendez, E., Caron, P. R., Lin, C., Murcko, M. A., Collett, M. S., and Rice, C. M. (1997) Bovine viral diarrhea virus NS3 serine proteinase: polyprotein cleavage sites, cofactor requirements, and molecular model of an enzyme essential for pestivirus replication., *Journal of virology 71*, 5312-22.
146. Rice, C. (1996) Flaviviridae: the viruses and their replication (B. N. Fields, D. M. Knipe, P. M. Howley, et al, Ed.) Fields vir., pp 931-959, Lippincott-Raven Publishers, Philadelphia, Pa.
147. Murray, C. L., Jones, C. T., and Rice, C. M. (2008) Architects of assembly: roles of Flaviviridae non-structural proteins in virion morphogenesis., *Nature reviews. Microbiology 6*, 699-708.
148. Tautz, N., Elbers, K., Stoll, D., Meyers, G., and Thiel, H. J. (1997) Serine protease of pestiviruses: determination of cleavage sites., *Journal of virology 71*, 5415-22.
149. Wiskerchen, M., and Collett, M. S. (1991) Pestivirus gene expression: protein p80 of bovine viral diarrhea virus is a proteinase involved in polyprotein processing., *Virology 184*, 341-50.
150. Donis, R. O., and Dubovi, E. J. (1987) Characterization of bovine viral diarrhoea-mucosal disease virus-specific proteins in bovine cells., *The Journal of general virology 68 (Pt 6)*, 1597-605.
151. Greiser-Wilke, I., Dittmar, K. E., Liess, B., and Moennig, V. (1992) Heterogeneous expression of the non-structural protein p80/p125 in cells infected with different pestiviruses., *The Journal of general virology 73 (Pt 1)*, 47-52.
152. Lackner, T., Thiel, H.-J., and Tautz, N. (2006) Dissection of a viral autoprotease elucidates a function of a cellular chaperone in proteolysis., *Proceedings of the National Academy of Sciences of the United States of America 103*, 1510-5.
153. Baigent, S. J., Zhang, G., Fray, M. D., Flick-Smith, H., Goodbourn, S., and McCauley, J. W. (2002) Inhibition of beta interferon transcription by noncytopathogenic bovine viral diarrhea virus is through an interferon regulatory factor 3-dependent mechanism., *Journal of virology 76*, 8979-88.

154. Lackner, T., Müller, A., König, M., Thiel, H.-J., and Tautz, N. (2005) Persistence of bovine viral diarrhea virus is determined by a cellular cofactor of a viral autoprotease., *Journal of virology 79*, 9746-55.
155. Lackner, T., Müller, A., Pankraz, A., Becher, P., Thiel, H.-J., Gorbalenya, A. E., and Tautz, N. (2004) Temporal modulation of an autoprotease is crucial for replication and pathogenicity of an RNA virus., *Journal of virology 78*, 10765-75.
156. Schweizer, M., and Peterhans, E. (2001) Noncytopathic bovine viral diarrhea virus inhibits double-stranded RNA-induced apoptosis and interferon synthesis., *Journal of virology 75*, 4692-8.
157. Weiland, E., Stark, R., Haas, B., Rümenapf, T., Meyers, G., and Thiel, H. J. (1990) Pestivirus glycoprotein which induces neutralizing antibodies forms part of a disulfide-linked heterodimer., *Journal of virology 64*, 3563-9.
158. Weiland, E., Ahl, R., Stark, R., Weiland, F., and Thiel, H. J. (1992) A second envelope glycoprotein mediates neutralization of a pestivirus, hog cholera virus., *Journal of virology 66*, 3677-82.
159. Hulst, M. M., Westra, D. F., Wensvoort, G., and Moormann, R. J. (1993) Glycoprotein E1 of hog cholera virus expressed in insect cells protects swine from hog cholera., *Journal of virology 67*, 5435-42.
160. König, M., Lengsfeld, T., Pauly, T., Stark, R., and Thiel, H. J. (1995) Classical swine fever virus: independent induction of protective immunity by two structural glycoproteins., *Journal of virology 69*, 6479-86.
161. Rümenapf, T., Stark, R., Meyers, G., and Thiel, H. J. (1991) Structural proteins of hog cholera virus expressed by vaccinia virus: further characterization and induction of protective immunity., *Journal of virology 65*, 589-97.
162. Zijl, M. van, Wensvoort, G., Kluyver, E. de, Hulst, M., Gulden, H. van der, Gielkens, A., Berns, A., and Moormann, R. (1991) Live attenuated pseudorabies virus expressing envelope glycoprotein E1 of hog cholera virus protects swine against both pseudorabies and hog cholera., *Journal of virology 65*, 2761-5.
163. Iqbal, M., Poole, E., Goodbourn, S., and McCauley, J. W. (2004) Role for bovine viral diarrhea virus Erns glycoprotein in the control of activation of beta interferon by double-stranded RNA., *Journal of virology 78*, 136-45.
164. Liang, D., Sainz, I. F., Ansari, I. H., Gil, L. H. V. G., Vassilev, V., and Donis, R. O. (2003) The envelope glycoprotein E2 is a determinant of cell culture tropism in ruminant pestiviruses., *The Journal of general virology 84*, 1269-74.

165. Kato, T., Furusaka, A., Miyamoto, M., Date, T., Yasui, K., Hiramoto, J., Nagayama, K., Tanaka, T., and Wakita, T. (2001) Sequence analysis of hepatitis C virus isolated from a fulminant hepatitis patient., *Journal of medical virology 64*, 334-9.
166. Buckwold, V. E., Beer, B. E., and Donis, R. O. (2003) Bovine viral diarrhea virus as a surrogate model of hepatitis C virus for the evaluation of antiviral agents., *Antiviral research 60*, 1-15.
167. Buckwold, V. E., Wei, J., Wenzel-Mathers, M., and Russell, J. (2003) Synergistic in vitro interactions between alpha interferon and ribavirin against bovine viral diarrhea virus and yellow fever virus as surrogate models of hepatitis C virus replication., *Antimicrobial agents and chemotherapy 47*, 2293-8.
168. Vassilev, V. B., Collett, M. S., and Donis, R. O. (1997) Authentic and chimeric full-length genomic cDNA clones of bovine viral diarrhea virus that yield infectious transcripts., *Journal of virology 71*, 471-8.
169. Deleersnyder, V., Pillez, A., Wychowski, C., Blight, K., Xu, J., Hahn, Y. S., Rice, C. M., and Dubuisson, J. (1997) Formation of native hepatitis C virus glycoprotein complexes., *Journal of virology 71*, 697-704.
170. Thiel, H. J., Stark, R., Weiland, E., Rümenapf, T., and Meyers, G. (1991) Hog cholera virus: molecular composition of virions from a pestivirus., *Journal of virology 65*, 4705-12.
171. Branza-Nichita, N., Durantel, D., Carrouée-Durantel, S., Dwek, R. A., and Zitzmann, N. (2001) Antiviral effect of N-butyldeoxynojirimycin against bovine viral diarrhea virus correlates with misfolding of E2 envelope proteins and impairment of their association into E1-E2 heterodimers., *Journal of virology 75*, 3527-36.

CHAPTER 2

NOVEL DNJ-DERIVED COMPOUNDS

2.1 INTRODUCTION

2.1.1 Creating a diversity of protein function through N-glycosylation

Glycosylation is an important post-translational modification that compensates for the limited expression of proteins by the mammalian genome in order to generate a diversity of proteins with varying functions and is by far one of the most common forms of protein modification (*1*). Part of N-linked glycosylation involves a series of glucose trimming reactions on the nascent glycoproteins, catalysed by host cell encoded α-glucosidases, generating mono-glucosylated proteins that associate with lectin-like chaperone proteins calnexin and calreticulin to assume their native conformations (*2*), (*3*). Many viruses therefore make use of this host cell machinery to process and assemble their envelope glycoproteins, without imposing detrimental influence on the N-glycosylation of host-encoded proteins.

2.1.2 Perturbation of the N-glycosylation pathway using ∝-glucosidase inhibitors

∝-glucosidase inhibitors act as putative glucose mimetics that reversibly compete with the glycoprotein substrates for binding sites on the α-glucosidases. Iminosugars are monosaccharide mimics with a nitrogen atom in place of the ring oxygen. These DNJ-containing compounds act as charge transition state analogues and inhibit ER ∝-glucosidases *in vitro* with submicromolar activity.

The induction of cytotoxicity from the inhibition of target enzymes such as ER ∝-glucosidases, as well as enzymes responsible for glycosphingolipid synthesis and glycogen breakdown has also been an area of concern. Moreover, the folding and assembly of some host proteins could also be compromised in the presence of prolonged ER glucosidase inhibition, leading to altered cellular physiology, such as

apoptosis or cellular transformation as a result of sustained unfolded protein response (*4*).

Nonetheless, the use of ER α-glucosidase inhibitors at a low level serves to disrupt the proper folding of certain viral envelope glycoproteins that accumulate and assemble in the ER, without affecting host cell viability (*5*). Even though most cellular proteins are dependent on the α-glucosidase-mediated folding pathway, certain cell lines deficient in α-glucosidase expression are still viable (*6*).

2.1.3 Limitations in anti-viral efficacy of *N*B-DNJ

*N*B-DNJ is the *N*-alkylated analogue of DNJ and exhibits its potency as an inhibitor of key N-glycan processing enzymes, α-glucosidases I and II, in the mammalian ER (*7*), (*8*), (*9*). It has been shown to be a better α-glucosidase inhibitor than DNJ in cultured HepG2 cells (*10*). *N*B-DNJ has been found to exhibit its anti-viral effects through α-glucosidase inhibition both *in vitro* (*11*) and *in vivo* (*12*). A concentration-dependent anti-viral effect of *N*B-DNJ against BVDV and HBV has also been reported in earlier studies (*13*), (*14*).

In spite of its anti-viral potency, *N*B-DNJ is limited to its relatively low efficacy, incapable of disrupting viral protein folding pathways completely. A possible explanation points to its low accessibility to its enzymatic targets, α-glucosidases I and II in the ER lumen or a loss of inhibitory activity from its weak deprotonation (pK_a = 6.6) (*15*) in the ER (pH 7.1) (*16*), (*17*). Even though the imino sugars readily and efficiently cross the plasma membrane into the cytosol, such that the concentration of the iminosugar in the cytosol is at equilibrium with the extracellular concentration, the rate of entry is not known. In fact, the concentration within the ER lumen is significantly lower than that supplied exogenously (*17*). It has been reported

that 1-10 000 times the concentration of iminosugar required to inhibit purified ER α-glucosidase I *in vitro* was necessary to achieve the same level of inhibition *in vivo* (*18*).

Although the inhibition of α-glucosidase is well tolerated in tissue culture and in animals, specific *in vivo* side effects, such as interference with intestinal carbohydrate digesting enzymes and the induction of gastrointestinal distress is seemingly unavoidable. Transient diarrhoea could ensue due to the inhibition of α-glucosidase activity of the intestinal sucrase/isomaltase complex at low dose (3 × 100 mg/day) *N*B-DNJ in the first Gaucher trial, although higher oral doses of *N*B-DNJ or traces of the compound that remained uncleared in the gut could result in toxic membrane perturbations (*19*).

To date, the initial phase II efficacy and safety study of *N*B-DNJ administered in combination with low-dose zidovudine (AZT) to symptomatic HIV-1 infected patients (*20*) and a phase I rising dose tolerability study of *N*B-DNJ in patients with acquired immunodeficiency syndrome (AIDS) and advanced AIDS related complex have been completed (*21*), (*22*). Slow accrual of *N*B-DNJ and the occurrence of adverse side effects such as granulocytopenia, dizziness, and paresthesia (*23*) in a study where *N*B-DNJ (Miglustat®) has been administered at doses of up to 3000 mg/day, approximately 10 times the recommended starting dose administered to Gaucher patients (*24*), for up to six months in HIV-positive patients. Besides, leukopenia and neutropenia have also been observed in a similar group of patients receiving 800 mg/day or above (*25*), highlights the exigency to develop DNJ-derived compounds with improved potency and bioavailability.

2.1.4 Structural modifications of existing DNJ derivatives

From a structural perspective, the imino sugar head group, DNJ, confers competitive α-glucosidase inhibition, whilst the nitrogen-linked alkyl side chain dictates potency, cytotoxicity (*26*), localization, uptake and tissue distribution. Earlier studies have attempted to increase anti-viral potency of iminosugars in cell- and animal-based assays through the alkylation of the ring nitrogen atom in imino sugars (*10*). *N*-nonyl-DNJ (*N*N-DNJ), for instance, demonstrated improved antiviral efficacies, with the 50% effective concentration of the anti-viral effect (EC_{50}) values in the low micromolar range, relative to DNJ and *N*B-DNJ, with EC_{50} values at the millimolar range (*27*), (*28*), (*29*), (*30*), (*31*), (*32*). Nonetheless, the long-term usage of long alkyl chain DNJ derivatives is limited to their unfavorable cytotoxicity profiles.

Interestingly, *N*-nonyl-deoxygalactonojirimycin (*N*N-DGJ) exhibits anti-BVDV activity even though it does not inhibit ER α-glucosidase activity due to the absence of a DNJ head group (*32*), (*31*), suggesting that in addition to α-glucosidase inhibition, DNJ derivatives with long N-alkylated side chains possess other unique anti-viral property.

As determined by cellular based assays, alkyl side chains of at least four carbons have been found to enhance the anti-viral activity of alkylated DNJs (*33*), (*34*), (*35*), whilst eight- to nine-carbons side chains were ideal for the inhibition of glycan processing and virus production (*36*), (*31*). Furthermore, alkyl side chains of at least eight carbons are associated with the activation of innate host defence pathways (*31*). A more recent study found that a four- to six-carbon side chain was optimal for α-glucosidase inhibition (*37*). A series of pulse-chase experiments has also shown that long alkyl chain imino sugar derivatives did not interfere with BVDV RNA

replication, viral protein synthesis and processing (*38*). Radio-labelled DNJ compounds with alkyl side chains greater than eight carbons showed a concentration-dependent cytotoxicity effect when administered to mice (*39*). Improved glucosidase inhibitory efficacy associated with increased cellular association, therefore also contributes to increased cytotoxicity of these DNJ compounds (*39*).

Undesired cytotoxicity of DNJ compounds with chain lengths greater than nine carbon atoms can be countered by introduction of oxygen atoms into the alkyl chain to decrease their lipophilic and amphiphilic character (*31*), (*34*). However, the further increase in polarity through the incorporation of three oxygen atoms within a 10-carbon or 14-carbon side chain led to a significant reduction in inhibitory activity in HepG2 cells (*36*). The position of the oxygen atom within the alkyl side chain also plays a critical role in influencing the inhibitory potential of the DNJ compound. Tan and colleagues found that an oxygen atom at position 7 reduced the hydrophobicity of N-decyl-DNJ more significantly than at position 3 (*34*).

Earlier studies have shown that iminosugars with alkyl chains terminating with cyclohexyl groups exhibit reduced toxicity and improved antiviral efficacy against BVDV and HBV (*34*). Table 2 provides an overview of selected DNJ-derived compounds. *N*-propylcyclohexyl-DNJ (***4***) and *N*-butylcyclohexyl-DNJ (***5***) were both shown to be active against a broad spectrum of viruses such as BVDV, West Nile virus (WNV) and DV, with ***5*** exhibiting anti-viral activity comparable to that of ***2***, but was relatively less toxic (*36*). Even though *N*-butyl(1-cyclohexenyl)-DNJ (***6***) and *N*-butyl(1-hydroxylcyclohexyl)-DNJ (***7***), both derivatives of ***5*** with DNJ head groups and 4-carbon side chains, were found to be well tolerated in MDBK cells with CC_{50} values >300μM, they were significantly less potent in anti-viral efficacy against BVDV relative to ***5*** (*40*).

The subsequent development of two more compounds, *N*-pentylcyclohexyl-DNJ (***8***) and *N*-pentyl-(1-hydroxycyclohexyl)-DNJ (***9***), by the same group combined the favourable characteristics of both ***2*** and ***5***, with similar EC_{50} at low micromolar concentrations against BVDV, DV and WNV (*40*), (*41*). ***9*** was found to be better tolerated in MDBK cells than ***8***, suggesting the importance of the hydroxyl group in reducing cytotoxicity and the former also demonstrated a 10-fold lower 50% cytotoxic concentration for cell growth (CC_{50}) value relative to ***5*** (*36*), (*42*), (*41*). The elimination of the hydroxyl group on the terminal chain and combination of an oxygenated alkyl side chain with a substituted terminal ring structure of ***9***, resulted in the generation of a series of DNJ analogues that exhibit better anti-viral properties and lower cytotoxicity, with *N*-6-hexyl(2-methylcyclohexyloxy)-DNJ (***10***) demonstrating the best anti-viral efficacy (*36*).

Other studies have shown that substituting the alkyl chain with a phenyl group, in place of the cyclohexyl group, such as *N*-benzyl-DNJ (***11***) and *N*-butylphenyl-DNJ (***12***), demonstrates more potent inhibition towards α-glucosidase I (*37*). These structure-activity relationship studies indicate that the combination of an increased oxygenated alkyl chain length and the substitution of the alkyl chain with a phenyl group is critical for achieving improved anti-viral potency and lower cytotoxicity.

N-(6'-(4"-Azido-2"-nitrophenylamino)hexyl)-1-deoxynojirimycin 1 (***13***) was previously synthesized in the group as a possible photoaffinity probe for ER α-glucosidases I and II. Interestingly, this compound found to be a highly potent α-glucosidase I inhibitor (IC_{50} of 17nM) based on an *in vitro* assay and also shown by a FOS analysis to exhibit inhibitory activity towards both ER α-glucosidases in cells (*43*). The *in vitro* comparison of inhibitory potency against purified rat liver ER α-

glucosidases I and II with $Glc_{1\square-3}$ $Man_5GlcNAc_1$-2AA-labelled substrates of ***1*** and ***13*** found that the inhibitory potency of the latter compound was 40 times more potent than the former (*43*).

Since alkylation of the ring nitrogen of DNJ-derived compounds leads to a series of new compounds that inhibit both α-glucosidases I and II to different extent (*44*), the aim of this chapter was to obtain structure-activity information by modifying the lead compound ***13*** through varying the length of the alkyl chain between DNJ head group. In addition, the aromatic moiety and the substitution pattern on the aromatic moiety were also altered, followed by FOS analyses on this modest library of DNJ-derived compounds to assess their inhibitory potency against α-glucosidases I and II in cells.

No.	Compound	Structure	Viral target(s)	Notes	Reference
1	*N*B-DNJ	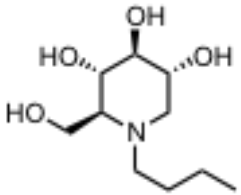	HCV, HIV, DV, BVDV	Approved by EPAR and FDA as a treatment option for type I Gaucher disease Limited anti-viral efficacy [a]TI_{BVDV} >40 - >25 TI_{HBV} >50 - >10	(25), (32), (22), (11), (8), (37), (1), (20)
2	*N*N-DNJ	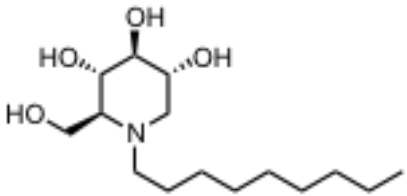	BVDV	More potent anti-viral than *N*B-DNJ Cytotoxic TI_{BVDV} >50 TI_{HBV} 175 - 17.5 TI_{WNV} 5-25 TI_{DV} 20-100	(9), (10), (62), (60), (18), (44), (37), (28)

3	*N*N-DGJ	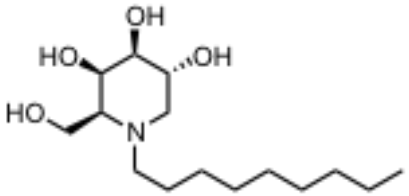	BVDV	Long alkyl chain confers anti-viral property Cytotoxic TI_{BVDV} >7.5	(44), (18),
4	*N*-propylcyclohexyl-DNJ (SP-173)	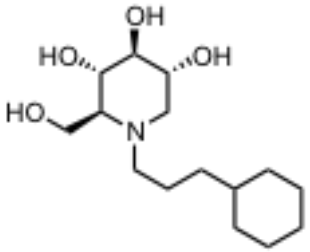	DV, BVDV, WNV	TI_{BVDV} >30 TI_{WNV} >100 TI_{DV} >33	(37), (53), (27), (28)
5	*N*-butylcyclohexyl-DNJ (SP-169)	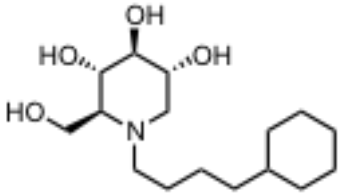	DV, BVDV, WNV, HBV	Comparable anti-viral efficacy to NN-DNJ, but less cytotoxic TI_{BVDV} > 100 TI_{HBV} = 16.7 TI_{WNV} >40 TI_{DV} >66	(37), (53), (28), (27)

6	*N*-butyl(1-cyclohexenyl)-DNJ (OSL-12-51)	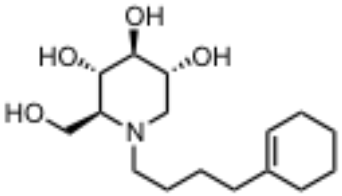	BVDV	CC_{50} >300µM	(28)
7	*N*-butyl(1-hydroxylcyclohexyl)-DNJ (OSL-12-31)	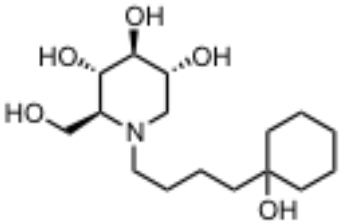	BVDV	CC_{50} >300µM	(28)
8	*N*-pentylcyclohexyl-DNJ (OSL-1)	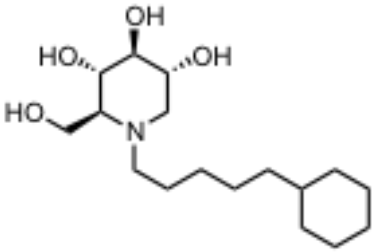	BVDV, WNV	Similar anti-viral efficacy as **9** against BVDV and WNV	(28), (27)
9	*N*-pentyl-(1-hydroxycyclohexyl)-DNJ (OSL95-II)	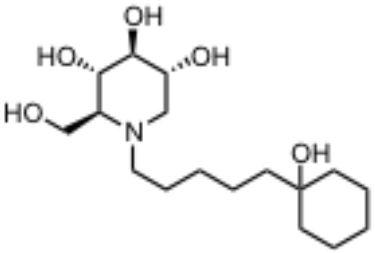	DV, BVDV, WNV	EC_{50} against DV at low micromolar range Better tolerated in MDBK cells than **8**	(28), (16), (27)

				TI_{BVDV} > 166 TI_{WNV} >9 TI_{DV} >50	
10	*N*-6-hexyl(2-methylcyclohexyloxy)-DNJ (PBDNJ0804)	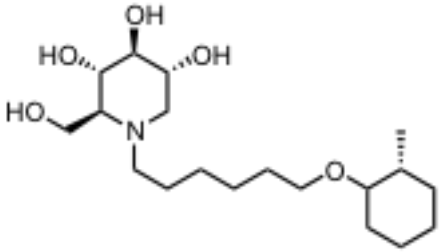	DV, BVDV, WNV	TI_{DV} almost 90-fold higher than **9**	(16)
11	*N*-benzyl-DNJ	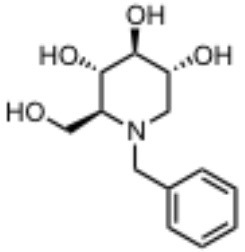	[b]ND	Phenyl substituent of alkyl chain more inhibitory to glucosidase I than the cyclohexyl groups in **4**, **5**, **9** and **10** Both half-life and steady-state distribution volume two-fold better than its *N*-methyl analogue	(3), (21)

12	*N*-butylphenyl-DNJ (SP-168)	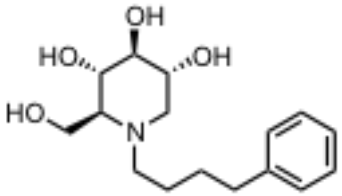	BVDV	Similar anti-viral efficacy to **11** TI_{BVDV} = 25	(3), (*36*)
13	NAP-DNJ (UV5, developed by United Therapeutics)	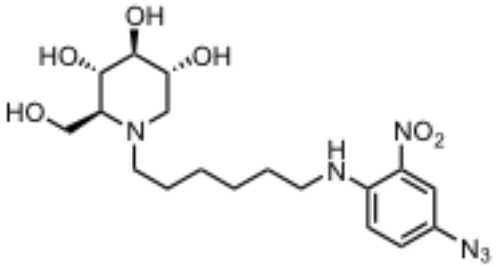	DV (Unpublished), BVDV, EBOV, MARV	Inhibits α-glucosidase II at nanomolar concentrations giving sustained anti-viral response, unique inhibitory property elucidated anti-viral mechanism of iminosugars TI_{BVDV} = 22.2 (Unpublished)	(*37*), (*42*), (*54*)
14	Castanospermine	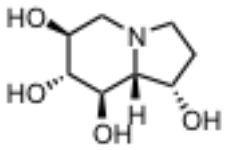	DV, WNV	Yellow fever virus and West Nile virus demonstrated partial and almost complete resistance respectively TI_{WNV} = 5 TI_{DV} >17	(*55*), (*39*)

15	6-O-butanoyl-castanospermine (Celgosivir, developed by Biowest Therapeutics Inc.)	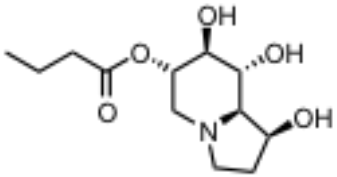	HCV, HIV, BVDV, DV	No deleterious consequences on normal lymphocyte function The only anti-HCV drug in clinical development that acts on host-directed glycosylation	(*56*), (*57*), (*58*), (*59*), (*60*), (*61*)
16	Nitoxozanide (NTZ)	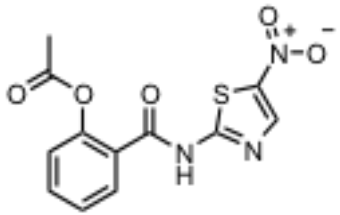	HCV, HBV, influenza virus	Phase II clinical studies completed. SVR rates at 79% and 80% in combination therapy studies relative to 50% with the standard of care with peginterferon plus ribavirin only Suppressed serum HBV DNA and reduced HBV e antigen in majority of patients with chronic hepatitis B	(*62*), (*63*)
17	*N*-9-methoxynonyl-DNJ (UV4, developed by United Therapeutics)	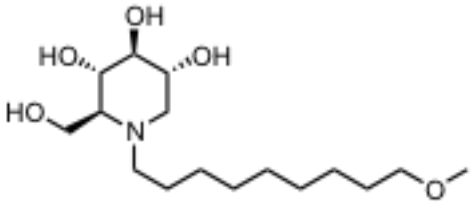	BVDV, EBOV, MARV	No significant weight loss or adverse effects seen 7 days after oral administration in BALB/c and C57/Bl/6 mice	(*54*)

[a]TI, Therapeutic index at MOI 1 = CC_{50}/EC_{50}

[b]ND, Not determined

With the exception of *N*B-DNJ, all compounds listed above are at the pre-clinical development stage.

Table 2 Overview of selected DNJ-derived compounds.

2.2 MATERIALS AND METHODS

2.2.1 Materials

AnalaR and HPLC grade solvents were from VWR International. Water was Milli-Q^{TM} grade. ***1*** was provided by Pharmacia. N-5-phenylpentyl-deoxynojirimycin and N-6-phenylhexyl DNJ were from United Therapeutics. All other reagents were from Sigma.

2.2.2 Cells

Mardin-Darby bovine kidney (MDBK) cells (European Collection of Animal Cell Cultures, Porton Down, United Kingdom) were grown in RPMI 1640 medium (GIBCO/BRL) supplemented with 10% BVDV-free fetal calf serum (PAA Laboratories, Teddington, United Kingdom), 2 mM L-glutamine, 50 units/ml penicillin and 50 μg/ml streptomycin (GIBCO) at 37°C in a humidified 5% CO_2 atmosphere. Cells were confirmed to be free of BVDV by reverse transcriptase-PCR (RT-PCR).

2.2.3 FOS isolation

MDBK cells were seeded at 1 x 10^6 cells/ plate in 6-well cell culture dishes and left to adhere at 37^{o}C, 5% CO_2 atmosphere for 12h before incubating with different concentrations of iminosugars for another 24h. Following cell culture, the medium was removed and the cells were washed three times with PBS by centrifugation. Washed cells were frozen at -20 °C for 20 minutes before thawing and Dounce homogenization in water. An aliquot was taken for protein concentration determination using the Pierce BCA (bicinchoninic acid) protein assay reagent,

following the manufacturer's instructions. The maximum recovery of FOS was performed using the following conditions. The homogenate from 1–2×10^6 cells (0.1–0.2 mg protein) was desalted and deproteinated by passage through a mixed-bed ion-exchange column [0.2 ml of AG50W-X12 (H^+, 100-200 mesh) over 0.4 ml of AG3-X4 (OH^-, 100-200 mesh)], pre-equilibrated with water (5×1 ml). The homogenate was added to the column, which was washed with 4×1 ml of water, and the eluate collected. The extracted and purified FOS were then dried under vacuum or by lyophilizing (*60*). Anthranilic acid was used to label the FOS (*61*) and the labelled oligosaccharides were purified by chromatography using Discovery Speed Amide-2 columns (*60*). The labelled oligosaccharides were stored at -20°C.

2.2.4 Purification of fluorescently labelled FOS

The labelled oligosaccharides were further purified by chromatography using Concanavalin A (ConA)-Sepharose 4B columns (100 ml packed resin). The column was pre-equilibrated with 2×1 ml of water followed by sequential 1 ml washes of 1 mM $MgCl_2$, 1 mM $CaCl_2$, 1 mM $MnCl_2$ and 2×1 ml of 50 mM Tris/HCl buffer, pH 7.2. The sample was added and allowed to pass through the column before washing with 2×1 ml of 50 mM Tris/HCl buffer, pH 7.2. The ConA-bound FOS were then eluted with 2×1 ml of hot (70 °C) 0.5 M methyl α-D-mannopyranoside in 50 mM Tris/HCl buffer, pH 7.2(*60*).

2.2.5 Carbohydrate analysis by NP-HPLC (normal-phase HPLC)

ConA-Sepharose purified 2-AA-labelled oligosaccharides were separated by NP-HPLC (Waters) using a 4.6×250 mm TSKgel Amide-80 column (Anachem) with slight modifications to the published method (*61*). Glucose units were determined,

following comparison with a 2-AA-labelled glucose oligomer ladder (derived from a partial hydrolysate of dextran) external standard using Peak Time software (developed in-house).

The peak area of each 2-AA-labelled species was measured using Waters Empower software and converted into molar amounts using an experimentally-derived conversion factor (i.e. using 2-AA labelling, comparing a standard oligosaccharide of known concentration and measurement of the peak area following HPLC separation) (*60*).

2.2.6 Synthesis of N-(6'-(4"-Azido-2"-nitrophenylamino)hexyl)-1-deoxynojirimycin (*13*)

Proton nuclear magnetic resonance spectra were recorded on a Bruker DPX 400 (400MHz) spectrometer and were calibrated according to the chemical shift of the deuterated solvent. Chemical shifts (δ) are quoted in ppm and coupling constants (J) in Hz. All organic reactions were carried out under nitrogen. Silica gel (230-400 mesh, 40-63μm) for column chromatography was purchased from Merck. Thin layer chromatography was carried out on aluminium sheets coated with $60F_{254}$ silica from Merck. Purification of ***13*** was carried out with Waters Sep-Pak® cartridges packed with reversed-phase sorbent C_{18}. Solvents were used as supplied (HPLC grade) and commercially available agents were used as supplied. Dimethylsulphoxide was purchased from Sigma.

2.3 RESULTS

2.3.1 Synthesis of NAP-DNJ

NAP-DNJ is an aryl azide structurally modified based on a similar DNJ backbone as *N*B-DNJ. It was previously synthesized for photo affinity labelling studies, since the 4-azido-2-nitrophenyl moiety makes the compound very stable in the dark as a suitable photo labile precursor.

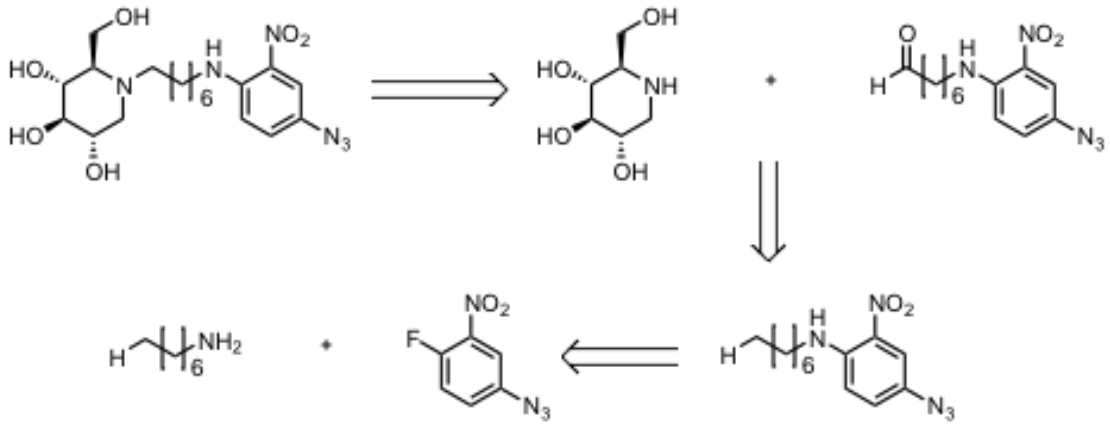

Figure 2.1 Retrosynthesis of NAP-DNJ.

The first step involves the coupling a flourine-substituted aromatic compound to an amino alcohol. This nucleophilic aromatic substitution reaction is followed by the oxidation of primary alcohol to an aromatic aldehyde by Dess-Martin periodinane. The substituted aromatic aldehyde is then coupled to DNJ by reductive amination using sodium cyanoborohydride. The following list of aromatic DNJ analogues follows the same retrosynthetic pathway as shown above.

2.3.1.1 6-(4'-Azido-2'-nitrophenylamino)hexan-1-ol

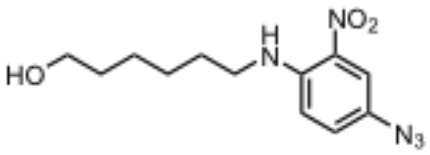

4-fluoro-3-nitrophenyl azide (380mg, 2.06mmol) was added to a stirred solution of 6-aminohexan-1-ol (241.3mg, 2.06mmol) and triethylmine (521.6µl, 3.8mmol) in 1,4-dioxne (5ml) at room temperature under nitrogen atmosphere in the dark. After 19h, t.l.c. (ethyl acetate : cyclohexane, 5:2) indicated a major product (R_f 0.41) and some starting material (R_f 0.75), both UV active. The solvents were removed *in vacuo* and the residue was partitioned between dichloromethane (10ml) and water (10ml). The aqueous later was extracted with dichloromethane (4 x 5ml) and the combined organic fractions were dried over magnesium sulphate and filtered. The solvent was removed *in vacuo*, and the crude residue was purified by flash chromatography (ethyl acetate : cyclohexane, 2:1) to afford 6-(4'-Azido-2'-nitrophenylamino)hexan-1-ol (451.1mg, 78.4%).

^{1}H NMR (CDCl3, 400MHz) δ_H: 8.02 (1H, a-br-s, ArNH), 7.86 (1H, d, H-3', $J_{3',5'}$ 2.7Hz), 7.13 (1H, dd, H-5', $J_{5',3'}$ 2.7Hz, $J_{5',6'}$ 9.2Hz), 6.86 (1H, d, H-6', $J_{6',5'}$ 9.2Hz), 3.69 (2H, t, CH_2-1, $J_{1,2}$ 9.2Hz), 3.31 (2H, td, CH_2-6, $J_{6,5}$ 7.0Hz), 1.82 -1.65 (4H, m, CH_2-5), 1.60 (2H, quintet, CH_2-2), 1.48 (4H, tt, CH_2-3, CH_2-4).

2.3.1.2 6-(4'-Azido-2'-nitrophenylamino)hexanal

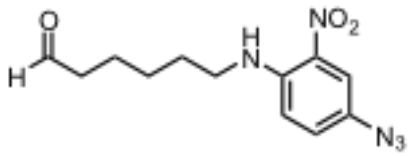

6-(4'-Azido-2'-nitrophenylamino)hexan-1-ol (270.28mg, 0.97mmol) and Dess-Martin periodinane (639mg, 1.51mmol) were stirred in dichloromethane (5.6ml) at room temperature under a nitrogen atmosphere in the dark. After 18h, t.l.c. (ethyl acetate : cyclohexane, 2:1) indicated formation of one product (R_f 0.34), leaving no starting material. The reaction was quenched with aqueous sodium hydroxide solution (1M, 60ml) and the mixture partitioned between water (25ml) and dichloromethane (30ml). The aqueous layer was extracted with dichloromethane (4 x 10ml) and the combined organic fractions dried over magnesium sulphate and filtered. The solvent was removed *in vacuo* and the crude residue was purified by flash chromatography (ethyl acetate : petroleum ether, 1:2) to afford 6-(4'-Azido-2'-nitrophenylamino)hexanal (220.5mg, 82%) as a red oil.

^{1}H NMR (CDCl3, 400MHz) δ_H: 9.79 (1H, t, CHO, $J_{CHO,2}$ 1.5Hz), 8.02 (1H, a-br-s, ArNH), 7.86 (1H, d, H-3', $J_{3',5'}$ 2.7Hz), 7.13 (1H, dd, H-5', $J_{5',3'}$ 2.7Hz, $J_{5',6'}$ 9.1Hz), 6.86 (1H, d, H-6', $J_{6',5'}$ 9.2Hz), 3.31 (2H, td, CH_2-6, $J_{6,5}$ 7.0Hz, $J_{6,NH}$ 5.4Hz), 2.50 (2H, td, Ch_2-2, $J_{2,3}$ 7.2Hz, $J_{2,1}$ 1.5Hz), 1.82-1.65 (4H, m, CH_2-3, CH_2-5), 1.48 (2H, m, CH_2-4).

2.3.1.3 N-(6’-(4”-Azido-2”-nitrophenylamino)hexyl)-1-deoxynojirimycin

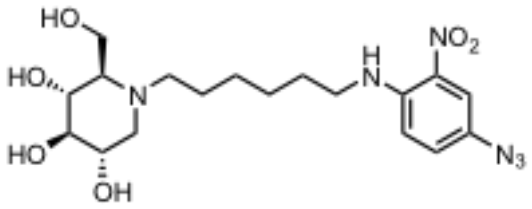

Deoxynojirimycin (50.7mg, 0.311mmol), 6-(4’-Azido-2’-nitrophenylamino)hexanal (103.4mg, 0.373mmol), glacial acetic acid (37.6µl, 0.66mmol) and sodium cyanoborohydride solution (423µl, 1.0M in tetrahydrofuran, 6.73mmol) were stirred in methanol (4.7ml) at room temperature under a nitrogen atmosphere in the dark. After 64h, the solvents were removed *in vacuo* and the residue was dissolved in chloroform (5ml) and water (5ml). The organic layer was extracted with water (3 x 5ml) and the combined aqueous layers were concentrated in vacuo. Sep Pak® C18 cartridges were conditioned with methanol (2ml each) and equilibrated with water (2ml each) and the aqueous was co-loaded with water (10ml) and then eluted with methanol (10ml). Solvent was removed *in vacuo* to afford N-(6’-(4”-Azido-2”-nitrophenylamino)hexyl)-1-deoxynojirimycin (56.5mg, 42.8%) as a red oil.

^{1}H NMR (DMSO, 400MHz) δ_H: 7.71 (1H, d, $J_{3”,5”}$ 2.8Hz, CH-3”), 7.35 (1H, dd, $J_{5”,6”}$ 9.2Hz, $J_{5”,3”}$ 2.8Hz, CH-5”), 7.14 (1H, d, $J_{6”,5”}$ 9.3Hz, CH-6”), 3.53 (1H, m, CH_2-6b), 3.71 (1H, d, $J_{6a,6b}$ 11.7Hz, CH_2-6a), 3.19 (1H, ddd, $J_{2,1a}$ 13.6Hz, $J_{2,3}$ 9.2Hz, $J_{2,1b}$ 4.2Hz, CH-2), 3.02 (1H, td, CH-4), 3.26 – 3.40 (2H, m, CH_2-6’), 2.90 (1H, td, $J_{3,2}$ 4.2Hz, CH-3), 2.74 (2H, m, CH_2-1b, CH_2-1’a), 2.37 (1H, m, CH_2-1’b), 1.94 (2H, m, CH_2-1a, CH-5), 1.61 (2H, m, CH_2-5’), 1.35 (4H, dt, CH_2-2’, CH_2-4’), 1.26 (2H, m, CH_2-3’).

2.3.2 DNJ-derived analogues

In addition to NAP-DNJ, a modest library of other DNJ analogues, comprised of short alkyl chain spacers (4-carbon, 5-carbon, 6-carbon or 7-carbon) with nitrobenzene group, was also previously synthesized according to the steps illustrated in Figure 2.1 (*62*). The structural variations of the DNJ derivatives are shown in Figure 2.2 and the full structures illustrated in Table 3.

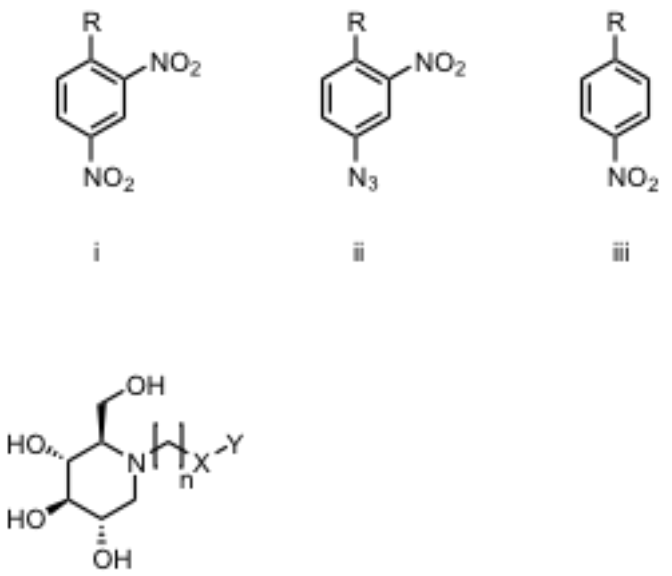

JR2: n=4, X=N, Y=i

JR3: n=5, X=N, Y=i

JR1: n=6, X=N, Y=i

NAP-DNJ: n=6, X=N, Y=ii

AR1: n=6, X=N, Y=iii

PH1: n=6, X=C, Y=Phenol

OP1: n=6, XY=N3

N5: n=4, X=C, Y=Phenol

N6: n=5, X=C, Y=Phenol

Figure 2.2 Variations of Aromatic DNJ Derivatives.

Based on the same DNJ backbone, the length of the linker alkyl chain and the aromatic ring at the end of the chain were varied. The aromatic ring structure either had the azide group removed or substituted with a nitro group.

Name of compound	Compound structure
N-(6’-(4”-Azido-2” nitrophenylamino)hexyl)-1-deoxynojirimycin 1 (NAP-DNJ)	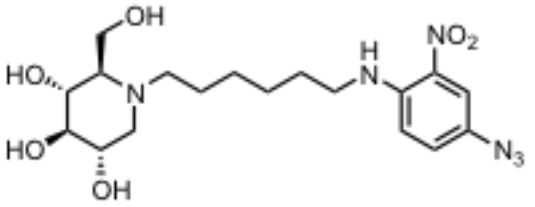
N-(6'-Azidohexyl)-1-deoxynojirimycin (OP1)	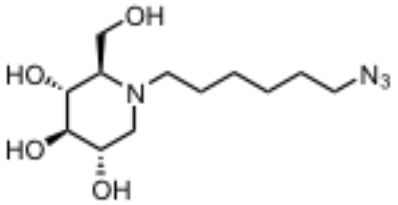
N-(6'-(4''-Nitrophenylamino)hexyl)-1-deoxynojirimycin (AR1)	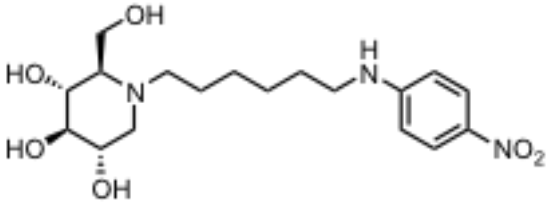
N-(7'-Phenylheptyl)-1-deoxynojirimycin (PH1)	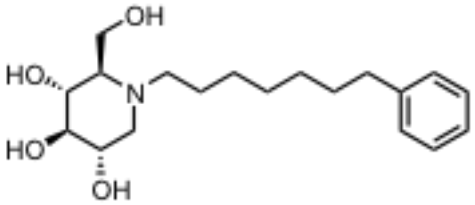
N-(6'-(2'',4''-Dinitrophenylamino)hexyl)-1-deoxynojirimycin (JR1)	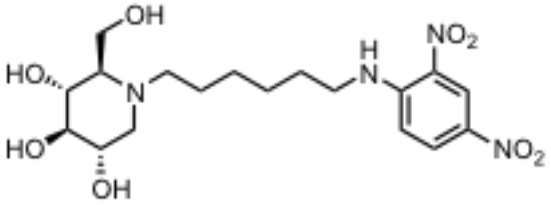
N-(4'-(2'',4''-Dinitrophenylamino)butyl)-1-deoxynojirimycin (JR2)	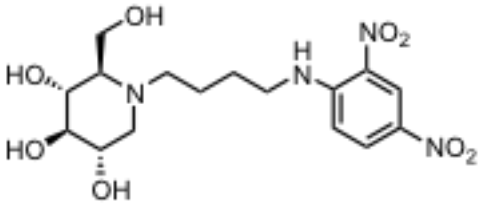

N-(5'-(2",4"-Dinitrophenylamino)pentyl)-1-deoxynojirimycin (JR3)	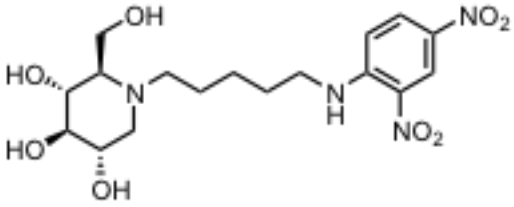
N-5-phenylpentyl-deoxynojirimycin (N5)	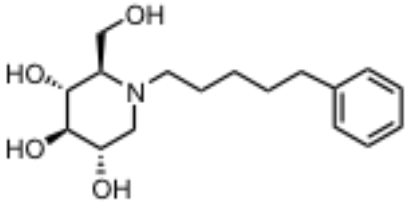
N-6-Phenylhexyl-deoxynojirimycin (N6)	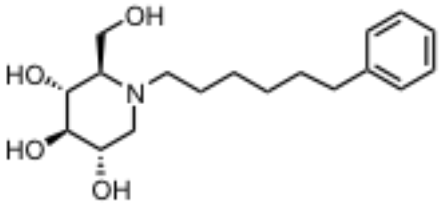

Table 3. Aromatic DNJ Derivatives

2.3.3 Comparison of inhibitory potency of DNJ-derived compounds against ER α-glucosidase activity

To establish and compare the cellular inhibitory potency of the library of DNJ derivatives against α-glucosidases I and II, MDBK and HL60 cells were incubated with various concentrations of these compounds over a 24h period and the FOS profile of the cells were characterized and quantitatively analysed following NP-HPLC separation of the FOS species. Figure 2.3 provides an overview of the steps involved in the FOS analysis.

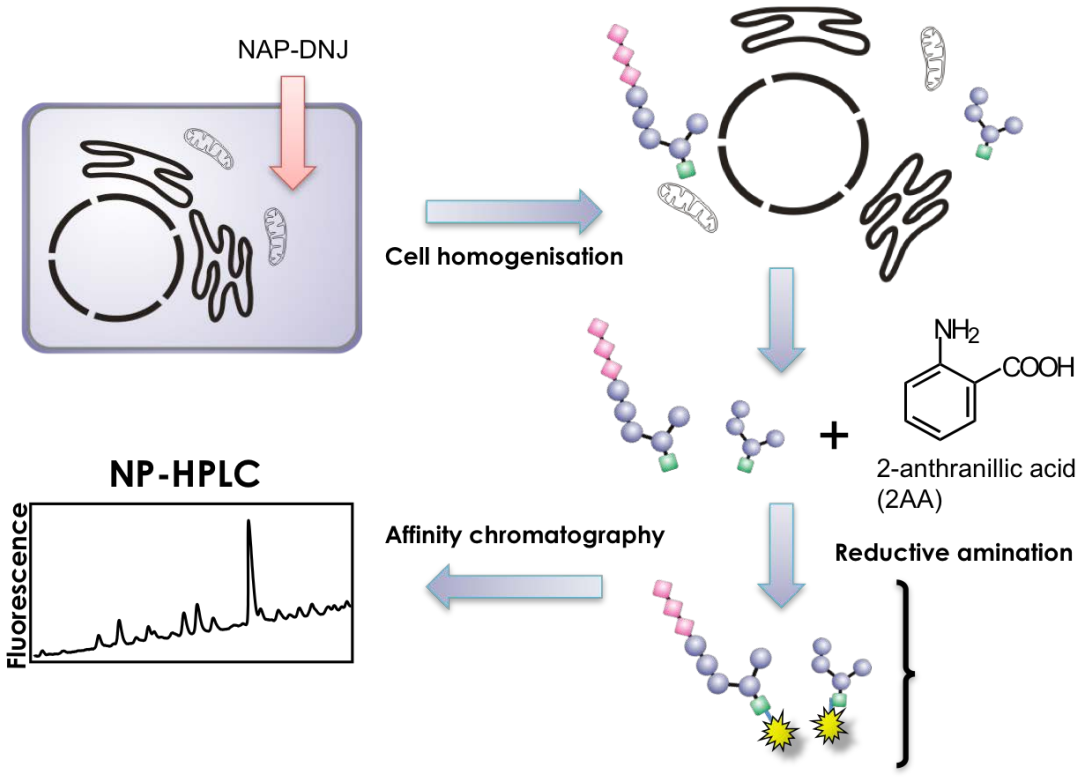

Figure 2.3 Isolation and analysis of FOS.

Peaks on the NP-HPLC chromatograms were identified based on known FOS standards with characteristic glucose units and digests of specific peaks with α-glucosidases I and/or II. The FOS isolated from each sample was normalised to either protein in the sample or to a cell-derived internal FOS standard such as M4N, both of which yield the same results.

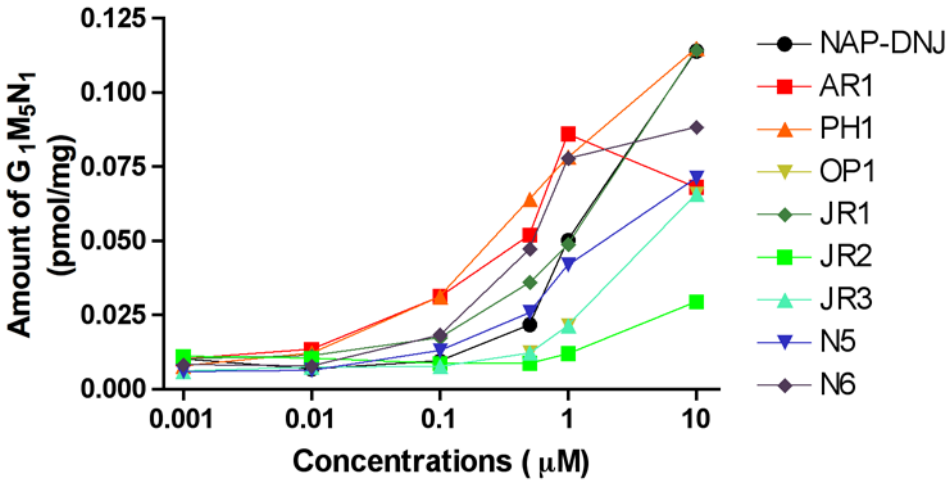

Figure 2.4 Production of mono-glucosylated FOS in MDBK cells.

MDBK cells were treated with increasing concentrations of DNJ compounds. Peak areas were measured in pmol following NP-HPLC analysis of labelled species and normalised to protein content in cells (pmol/mg).

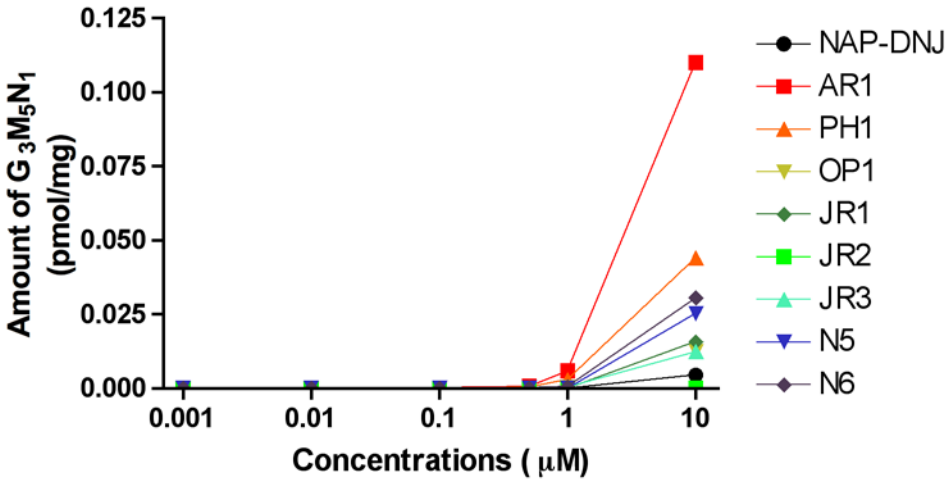

Figure 2.5 Production of tri-glucosylated FOS in MDBK cells.

MDBK cells were treated with increasing concentrations of DNJ compounds. Peak areas were measured in pmol following NP-HPLC analysis of labelled species and normalised to protein content in cells (pmol/mg).

NAP-DNJ exhibited the strongest inhibitory potency against α-glucosidase II at 10μM relative to the other compounds (Figure 2.4), with PH1 demonstrating comparable potency. However, NAP-DNJ was not able to inhibit α-glucosidase I activity until 10μM, whilst PH1 was able to do so at a concentration 20 fold less (Figure 2.5). NAP-DNJ was chosen for further investigations in this study since α-glucosidase II activity could be perpetuated up to 1μM, without inhibiting α-glucosidase I activity.

NAP-DNJ has previously been reported to demonstrate a more potent inhibitory effect on the ER α-glucosidases I and II, in cells and *in vitro*, relative to *N*B-DNJ (*43*).

Therefore, the inhibitory activity of both *N*B-DNJ and NAP-DNJ against α-glucosidases I and II in cell culture was further tested and compared by incubating both MDBK and HL60 cells with various concentrations of *N*B-DNJ or NAP-DNJ over a 24-hour period.

2.3.4 Comparison of inhibitory potency of NAP-DNJ and *N*B-DNJ for ER α-glucosidase activity in MDBK cells

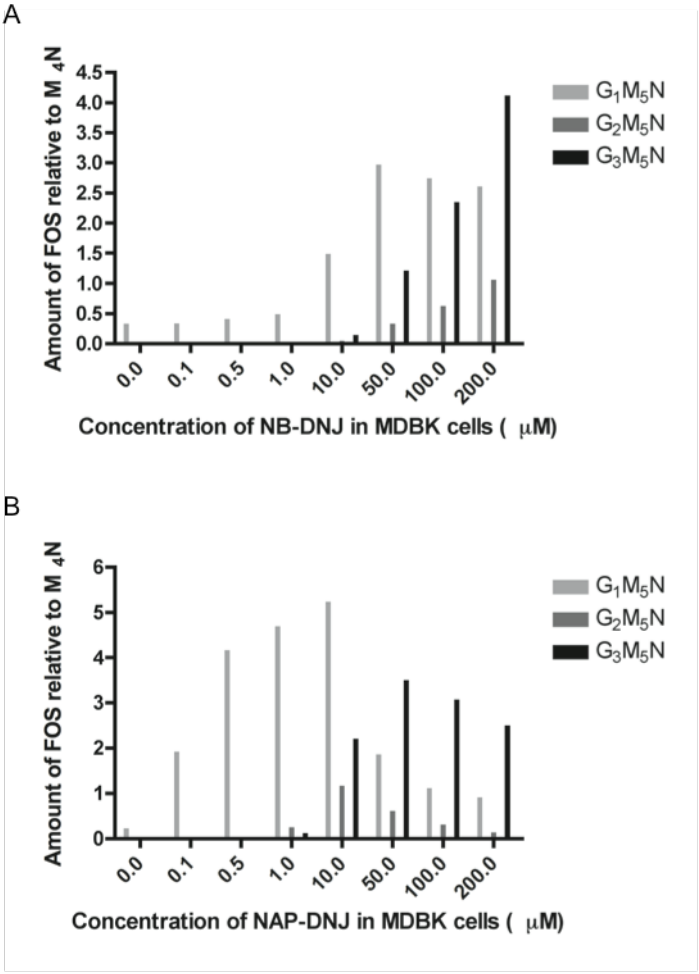

Figure 2.6: NP-HPLC analysis of 2-AA labelled free oligosaccharides (FOS) extracted from MDBK cells.

Production of mono-glucosylated FOS ($Glc_1Man_5GlcNAc_1$), di-glucosylated FOS ($Glc_2Man_5GlcNAc_1$) and tri-glucosylated FOS ($Glc_3Man_5GlcNAc_1$) in MDBK cells in the presence of increasing *N*B-DNJ (A) or NAP-DNJ (B) concentration for 24 h. Labelled FOS were separated using NP-HPLC and peak areas in pmol corresponding to mono-, di- and tri-glucosylated oligosaccharides were normalised to M_4N. The structures of the FOS annotated here are shown in Appendix 1.

At concentrations 10μM or less of each DNJ analogue, the production of both mono- and tri-glucosylated FOS in NAP-DNJ -treated cells was higher than that in *N*B-DNJ -treated cells, as shown in Figure 2.6. NAP-DNJ is thus more capable than *N*B-DNJ at inhibiting both glucosidases I and II at low concentrations.

2.3.5 Comparison of inhibitory potency of NAP-DNJ and *N*B-DNJ for ER α-glucosidase activity in HL60 cells

Similar experiments were performed in HL60 cells. The results are shown in Figure 2.7.

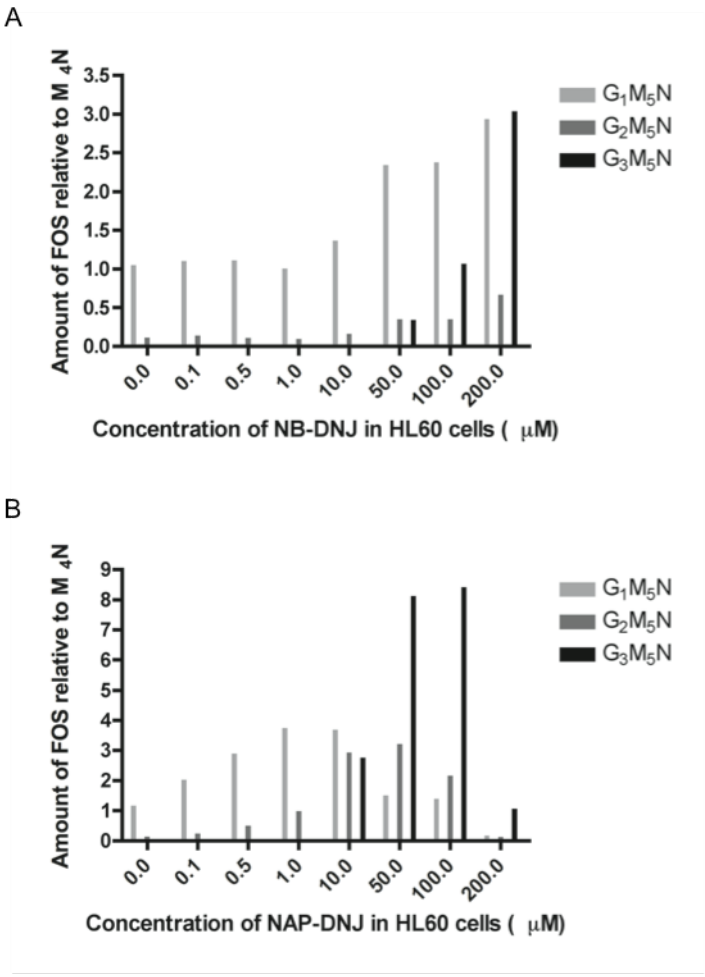

Figure 2.7: NP-HPLC analysis of 2-AA labelled FOS extracted from HL60 cells.

Production of mono-glucosylated FOS ($Glc_1Man_5GlcNAc_1$), di-glucosylated FOS ($Glc_2Man_5GlcNAc_1$) and tri-glucosylated FOS ($Glc_3Man_5GlcNAc_1$) in HL60 cells in the presence of increasing *N*B-DNJ (A) or NAP-DNJ (B) concentration for 24 h. Labelled FOS were separated using NP-HPLC and peak areas in pmol corresponding to mono-, di- and tri-glucosylated oligosaccharides were normalised to M_4N. The structures of the FOS annotated here are shown in Appendix 1

Similar to the results obtained in MDBK cells, the production of both mono- and tri-glucosylated FOS in NAP-DNJ -treated cells is higher than that in *N*B-DNJ -treated cells at concentrations 10μM or less of each DNJ analogue. See Figure 2.7.

As seen in both cell lines, only 0.1μM of NAP-DNJ compared to 10μM of *N*B-DNJ, was needed to evoke the same amount of G_1M_5N production, accounting for 100 times stronger inhibitory effect of NAP-DNJ on α-glucosidase II inhibition in cells.

The amount of G_3M_5N also increased with higher concentrations of NAP-DNJ. This is followed by a consequential decrease in the amount of G_1M_5N produced. At a similar concentration of 10μM, more G_3M_5N was produced in cells treated with NAP-DNJ as compared to those treated with *N*B-DNJ, suggesting a more potent inhibitory effect of NAP-DNJ on α-glucosidase I inhibition in cells.

The production of the di-glucosylated species were significantly lower than the mono- and the tri-glucosylated species in both cell lines following treating with either compound, therefore the detection of the latter two species were sufficient to account for α-glucosidase II and I inhibition respectively.

The unique inhibitory profile of NAP-DNJ against both ER α-glucosidases I and II also makes it a suitable compound in exclusively targeting α-glucosidase II activity at lower concentrations and both α-glucosidases at higher concentrations, allowing for the elucidation of the relative importance of both glucosidases driving an anti-viral mechanism.

2.4 DISCUSSION

All compounds tested in the FOS assays exhibited α-glucosidase II inhibition and were found to be more potent α-glucosidase II inhibitors than *N*B-DNJ in a previous study (*62*). PH1 was consistently found to be a significant α-glucosidase II inhibitor at all concentrations tested relative to the other compounds, suggesting that the nitrogen atom between the alkyl chain and the aromatic ring and the electron withdrawing groups on the aromatic ring does not play a significant role in glucosidase inhibition. On the contrary, it could hinder inhibition. The presence of an aromatic ring was also essential for potent α-glucosidase II inhibition since both NAP-DNJ and PH1 exhibited the strongest α-glucosidase inhibition. However, JR2 was found to be the poorest α-glucosidase II inhibitor amongst the compounds, suggesting that the presence of more than 4 carbon atoms on the alkyl linker chain was necessary for efficient α-glucosidase II inhibition. In fact, a compound with an alkyl linker chain of 7 atoms was found to be the most potent inhibitor.

Only JR1 displayed any form on α-glucosidase I inhibition amongst the dinitro compounds, highlighting the importance of alkyl linker chain length in discriminating between α-glucosidase I and II inhibition. Presence of electron withdrawing groups

were also found to decrease α-glucosidase inhibition since AR1 was found to be more potent than JR1 at inhibiting both α-glucosidases I and II.

Based on the FOS analyses of *N*B-DNJ and NAP-DNJ in MDBK cells, it was found that both compounds exhibit a more potent cellular inhibition of α-glucosidase II compared to α-glucosidase I (Figures 2.6 and 2.7) since the inhibition of α-glucosidase II occurred at lower concentrations whilst the inhibition of α-glucosidase I occurred at higher concentrations. This trend was more pronounced in cells treated with NAP-DNJ. The observation is in direct contrast with the *in vitro* inhibition by *N*B-DNJ, where based on IC_{50} values, the inhibition of α-glucosidase II was approximately 100-fold weaker than inhibition of α-glucosidase I, irrespective of mannose structure or number of N-acetylglucosamine residues at the reducing terminus (*64*). It has been proposed that the removal of the first and second glucose residues by α-glucosidase I and II respectively occurs at close to their limiting rates (V_{max}) in cells, whereas the rate of removal of the proximal glucose residue does not occur close to the V_{max}, hence the competitive inhibitor has a much greater effect on the rate in the latter (*64*). This explains the spike in the production of mono-glucosylated FOS at low concentrations of the inhibitors in cells.

Based on the FOS profiles of these DNJ-derived compounds, it appears that the considerable exclusive inhibition of α-glucosidase II could be achieved with concentrations of NAP-DNJ up to 1μM. Therefore, the discrimination between α-glucosidase I and II activities can be followed with precision using NAP-DNJ,

allowing further mechanistic studies of iminosugars and their anti-viral properties. Even though PH1 was found to be a more potent α-glucosidase II inhibitor compared to NAP-DNJ, the former triggered α-glucosidase I inhibition at 0.5μM, therefore lowering the concentration threshold for exclusive α-glucosidase II inhibition.

Previous *in vitro* as well as cell-based glucosidase inhibition assays using iminosugars have provided comparative insights into their differing glucosidase inhibitory potency (*42*), (*65*), (*51*), (*43*). Interestingly, there appears to be a direct pharmacological equivalence between the *in vitro* and cell-based inhibitory potency demonstrated by these iminosugars. Unlike in the cell-based assays, membrane permeability, ER entry, residency time did not play a part in the *in vitro* assays. Therefore some iminosugars are better than others at targeting their DNJ head groups to the active site of α-glucosidase, and this differing ability to mediate a complement fit is probably attributed to the stereochemistry of the compounds. They vary in alkyl chain length and functional groups and these differences could either facilitate complementary binding or impose varying degrees of steric hindrance that impede binding. In fact, it has previously been hypothesized that the incorporation of an aromatic group in DNJ analogues serves to coordinate this binding (*37*). This explains the differences in inhibitory potency demonstrated by different iminosugars. The absence of the crystal structure of α-glucosidases and hence the lack of docking experiments to identify a model of best fit between enzyme and substrate make it challenging to further validate this hypothesis.

2.5 REFERENCES

1. Vigerust, D. J., and Shepherd, V. L. (2007) Virus glycosylation: role in virulence and immune interactions., *Trends in microbiology 15*, 211-8.

2. Wei-Jia Ou, Pamela H. Cameron, D. Y. T. & J. J. M. B. (1993) Association of folding intermediates of glycoproteins with calnexin during protein maturation., *Nature 364*, 771-776.

3. Zapun, a, Petrescu, S. M., Rudd, P. M., Dwek, R. a, Thomas, D. Y., and Bergeron, J. J. (1997) Conformation-independent binding of monoglucosylated ribonuclease B to calnexin., *Cell 88*, 29-38.

4. Durantel, D., Alotte, C., and Zoulim, F. (2007) Glucosidase inhibitors as antiviral agents for hepatitis B and C., *Current opinion in investigational drugs (London, England : 2000) 8*, 125-9.

5. Dwek, R. a, Butters, T. D., Platt, F. M., and Zitzmann, N. (2002) Targeting Glycosylation As a Therapeutic Approach, *Nature Reviews Drug Discovery 1*, 65-75.

6. Helenius, a. (1995) Calnexin Fails to Associate with Substrate Proteins in Glucosidase-deficient Cell Lines, *Journal of Biological Chemistry 270*, 26060-26062.

7. Grinna, L. S., and Robbins, P. W. (1980) Substrate specificities of rat liver microsomal glucosidases which process glycoproteins., *The Journal of biological chemistry 255*, 2255-8.

8. Michael JM, K. S. (1980) Partial purification and characterization of the glucosidases involved in the processing of asparagine-linked oligosaccharides, *Archives of biochemistry and biophysics 199*, 249-258.

9. Spiro RG, Spiro MJ, B. V. (1979) Processing of carbohydrate units of glycoproteins. Characterization of a thyroid glucosidase., *Journal of Biological Chemistry 254*, 7659-7667.

10. Tan, a, Broek, L. van den, Boeckel, S. van, Ploegh, H., and Bolscher, J. (1991) Chemical modification of the glucosidase inhibitor 1-deoxynojirimycin. Structure-activity relationships., *The Journal of biological chemistry 266*, 14504-10.

11. Gruters, R. A., Neefjes, J. J., Tersmette, M., Goede, R. E. de, Tulp, A., Huisman, H. G., Miedema, F., and Ploegh, H. L. (1987) Interference with HIV-induced syncytium formation and viral infectivity by inhibitors of trimming glucosidase., *Nature 330*, 74-7.

12. Karlsson, G. B., Butters, T. D., Dwek, R. a, and Platt, F. M. (1993) Effects of the imino sugar N-butyldeoxynojirimycin on the N-glycosylation of recombinant gp120., *The Journal of biological chemistry 268*, 570-6.

13. Branza-nichita, N., Durantel, D., Carroue, S., Dwek, R. A., and Zitzmann, N. (2001) Antiviral Effect of N-Butyldeoxynojirimycin against Bovine Viral Diarrhea Virus Correlates with Misfolding of E2 Envelope Proteins and Impairment of Their Association into, *Journal of virology 75*, 3527-3536.

14. Block, T. M., and Jordan, R. (2001) Iminosugars as possible broad spectrum anti hepatitis virus agents: the glucovirs and alkovirs., *Antiviral chemistry & chemotherapy 12*, 317-25.

15. Brumshtein, B., Greenblatt, H. M., Butters, T. D., Shaaltiel, Y., Aviezer, D., Silman, I., Futerman, A. H., and Sussman, J. L. (2007) Crystal structures of complexes of N-butyl- and N-nonyl-deoxynojirimycin bound to acid beta-glucosidase: insights into the mechanism of chemical chaperone action in Gaucher disease., *The Journal of biological chemistry 282*, 29052-8.

16. Mellor, H. R., Neville, D. C. a, Harvey, D. J., Platt, F. M., Dwek, R. a, and Butters, T. D. (2004) Cellular effects of deoxynojirimycin analogues: uptake, retention and inhibition of glycosphingolipid biosynthesis., *The Biochemical journal 381*, 861-6.

17. Mellor, H. R., Neville, D. C. a, Harvey, D. J., Platt, F. M., Dwek, R. a, and Butters, T. D. (2004) Cellular effects of deoxynojirimycin analogues: inhibition of N-linked oligosaccharide processing and generation of free glucosylated oligosaccharides., *The Biochemical journal 381*, 867-75.

18. Broek, L. A. van den, Kat-Van Den Nieuwenhof, M. W., Butters, T. D., and Van Boeckel, C. A. (1996) Synthesis of alpha-glucosidase I inhibitors showing antiviral (HIV-1) and immunosuppressive activity., *The Journal of pharmacy and pharmacology 48*, 172-8.

19. Mellor, H. R., Platt, F. M., Dwek, R. A., and Butters, T. D. (2003) Membrane disruption and cytotoxicity of hydrophobic N-alkylated imino sugars is independent of the inhibition of protein and lipid glycosylation., *The Biochemical journal 374*, 307-14.

20. Fischl, M. A., Resnick, L., Coombs, R., Kremer, A. B., Pottage, J. C., Fass, R. J., Fife, K. H., Powderly, W. G., Collier, A. C., and Aspinall, R. L. (1994) The safety and efficacy of combination N-butyl-deoxynojirimycin (SC-48334) and zidovudine in patients with HIV-1 infection and 200-500 CD4 cells/mm3., *Journal of acquired immune deficiency syndromes 7*, 139-47.

21. (NIAID), N. I. of A. and I. D. (2005) Phase I Rising Dose Tolerability Study of SC-48334 in Patients With Acquired Immunodeficiency Syndrome (AIDS) and Advanced AIDS Related Complex.

22. Service, N. A. C. T. I. (2005) Phase II Study of the Safety and Surrogate Marker Efficacy of Butyldeoxynojirimycin (SC-48334) and AZT in Symptomatic HIV-1 Infected Patients With 200 - 500 CD4+ Cells/mm3.

23. Tierney, M., Pottage, J., Kessler, H., Fischl, M., Richman, D., Merigan, T., Powderly, W., Smith, S., Karim, A., and Sherman, J. (1995) The tolerability and pharmacokinetics of N-butyl-deoxynojirimycin in patients with advanced HIV disease (ACTG 100). The AIDS Clinical Trials Group (ACTG) of the National Institute of Allergy and Infectious Diseases., *Journal of acquired immune deficiency syndromes and human retrovirology : official publication of the International Retrovirology Association 10*, 549-53.

24. Heitner, R., Elstein, D., Aerts, J., Weely, S. van, and Zimran, A. Low-dose N-butyldeoxynojirimycin (OGT 918) for type I Gaucher disease., *Blood cells, molecules & diseases 28*, 127-33.

25. Drug Bank. (2005) Miglustat (http://www.drugbank.ca/drugs/DB00419).

26. Bhudevi, B. (2001) Fluorogenic RT–PCR assay (TaqMan) for detection and classification of bovine viral diarrhea virus, *Veterinary Microbiology 83*, 1-10.

27. Block, T. M., Lu, X., Mehta, A. S., Blumberg, B. S., Tennant, B., Ebling, M., Korba, B., Lansky, D. M., Jacob, G. S., and Dwek, R. A. (1998) Treatment of chronic hepadnavirus infection in a woodchuck animal model with an inhibitor of protein folding and trafficking., *Nature medicine 4*, 610-4.

28. Branza-Nichita, N., Durantel, D., Carrouée-Durantel, S., Dwek, R. A., and Zitzmann, N. (2001) Antiviral effect of N-butyldeoxynojirimycin against bovine viral diarrhea virus correlates with misfolding of E2 envelope proteins and impairment of their association into E1-E2 heterodimers., *Journal of virology 75*, 3527-36.

29. Zitzmann, N., Mehta, a S., Carrouée, S., Butters, T. D., Platt, F. M., McCauley, J., Blumberg, B. S., Dwek, R. a, and Block, T. M. (1999) Imino sugars inhibit the formation and secretion of bovine viral diarrhea virus, a pestivirus model of hepatitis C virus: implications for the development of broad spectrum anti-hepatitis virus agents., *Proceedings of the National Academy of Sciences of the United States of America 96*, 11878-82.

30. Wu, S.-fen, Lee, C.-jang, Liao, C.-len, Dwek, R. A., Zitzmann, N., and Lin, Y.-ling. (2002) Antiviral Effects of an Iminosugar Derivative on Flavivirus Infections, *Journal of virology 76*, 3596-3604.

31. Durantel, D., Branza-nichita, N., Carroue, S., Butters, T. D., Dwek, R. A., and Zitzmann, N. (2001) Study of the Mechanism of Antiviral Action of Iminosugar Derivatives against Bovine Viral Diarrhea Virus, *Journal of virology 75*, 8987-8998.

32. Pavlović, D., Neville, D. C. a, Argaud, O., Blumberg, B., Dwek, R. a, Fischer, W. B., and Zitzmann, N. (2003) The hepatitis C virus p7 protein forms an ion channel that is inhibited by long-alkyl-chain iminosugar derivatives., *Proceedings of the National Academy of Sciences of the United States of America 100*, 6104-8.

33. Mehta, a, Carrouée, S., Conyers, B., Jordan, R., Butters, T., Dwek, R. a, and Block, T. M. (2001) Inhibition of hepatitis B virus DNA replication by imino sugars without the inhibition of the DNA polymerase: therapeutic implications., *Hepatology (Baltimore, Md.) 33*, 1488-95.

34. Tan, a, Broek, L. van den, Bolscher, J., Vermaas, D. J., Pastoors, L., Boeckel, C. van, and Ploegh, H. (1994) Introduction of oxygen into the alkyl chain of N-decyl-dNM decreases lipophilicity and results in increased retention of glucose residues on N-linked oligosaccharides., *Glycobiology 4*, 141-9.

35. Zitzmann, N., Mehta, a S., Carrouée, S., Butters, T. D., Platt, F. M., McCauley, J., Blumberg, B. S., Dwek, R. a, and Block, T. M. (1999) Imino sugars inhibit the formation and secretion of bovine viral diarrhea virus, a pestivirus model of

hepatitis C virus: implications for the development of broad spectrum anti-hepatitis virus agents., *Proceedings of the National Academy of Sciences of the United States of America 96*, 11878-82.

36. Mehta, A., Ouzounov, S., Jordan, R., Simsek, E., Lu, X., Moriarty, R. M., Jacob, G., Dwek, R. a, and Block, T. M. (2002) Imino sugars that are less toxic but more potent as antivirals, in vitro, compared with N-n-nonyl DNJ., *Antiviral chemistry & chemotherapy 13*, 299-304.

37. Alonzi, D. S., Dwek, R. a, and Butters, T. D. (2009) Improved cellular inhibitors for glycoprotein processing α-glucosidases: biological characterisation of alkyl- and arylalkyl-N-substituted deoxynojirimycins, *Tetrahedron: Asymmetry*, Elsevier Ltd *20*, 897-901.

38. Mehta, A. S., Gu, B., Conyers, B., Ouzounov, S., Wang, L., Moriarty, R. M., Dwek, R. A., and Block, T. M. (2004) alpha-Galactosylceramide and Novel Synthetic Glycolipids Directly Induce the Innate Host Defense Pathway and Have Direct Activity against Hepatitis B and C Viruses, *Antimicrobial agents and chemotherapy 48*, 2085-2090.

39. Mellor, H. R., Nolan, J., Pickering, L., Wormald, M. R., Platt, F. M., Dwek, R. A., Fleet, G. W. J., and Butters, T. D. (2002) Preparation, biochemical characterization and biological properties of radiolabelled N-alkylated deoxynojirimycins., *The Biochemical journal 366*, 225-33.

40. Gu, B., Mason, P., Wang, L., Norton, P., Bourne, N., Moriarty, R., Mehta, A., Despande, M., Shah, R., and Block, T. (2007) Antiviral profiles of novel iminocyclitol compounds against bovine viral diarrhea virus, West Nile virus, dengue virus and hepatitis B virus., *Antiviral chemistry & chemotherapy 18*, 49-59.

41. Gu B, Block TM, Moriarty RM, Deshpande MN, Shah RC, G. (2009) Iminosugar compounds with antiflavirus activity (Patent No. 20090042268).

42. Chang, J., Wang, L., Ma, D., Qu, X., Guo, H., Xu, X., Mason, P. M., Bourne, N., Moriarty, R., Gu, B., Guo, J.-T., and Block, T. M. (2009) Novel imino sugar derivatives demonstrate potent antiviral activity against flaviviruses., *Antimicrobial agents and chemotherapy 53*, 1501-8.

43. Rawlings, A. J., Lomas, H., Pilling, A. W., Lee, M. J.-R., Alonzi, D. S., Rountree, J. S. S., Jenkinson, S. F., Fleet, G. W. J., Dwek, R. a, Jones, J. H., and Butters, T. D. (2009) Synthesis and biological characterisation of novel N-alkyl-deoxynojirimycin alpha-glucosidase inhibitors., *Chembiochem : a European journal of chemical biology 10*, 1101-5.

44. Lesur, B; Ducep, JB; Lalloz, MN; Ehrhard, A; Danzin, C. (1997) New deoxynojirimycin derivatives as potent inhibitors of intestinal α-glucohydrolases, *Bioorganic & Medicinal Chemistry Letters 7*, 355-360.

45. Gruters RA, Neefjes JJ, Tersmette M, de Goede RE, Tulp A, Huisman HG, Miedema F, P. H. (1987) Interference with HIV-induced syncytium formation and viral infectivity by inhibitors of trimming glucosidase, *Nature 330*, 74-77.

46. Fischer, P. B., Karlsson, G. B., Dwek, R. a, and Platt, F. M. (1996) N-butyldeoxynojirimycin-mediated inhibition of human immunodeficiency virus entry correlates with impaired gp120 shedding and gp41 exposure., *Journal of virology 70*, 7153-60.

47. (2003) US FDA Medical Review.

48. EPAR. (2002) European Public Assessment Report Zavesca [Miglustat].

49. Faber, E. D., Broek, L. A. van den, Oosterhuis, E. E., Stok, B. P., and Meijer, D. K. (1998) The N-benzyl derivative of the glucosidase inhibitor 1-deoxynojirimycin shows a prolonged half-life and a more complete oral absorption in the rat compared with the N-methyl analog., *Drug delivery 5*, 3-12.

50. Ramstedt U, Klose B, Zitzmann N, Dwek RA, B. T. (2011) Iminosugars and methods of treating foliviral diseases (Patent No. 12/873708).

51. Whitby, K., Pierson, T. C., Geiss, B., Lane, K., Engle, M., Zhou, Y., Doms, R. W., and Diamond, M. S. (2005) Castanospermine , a Potent Inhibitor of Dengue Virus Infection In Vitro and In Vivo, *Journal of virology 79*, 8698-8706.

52. Pan, Y. T., Ghidoni, J., and Elbein, A. D. (1993) The effects of castanospermine and swainsonine on the activity and synthesis of intestinal sucrase., *Archives of biochemistry and biophysics 303*, 134-44.

53. Kang, M. S. (1996) Uptake and metabolism of BuCast: a glycoprotein processing inhibitor and a potential anti-HIV drug., *Glycobiology 6*, 209-16.

54. Taylor, D. L., Sunkara, P. S., Liu, P. S., Kang, M. S., Bowlin, T. L., and Tyms, A. S. (1991) 6-0-butanoylcastanospermine (MDL 28,574) inhibits glycoprotein processing and the growth of HIVs., *AIDS (London, England) 5*, 693-8.

55. Bridges, C. G., Brennan, T. M., Taylor, D. L., McPherson, M., and Tyms, a S. (1994) The prevention of cell adhesion and the cell-to-cell spread of HIV-1 in vitro by the alpha-glucosidase 1 inhibitor, 6-O-butanoyl castanospermine (MDL 28574)., *Antiviral research 25*, 169-75.

56. Schul, W., Liu, W., Xu, H.-Y., Flamand, M., and Vasudevan, S. G. (2007) A dengue fever viremia model in mice shows reduction in viral replication and suppression of the inflammatory response after treatment with antiviral drugs., *The Journal of infectious diseases 195*, 665-74.

57. Whitby, K., Taylor, D., Patel, D., Ahmed, P., and Tyms, A. S. (2004) Action of celgosivir (6 O-butanoyl castanospermine) against the pestivirus BVDV: implications for the treatment of hepatitis C., *Antiviral chemistry & chemotherapy 15*, 141-51.

58. Keeffe, E. B., and Rossignol, J.-F. (2009) Treatment of chronic viral hepatitis with nitazoxanide and second generation thiazolides., *World journal of gastroenterology : WJG 15*, 1805-8.

59. Rossignol, J. F., La Frazia, S., Chiappa, L., Ciucci, A., and Santoro, M. G. (2009) Thiazolides, a new class of anti-influenza molecules targeting viral hemagglutinin at the post-translational level., *The Journal of biological chemistry 284*, 29798-808.

60. Alonzi, D. S., Neville, D. C. a, Lachmann, R. H., Dwek, R. a, and Butters, T. D. (2008) Glucosylated free oligosaccharides are biomarkers of endoplasmic-reticulum alpha-glucosidase inhibition., *The Biochemical journal 409*, 571-80.

61. Neville, D. C. A., Coquard, V., Priestman, D. A., Vruchte, D. J. M. te, Sillence, D. J., Dwek, R. A., Platt, F. M., and Butters, T. D. (2004) Analysis of fluorescently labeled glycosphingolipid-derived oligosaccharides following ceramide glycanase digestion and anthranilic acid labeling., *Analytical biochemistry 331*, 275-82.

62. Rawlings, A. J. (2006) Glucosidase Inhibitors, University of Oxford.

63. Spiro, R. G. (2004) Role of N-linked polymannose oligosaccharides in targeting glycoproteins for endoplasmic reticulum-associated degradation., *Cellular and molecular life sciences : CMLS 61*, 1025-41.

64. Alonzi, D. S., Neville, D. C. a, Lachmann, R. H., Dwek, R. a, and Butters, T. D. (2008) Glucosylated free oligosaccharides are biomarkers of endoplasmic-reticulum alpha-glucosidase inhibition., *The Biochemical journal 409*, 571-80.

65. Chang, J., Schul, W., Butters, T. D., Yip, A., Liu, B., Goh, A., Lakshminarayana, S. B., Alonzi, D., Reinkensmeier, G., Pan, X., Qu, X., Weidner, J. M., Wang, L., Yu, W., Borune, N., Kinch, M. A., Rayahin, J. E., Moriarty, R., Xu, X., Shi, P.-Y., Guo, J.-T., and Block, T. M. (2011) Combination of α-glucosidase inhibitor and ribavirin for the treatment of dengue virus infection in vitro and in vivo., *Antiviral research 89*, 26-34.

CHAPTER 3
ANTI-VIRAL ANALYSES OF DNJ-DERIVED COMPOUNDS

3.1 INTRODUCTION

Glycosylation is an important post-translational modification that plays a crucial role in the folding process of N-linked glycoproteins. ER α-glucosidases are responsible for the stepwise removal of the three glucose residues on N-linked glycans attached to nascent polypeptides to allow the association of mono-glucosylated folding intermediates with the lectin-like ER chaperones calnexin and calreticulin (*1*), (*2*). ER-budding viruses such as the flavivirus genera pestiviruses are found to be highly reliant on this chaperone-mediated protein folding pathway and therefore perturbation of this process using α-glucosidase inhibitors, such as iminosugars, compromises the biogenesis of viral glycoproteins, leading to reduced infectivity (*3*), (*4*), (*5*). Low concentrations of iminosugars have previously demonstrated broad-spectrum anti-viral activity by reducing pre-budding complexes available for virion morphogenesis, maturation, secretion and infection (*6*), (*7*), (*8*), without affecting host cell viability (*9*), (*10*), (*11*). In addition, since the anti-viral mechanism of iminosugars is host driven, the emergence of viral escape mutants to virally coded therapeutics is avoided (*12*).

BVDV is a small, enveloped pestivirus of the Flaviviridae family that infects cattle, resulting in large annual economic losses to the global cattle industry. This virus has a single-stranded, positive-sense RNA genome of approximately 12,600 nucleotides (*13*). The polypeptide precursor is transcribed from a single large open reading frame and subsequently co- and posttranslationally processed into non-structural and structural proteins, including the envelope glycoproteins E1 and E2 that carry two, and four potential N-glycosylation sites,

respectively (*13*). E1 and E2 associate through disulfide bonds (*14*), (*15*) to form a dimer, responsible for establishing viral entry and infection in mammalian host cells. Iminosugars have been shown to inhibit the interaction between calnexin and BVDV E2 and most likely E1 glycoprotein, resulting in misfolding and a decrease in E1E2 heterodimer formation (*16*). In addition, long alkyl-chained iminosugars, such as *N*N-DNJ, have been shown to induce an increase in the amount of BVDV E2E2 dimers within the ER and the subsequent enrichment of these homodimers on secreted virus particles, leading to reduced infectivity (*7*). Another long alkyl-chained iminosugar, N-(6'-4"-azido-2"-nitrophenylamino) hexyl-1-deoxynojirimycin (NAP-DNJ), has been shown to have a more potent inhibitory activity against ER α-glucosidases I and II both *in vitro* and *in cellulo* according to a previously established structure-activity study, compared to *N*B-DNJ, an iminosugar approved for Type I Gaucher treatment (*17*). Protonation of the iminosugar nitrogen resembles the positively charge oxo-carbonium-like transition state formed during hydrolysis (*18*), and therefore reversibly competes with glucose substrates for the active sites of α-glucosidases.

In this study, the anti-viral mechanism of NAP-DNJ against BVDV was investigated for the first time. NAP-DNJ treatment resulted in decreased release of progeny virus, thus highlighting the influence of host-directed α-glucosidase inhibition on the biogenesis, packaging, assembly and infectivity of BVDV E1 and E2 glycoproteins. Enzymatic assays carried out in this study also shed light on the differences in the glycan compositions of intra-cellular E2 and E2 on the surface of the secreted virions following NAP-DNJ treatment. More importantly, the unique inhibitory property of NAP-DNJ against ER α-glucosidases I and II served to elucidate the roles that these luminal enzymes play in the replicative cycle of

flaviviruses. The potential of using NAP-DNJ to treat filoviral diseases under different clinical scenarios was also examined and discussed in this study.

3.2 MATERIALS AND METHODS

3.2.1 Materials

AnalaR and HPLC grade solvents were from VWR International. Rat liver α-glucosidase II (80mM triethylamine buffer, pH 7, containing 0.15M NaCl and 10% glycerol, 5m-units/ml) was purified as described previously (*19*), (*20*). PNGase F and Endo H_f were purchased from New England Biolabs, UK. All other reagents were from Sigma.

3.2.2 Cells, virus and inhibitors

MDBK cells (European Collection of Animal Cell Cultures, Porton Down, United Kingdom) were grown in RPMI 1640 medium (GIBCO/BRL) supplemented with 10% BVDV-free fetal calf serum (PAA Laboratories, Teddington, United Kingdom), 2 mM L-glutamine, 50 units/ml penicillin and 50 μg/ml streptomycin (GIBCO) at 37°C in a humidified 5% CO_2 atmosphere. Cells were confirmed to be free of BVDV by RT-PCR. Cytopathic BVDV-1-NADL (National Animal Disease Laboratory; American Type Culture Collection, Manassas, Va.) virus was provided by N. Zitzmann (University of Oxford). NAP-DNJ was synthesised as described in chapter 2.

3.2.3 Antibodies

Monoclonal antibodies MAb214 and MAb103/105 raised against BVDV E2 glycoprotein and BVDV NS2/NS3 protein respectively were purchased from the Veterinary Laboratories Agency, Weybridge, United Kingdom. The anti-calnexin polyclonal antibody was purchased from Bioquote Limited, York, United Kingdom. The anti-glyceraldehyde 3-phosphate

dehydrogenase (GAPDH) polyclonal antibody was purchased from Sigma, UK. The anti-rabbit and anti-mouse horseradish peroxidase-conjugated secondary antibodies were from AbCam, UK.

3.2.4 Western blotting following virus infection

MDBK cells were seeded at 3.64 x 10^6 cells/ plate in 60mm cell culture dishes and infected with BVDV-1-NADL at a multiplicity of infection (MOI) of 1 fluorescent focus units (FFU)/cell, for 4h at 37ºC, 5% CO_2 atmosphere. After the inoculum was removed, the cells were washed with phosphate-buffered saline (PBS). The cells were then treated with different concentrations of NAP-DNJ in RPMI 1640 medium. At 24h post-infection (p.i.), the cells were harvested using cell scrapers. The culture medium was subjected to centrifugation at 1300g for 10 minutes, followed by ultra-centrifugation at 100 000g for 4 hours at 4ºC. Lysis buffer containing 50mM Tris-HCl buffer, pH 7.5, 0.5% (v/v) Triton X-100, 150 mM NaCl, 2 mM EDTA and a mixture of protease inhibitors (Sigma) (designated Triton-TSE buffer), was added to both the virus pellet and the harvested cells for 1h on ice. The lysed samples were centrifuged at 13 793g for 5 minutes and 10µl of the supernatant was subjected to protein assay using the bicinchoninic acid protein assay kit (Pierce, Rockford, Ill.) to determine the total amount of protein in the lysates. Protein samples separated by sodium dodecyl sulfate-polyacrylamide gel electrophoresis (SDS-PAGE) under non-reducing conditions were transferred to PVDF membranes using a semidry electroblotter (Millipore). Membranes were probed with anti-BVDV E2 antibodies (dilution, 1/1,000) or anti-calnexin antibodies (dilution, 1/4,000) followed by horse-radish peroxidase (HRP) conjugated anti-mouse (dilution, 1/2,000) or anti-rabbit (dilution, 1/10,000) antibodies

respectively. Calnexin and E2 proteins were detected using an enhanced-chemiluminescence detection system (GE Healthcare, UK) and X-ray film (GE Healthcare, UK) by following the manufacturer's instructions.

3.2.5 Carbohydrate analysis by NP-HPLC (normal-phase HPLC)

MDBK cells were seeded at 3.6 x 10^6 cells/ plate in 60mm cell culture dishes and infected with cytopathic BVDV at a multiplicity of infection (MOI) of 1 FFU/cell, for 4h at 37^{o}C, 5% CO_2 atmosphere, prior to growth in fresh medium containing NAP-DNJ at various concentrations. Twenty-four hours p.i., FOS was extracted and purified as described previously (*21*). Anthranilic acid was used to label the FOS, as published (*22*) and the labelled oligosaccharides were purified by chromatography using Discovery Speed Amide-2 columns (*21*). The labelled oligosaccharides were further purified by chromatography using ConA-Sepharose 4B columns (100 ml packed resin) as described previously (*21*). ConA-Sepharose purified 2-AA-labelled oligosaccharides were separated by NP-HPLC (Waters) using a 4.6 X 250 mm TSKgel Amide-80 column (Anachem) (*22*), as described previously (*23*). The peak areas obtained were normalised to protein content in each sample.

3.2.6 Fluorescent antibody detection of virus

MDBK cells were either seeded in 96-well microtitration plates at 8 X 10^4 cells/ well or in six-well plates at 1.75 X 10^6 cells/ well and left to adhere for 4h at 37^{o}C, 5% CO_2 atmosphere to produce a confluent monolayer. The culture supernatant was harvested from NAP-DNJ treated BVDV-infected MDBK cells and the cell monolayers were inoculated with the culture supernatant following 5-fold serial dilutions in a final volume of 50µl in the 96-well microtitration plates or with 500µl of the culture supernatant, RNA normalised or

not. Viral adsorption was allowed to proceed for 1h at 37ºC before the inocula was discarded and monolayers washed twice with PBS. The infected monolayer was incubated at 37ºC for 24h before the monolayers were washed twice with PBS and the cells were fixed for 30mins with 4% (v/v) paraformaldehyde for 30 min and washed with PBS. They were then subjected to blocking in a 5% (w/v) milk-PBS solution for 30 min, and permeabilized with 1% (v/v) Triton X-100 for 20 min. The cells were washed with 1% (v/v) Tween-PBS and incubated with the primary antibody MAb103/105 (1:500 dilution) for 1h, followed by washing three times with 1% (v/v) Tween-PBS. Antibody-labeled cells were detected by incubation of the cells for 1h with an anti-mouse fluorescein isothiocyanate (FITC)-conjugated secondary antibody (1:500 dilution; Sigma) followed by washing three times with 1% (v/v) Tween-PBS. The nuclei were stained with 4',6-diamidino-2-phenylindole (DAPI; Vector Laboratories Inc.). Cells that were labeled with fluorescent antibody were observed and evaluated using an inverted Nikon Eclipse TE200-U microscope, equipped with a Fluor 10X objective lens, and FITC and UV filter sets. Images were captured with DXM1200F digital camera and Nikon ACT-1 2.70 software. Fluorescent foci that were located within the 32mm^2 area of each well were counted, and virus titers were calculated and expressed as FFU per ml. Triplicate wells were used for each sample.

3.2.7 Real-time RT-PCR analysis of virus samples

To concentrate the virus containing culture medium harvested from the infected cells, an aliquot of 500µl was concentrated (molecular weight cutoff, 10 kDa; Centricon filter; Millipore) to 140µl. A QIAamp viral RNA purification kit (Qiagen, Crawley, United Kingdom) was used to purify the RNA from the virus in the concentrated supernatants to

yield 50µl of RNA per sample, according to the manufacturer's instructions. The purified RNA samples were treated with DNase (90 min at 37°C, 20 min at 80°C). Real-time RT-PCR was carried out with a Qiagen SYBR green Quantitect RT-PCR kit, using primers that amplify a 334-bp portion of the NS2-coding sequence (forward primer, 5'-AGA AAA CAC AGA AAC CCG ACA GAC-3'; reverse primer, 5'-TTC CAC CAC TAT TGT AGC ATC CG-3'). An Opticon 2 real-time PCR machine (Bio-Rad) was used to carry out the following reactions: 50°C for 30 min, 15min incubation at 95°C followed by 35 cycles of 15s at 95°C, 1 min at 50°C, and 1 min at 72°C and a final extension for 7 min at 72°C. Internal standards prepared from a highly concentrated cp BVDV supernatant were used to generate standard curves.

3.2.8 Cell proliferation assay

A CellTiter 96® aqueous non-radioactive cell proliferation assay kit (Promega) was used to measure cellular cytotoxicity of NAP-DNJ according to the manufacturer's instructions. Briefly, 3 $X10^3$ MDBK cells were seeded into each well of a 96-well plate. Twenty-four hours later, the medium was removed and different concentrations of NAP-DNJ were added. The plates were incubated at 37°C for 18h, 24h, 42h, 48h, 66h and 72h. At the specified time points, 20µl of 3-(4,5-dimethylthiazol-2-yl)-5-(3-carboxymethoxyphenyl)-2-(4-sulfophenyl)-2*H*-tetrazolium) (MTS)–phenazine methosulfate was added to each well and the samples were incubated at 37°C for 2h. The absorbance was read at 490 nm with a UVmax plate reader (Molecular Devices). Each sample was analysed in triplicate, and the results were extrapolated to those of the non-inhibitor treated cells, which served as the 100% viability

control. The cytotoxic concentration (CC_{50}) was determined as the concentration at which 50% of the absorbance at 490nm was obtained relative to untreated control cells.

3.2.9 Immunoprecipitation

Cells were lysed with 2% CHAPS (3-[(3-chloramidopropyl)-dimethylammonio]-1-propanesulfonate) in HSE buffer (50mM HEPES buffer, pH 7.5, containing 200mM NaCl, 2mM EDTA plus protease inhibitors) on ice for 1h. The lysates were centrifuged at 13 793g for 15 minutes and pre-cleared with 20µl of protein A-Sepharose for 1h at 4°C. The pre-cleared lysates were incubated with rabbit polyclonal anti-calnexin antibodies (diluted 1:200) overnight at 4°C. Protein A-sepharose (30µl) was then added to the supernatants, and incubated for 1h at 4°C. The protein A-sepharose was washed six times with 0.5% CHAPS/ HSE buffer. In some experiments, the terminal glucose residue from glycoprotein substrates was removed using purified rat liver ER α-glucosidase II (10µl) which was added to the immunoprecipitated complex and incubated for 24h at 37°C. The immunoprecipitated complexes were eluted by boiling at 100°C the samples for 10min in SDS-PAGE sample buffer. Samples were analyzed using SDS-PAGE.

3.2.10 Endoglycosidase treatment

MDBK cells were grown in 6-well plates and infected with BVDV at MOI of 1 for 24h with or without NAP-DNJ. The cells were harvested by scrapers and centrifuged at 1300g for 5mins to obtain a cell pellet. The culture medium was also harvested and centrifuged at 100 000g for 4h at 4ºC to yield a viral pellet. Triton-TSE buffer plus protease inhibitors (Sigma) were added to lyse the viral and cell pellets respectively on ice for 1h. The lysates were then

subjected to centrifugation at 13 793g for 5 minutes. Portion of lysates were treated with PNGase F (New England Biolabs), Endo H_f (New England Biolabs), endomannosidase (*24*) or rat liver α-glucosidase II for 12h at 37°C. BVDV E2 was detected by western blot using MAb214 antibody followed by horse-radish peroxidase (HRP) conjugated anti-mouse antibody.

3.3 RESULTS

3.3.1 Cell proliferation assay

NAP-DNJ has been reported to demonstrate potent inhibitory activity against ER α-glucosidases I and II (see chapter 2). However, the anti-viral efficacy and mechanism of this DNJ-derived compound has yet been addressed. NAP-DNJ was reconstituted in dimethyl sulfoxide (DMSO), therefore an MTS-based cell proliferation assay was carried out to identify the maximum concentration of NAP-DNJ that could be used without causing a significant decrease in cell viability. Based on the optical density readings obtained at 490nm shown in Figure 3.1, majority of the cells remained viable up to 50μM NAP-DNJ over a 72h period. There was a reduction in viable cells following treatment with NAP-DNJ greater than 150μM after 18h.Treatment of MDBK cells with a NAP-DNJ concentration of 100μM or above for 24h resulted in reduced cell proliferation (Table 4). The concentration of NAP-DNJ required to reduce cell viability by 50% (CC_{50}) in 24h was found to be 158.9μM (Table 4). Consequently, the maximum concentration of NAP-DNJ used in this study was 75μM, as no apparent cytotoxicity was observed.

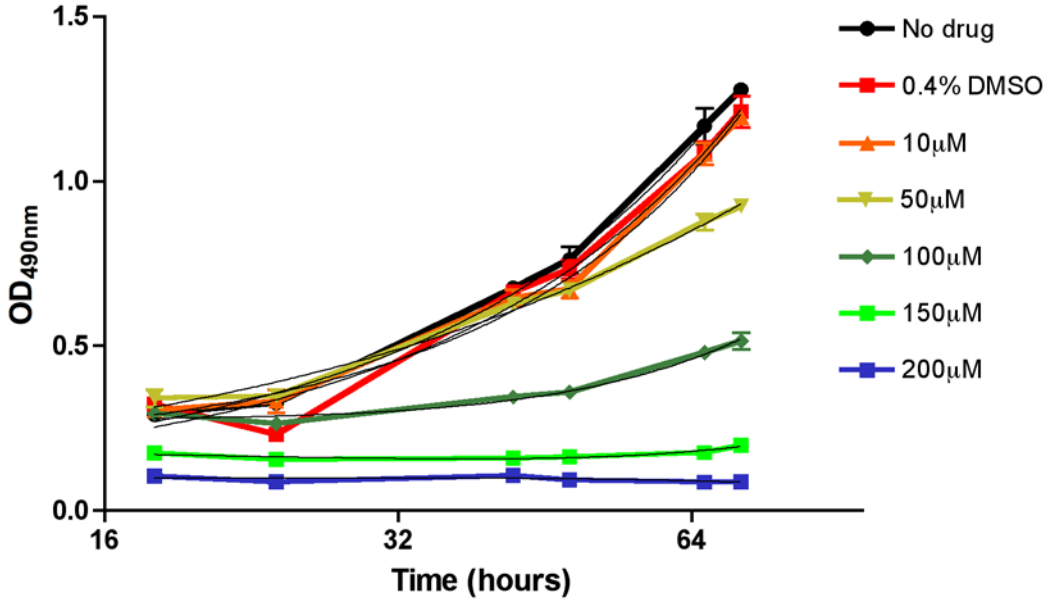

Figure 3.1 Cytotoxicity effects of NAP-DNJ in MDBK cells.

MDBK cells were treated with different concentrations of NAP-DNJ (10μM, 50μM, 100μM, 150μM and 200μM) over 18, 24, 42, 48, 66 and 72h, or the presence of 0.4% DMSO only as control. Following addition of MTS reagents, optical density was measured at 490nm.

	Incubation period (hours)					
	18	24	42	48	66	72
CC_{50} of NAP-DNJ (μM)	178.9	158.9	111.7	102.5	82.8	81.7

Table 4. The 50% cytotoxic concentration (CC_{50}) of NAP-DNJ. The CC_{50} values of NAP-DNJ in MDBK cells were determined at 18, 24, 42, 48, 66 and 72h post-treatment.

3.3.2 Inhibition of ER α-glucosidases by NAP-DNJ

DNJ and its alkyl analogues inhibit ER α-glucosidases I- and II-mediated trimming of glucose residues on glycoproteins. This results in an increase of misfolded glycoproteins with glucosylated high-mannose oligosaccharides, which are targeted for ER-associated degradation (ERAD). ERAD involves the removal of oligosaccharides as well as protein degradation, thereby resulting in an increase in free oligosaccharides (FOS) in the cell (*25*). The detection of $Glc_1Man_5GlcNAc_1$ (G_1M_5N) and $Glc_2Man_5GlcNAc_1$ (G_2M_5N) in a FOS analysis (*21*), is therefore indicative of ER α-glucosidase II inhibition, whilst detection of $Glc_3Man_5GlcNAc_1$ (G_3M_5N) indicates α-glucosidase I inhibition (See figure *in vitro*). FOS analyses were carried out on uninfected and BVDV-infected MDBK cells over a concentration range of NAP-DNJ from 0.1μM to 75μM, to probe for the amounts of mono- and tri-glucosylated species accumulating, as illustrated in Figure 3.2A. The glycan profiles obtained from both the uninfected and BVDV-infected cells subjected to NAP-DNJ treatments were similar, where the production of $Glc_1Man_5GlcNAc_1$ peaked at 5μM NAP-DNJ, indicative of α-glucosidase II inhibition, whilst the production of $Glc_3Man_5GlcNAc_1$ plateaus indefinitely at higher NAP-DNJ concentrations, as a result of α-glucosidase I inhibition. The production of G_2M_5N following NAP-DNJ treatment was almost negligible compared to the significantly higher productions of G_1M_5N and G_3M_5N, therefore the

detection of the latter two glycoforms would be sufficient to account for α-glucosidase II and I inhibition respectively.

The increased potency of NAP-DNJ relative to *N*B-DNJ allows discrimination of α-glucosidase I and II inhibition to probe the dependency of BVDV envelope glycoproteins on chaperone-mediated protein folding pathways (See chapter 2).

A

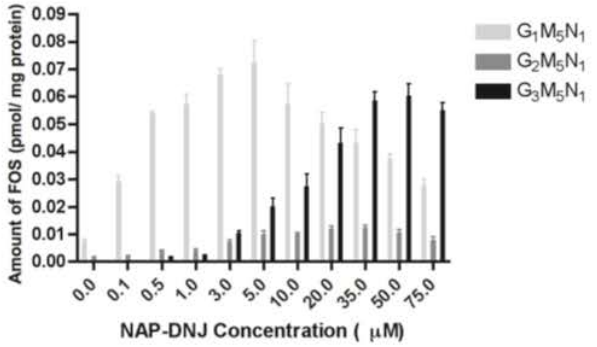
Amount of FOS (pmol/ mg protein)
0.09
0.08
0.07
0.06
0.05
0.04
0.03
0.02
0.01
0.00
0.0 0.1 0.5 1.0 3.0 5.0 10.0 20.0 35.0 50.0 75.0
NAP-DNJ Concentration (μM)
$G_1M_5N_1$
$G_2M_5N_1$
$G_3M_5N_1$

B

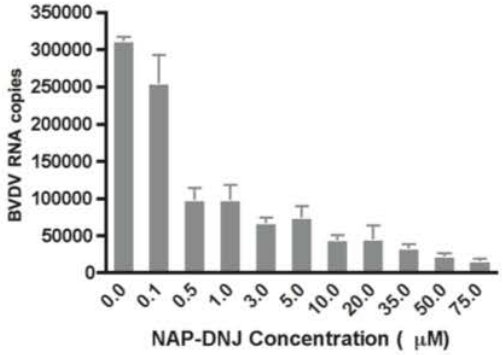
BVDV RNA copies
350000
300000
250000
200000
150000
100000
50000
0
0.0 0.1 0.5 1.0 3.0 5.0 10.0 20.0 35.0 50.0 75.0
NAP-DNJ Concentration (μM)

C

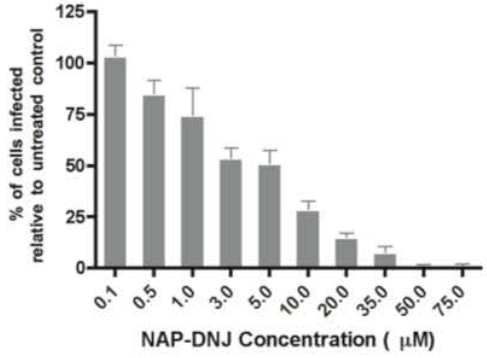
% of cells infected relative to untreated control
125
100
75
50
25
0
0.1 0.5 1.0 3.0 5.0 10.0 20.0 35.0 50.0 75.0
NAP-DNJ Concentration (μM)

D

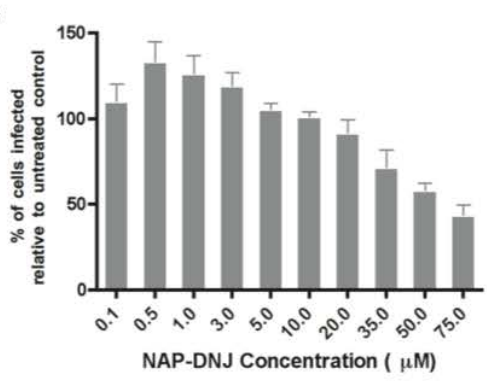
% of cells infected relative to untreated control
150
100
50
0
0.1 0.5 1.0 3.0 5.0 10.0 20.0 35.0 50.0 75.0
NAP-DNJ Concentration (μM)

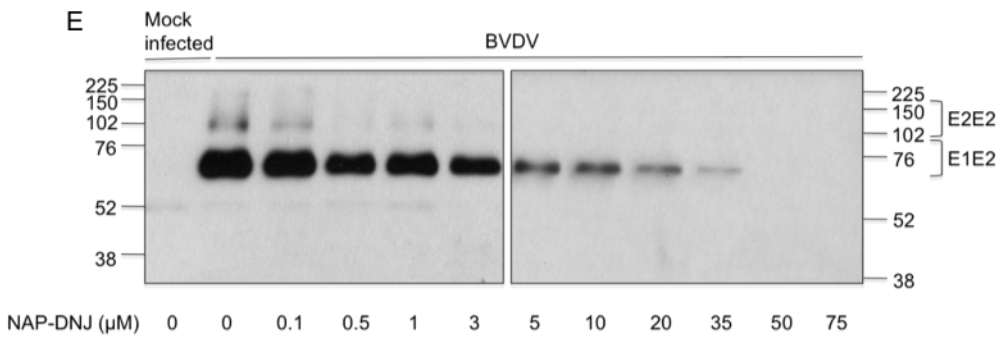

Figure 3.2 Decreased virion secretion as a result of ER α-glucosidase inhibition.

Production of mono-glucosylated FOS ($Glc_1Man_5GlcNAc_1$), di-glucosylated FOS ($Glc_2Man_5GlcNAc_1$) and tri-glucosylated FOS ($Glc_3Man_5GlcNAc_1$) in the presence of increasing NAP-DNJ concentration for 24 h. FOS were separated using NP-HPLC and peak areas corresponding to mono-, di- and tri-glucosylated oligosaccharides, normalised to protein concentration. The data were obtained from three experiments with standard deviation shown (A). MDBK cells were either infected with BVDV at an MOI of 1 or mock-infected and grown in the presence or absence of NAP-DNJ at the concentrations indicated. Twenty-four hours p.i., the spent medium was harvested and subjected to real time RT-PCR analysis to quantify the secreted viral RNA levels (B) or used to infect naïve MDBK cells directly, with the volumes of the inocula standardized (C). Following RT-PCR, viral RNA copies of each sample were normalised and used to re-infect naive MDBK cells (D). Twenty-four hours p.i, the cells were fixed and probed with a monoclonal antibody against the BVDV NS2 and NS3 proteins, followed by incubation with an anti-mouse FITC-conjugated secondary antibody whilst cell nuclei were stained with DAPI. Since cytotoxic effects persist beyond 75μM NAP-DNJ, EC_{50} was estimated assuming complete abolishment of viral activity at higher NAP-DNJ concentrations. The number of infected cells was expressed as a

percentage of total number of cells. Assembly of the viral proteins in the harvested spent medium was analyzed by SDS–12% PAGE under non-reducing conditions followed by Western blotting using MAb 214 (E).

3.3.3 NAP-DNJ reduced virion secretion by inhibiting ER α-glucosidase II

Previous studies have shown that *N*B-DNJ and to a greater extent *N*N-DNJ prevented the secretion of infectious BVDV when MDBK cells were infected with the HCV surrogate virus (*11*). To find out whether NAP-DNJ, a supposedly more potent α-glucosidase inhibitor relative to *N*B-DNJ and NN-DNJ, exhibits similar or more potent anti-BVDV properties, a series of assays were carried out. In order to monitor the amount of virus secreted in the culture supernatant of NAP-DNJ treatment of BVDV-infected MDBK cells, the amount of viral RNA copies in the culture medium was quantified using real time RT-PCR. Viral RNA copies decreased by three-fold at 1μM NAP-DNJ compared to untreated samples (Figure 3.2B). This coincides with the exclusive inhibition of α-glucosidase II (Figure 3.2A). The decline in viral RNA copies from infected cells that were treated with NAP-DNJ at concentrations higher than 3μM became less pronounced, when the inhibition of ER α-glucosidase I begins (Figure 3.2B), suggesting that ER α-glucosidase II inhibition could be exclusively responsible for the impairment of virion production and secretion.

The culture supernatant was also used to re-infect naïve MDBK cells. Fluorescent focus assay, a variation of the conventional plaque assay (*26*), was carried out on these cells

against the BVDV NS2-NS3 epitope after 24h and revealed a sharp decline in viral infectivity as shown in Figure 3.2C, indicating a reduction in infectivity of progeny virus.

3.3.4 Inhibition of both ER α-glucosidases I and II by NAP-DNJ contributes to a combined anti-viral effect in BVDV infected cells

In order to confirm that the drop in viral infectivity seen above was not exclusively due to decreased viral RNA secretion, the RT-PCR quantitated viral RNA copies across all the NAP-DNJ-treated and -untreated samples as described above were normalised to the same amount of viral RNA copies in the medium from infected cells treated with 75μM NAP-DNJ. The normalised virus medium was then used to re-infect naïve MDBK cells over a 24h period and fluorescent focus assay against the BVDV NS2-NS3 epitope depicted in Figure 3.2D shows the decrease in viral infectivity starting at 5μM of NAP-DNJ. At 75μM of NAP-DNJ, viral infectivity levels dropped to less than 50% that of the NAP-DNJ-untreated BVDV-infected control.

Inhibition of ER α-glucosidase I begins at 5μM of NAP-DNJ treatment, as indicated by the production of tri-glucosylated glycans in Figures 3.2A, and continued to persist and escalate until the production peaks and plateaued at 75μM of NAP-DNJ. This ER α-glucosidase I inhibitory range coincides with the decline in viral infectivity of the virus as described above, strongly suggesting that ER α-glucosidase I inhibiton is responsible for impairing viral functionality in progeny virus.

The decrease in virion secretion was further confirmed by decrease in amount of E1E2 and E2E2 dimers present in the culture supernatant of NAP-DNJ treated BVDV-infected cells compared to untreated cells (Figure 3.2E). No monomers were detected in the culture supernatant of BVDV-infected cells.

3.3.5 Prolonged exclusive α-glucosidase II inhibition was sufficient to sustain anti-viral efficacy

In order to determine where the NAP-DNJ-mediated inhibition of α-glucosidase I or II or both triggers a more potent anti-viral effect, MDBK cells were infected with BVDV at MOI 1 or 0.1 and subsequently treated with 1µM (exclusive α-glucosidase II inhibition) or 75µM NAP-DNJ (inhibition of both α-glucosidases I and II) for 24h. The titre of virus secreted into the culture medium was determined by fluorescent antibody detection assay. There was a >60% reduction in virus titre following 1µM NAP-DNJ treatment and >95% decrease with 75µM NAP-DNJ compared with untreated BVDV infected cells (Figure 3.3A, Treatment A). Thus, although exclusive α-glucosidase II inhibition was sufficient to decrease viral infectivity, inhibition of both α-glucosidases was necessary to impose a relatively more potent anti-viral capability.

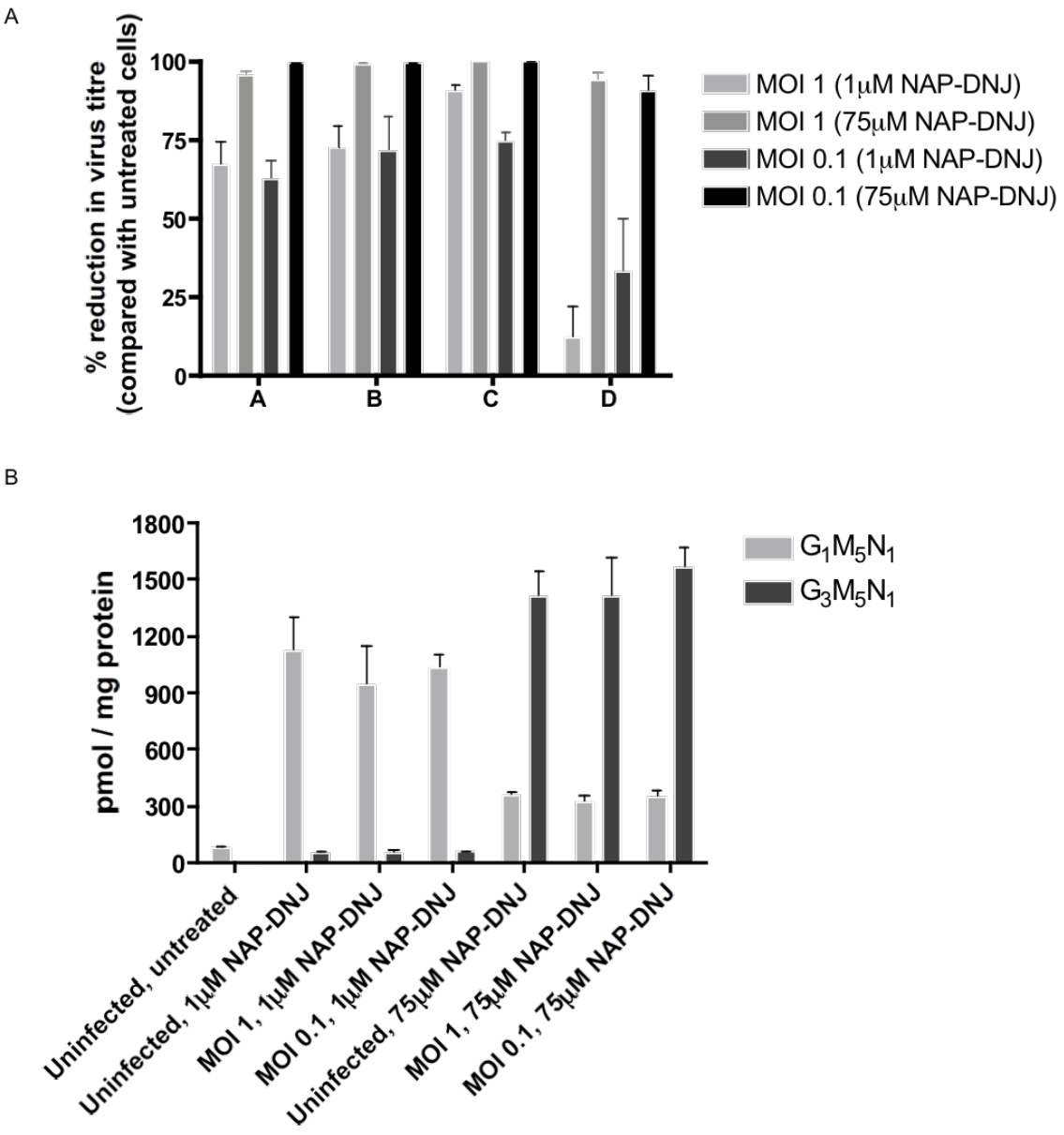

Figure 3.3 Sustained α-glucosidase II inhibition led to reduced virus titre, whilst inhibition of both α-glucosidases results in a more pronounced anti-viral response.

MDBK cells were incubated with or without BVDV infection at MOI of 1 or 0.1 for 4h (A) or 1h (B) and treated with 1μM or 75μM NAP-DNJ either post-infection (A) or at the time of infection (B). MDBK cells were pre-treated with 1μM or 75μM NAP-DNJ for 24h before

BVDV infection at MOI 1 or 0.1 for 1h. Cells were either treated with 1μM or 75μM NAP-DNJ at the time of infection (C) or remained untreated (D). Twenty-four hours post-infection, spent medium harvested was subjected to serial dilution and used to inoculate naïve cells for 24h. The cells were fixed and probed with a monoclonal antibody against the BVDV NS2 and NS3 proteins, followed by incubation with an anti-mouse FITC-conjugated secondary antibody whilst cell nuclei were stained with DAPI. Virus titre was determined based on the number of fluorescent focus units with each treatment and percentage reduction of virus titre was calculated relative to untreated control. The data were obtained from three experiments with standard deviation shown. Production of monoglucosylated FOS ($Glc_1Man_5GlcNAc_1$) and triglucosylated FOS ($Glc_3Man_5GlcNAc_1$) in the presence of 1μM or 75μM NAP-DNJ for 48 h. FOS were separated using NP-HPLC and peak areas corresponding to mono- and tri-glucosylated oligosaccharides, normalised to protein concentration. The data were obtained from three experiments with standard deviation shown (E).

The three-fold decrease in BVDV RNA copies (Figure 3.3B) and >60% decrease in secreted virion progeny (Figure 3.3A, Treatment A) following 1μM NAP-DNJ treatment indicated that the exclusive inhibition of α-glucosidase II significantly disrupted viral glycoprotein processing leading to a reduction in virus titre. To determine whether this anti-viral effect could be enhanced by prolonged treatment with 1μM NAP-DNJ, MDBK cells were treated with 1μM NAP-DNJ 1h post-infection for 24h. The virus titre of the culture supernatant was then determined by fluorescent antibody detection assay. Following 24h of 1μM NAP-DNJ

treatment post BVDV infection, virus titre fell by >70% (Figure 3.3A, Treatment B), compared with ~100% reduction in viral infectivity in the progeny virus was observed following inhibition of both α-glucosidases at 75μM NAP-DNJ (Figure 3.3A, Treatment B).

MDBK cells were also pre-treated with NAP-DNJ for 24h prior to BVDV infection in order to determine whether the compound was capable of conferring a protective effect on naïve cells. Pre-treatment with 1μM NAP-DNJ 24h before and during infection resulted in an 80% reduction in secreted progeny compared with untreated cells (Figure 3.3A, Treatment C). This pre-treatment with 1μM NAP-DNJ and hence inhibition of α-glucosidase II prior to infection, resulted in protection against BVDV. Pre-treatment with 1μM NAP-DNJ 24h before infection and no drug treatment thereafter also resulted in a significant drop in virus titre (Figure 3.3A, Treatment D). Analysis of the FOS in treatment D samples confirmed that α-glucosidase II inhibition was maintained throughout the 48h incubation period. No difference in FOS profiles was obtained when infected and non-infected cells were analyzed (Figure 3.3B). Altogether, the data indicated that inhibition of α-glucosidase II at 1μM NAP-DNJ significantly protects against BVDV infection.

3.3.6 NAP-DNJ-mediated inhibition of ER α-glucosidases alters the glycosylation of intra-cellular BVDV envelope glycoproteins

To determine that NAP-DNJ affected the biogenesis of viral glycoproteins within host cells, infected cells treated with or without NAP-DNJ were lysed and the lysates were subjected to western blotting using anti-BVDV E2 MAb214. Figure 3.4A shows a decreased production of intra-cellular viral glycoproteins, both monomers and dimers, in a concentration-dependent manner. Taken together, the reduction in intra- and extra-cellular viral glycoproteins, viral RNA copies and infectious titre suggest that NAP-DNJ mediated inhibition of both α-glucosidases resulted in a reduced synthesis of viral glycoproteins, decreasing the amount of pre-budding complexes available to be assembled and packaged into infectious progeny virions.

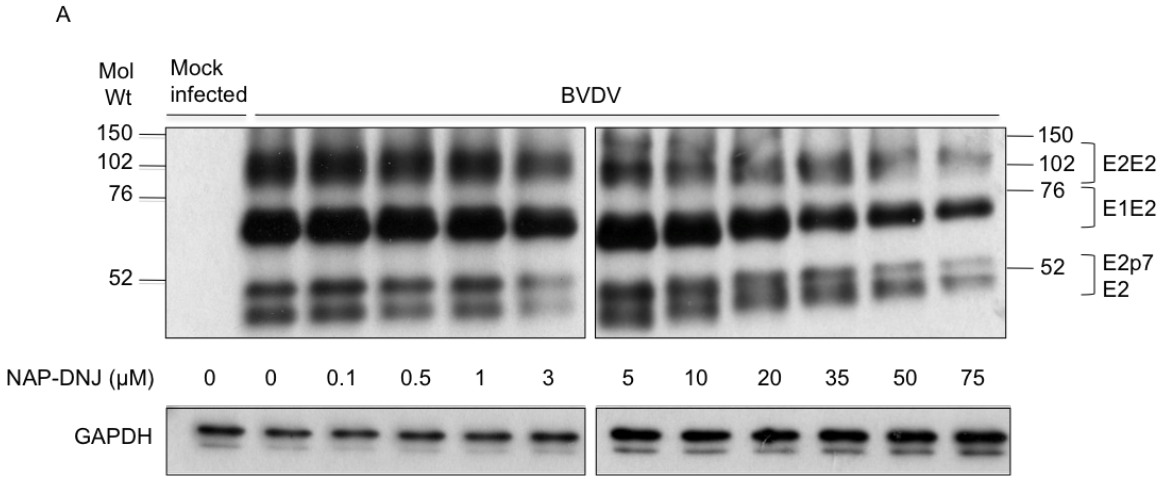

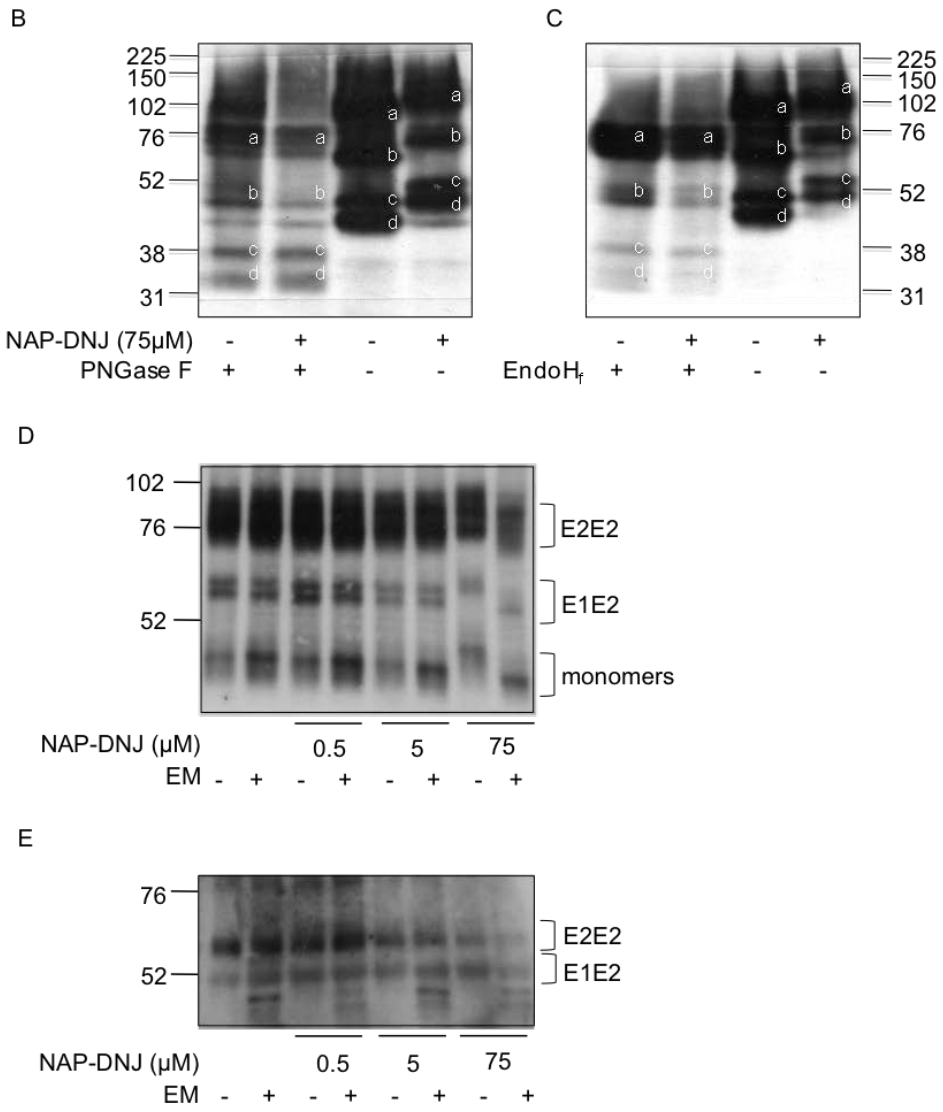

Figure 3.4 Glycan composition of BVDV E2 glycoprotein following NAP-DNJ treatment. MDBK cells were either infected with BVDV or mock-infected at an MOI of 1 and grown in the absence or presence of NAP-DNJ at the concentrations indicated. Twenty-four hours p.i., the cells were lysed. Assembly of the viral proteins was analyzed by SDS–12% PAGE followed by western blotting using MAb 214. GAPDH was detected on the same membrane as a loading control (A). The same lysates were separately prepared following treatment with or without NAP-DNJ and subjected to treatment with PNGase F (B) or Endo

H_f (C) or with recombinant human endomannosidase catalytic fragment (D) respectively at 37°C for 24h. Spent medium was also subjected to treatment with recombinant human endomannosidase catalytic fragment (E) at 37°C for 24h. Water (B), (C) or PBS (D), (E) was used in place of the enzymes to serve as negative controls. The viral proteins were analyzed by SDS–12% (B), (C) or SDS–7.5% (D), (E) PAGE followed by western blotting using MAb 214. The viral proteins were labelled as such: E2-E2 homodimers (a), E1-E2 heterodimers (b), E2-p7 (c) and E2 (d).

There was also an upward band shift trend in all E2-associated viral proteins from 3μM NAP-DNJ to 75μM NAP-DNJ (Figure 3.4A), the concentration range of NAP-DNJ at which inhibition of ER α-glucosidase I occurred (Figure 3.2A). In order to determine whether the observed reduced electrophoretic mobility of the intra-cellular BVDV envelope glycoproteins in NAP-DNJ treated cells was due to alterations in carbohydrate modifications, lysates of BVDV-infected cells treated with or without 75μM NAP-DNJ were digested with PNGase F digestions then analysed by western blot. Following PNGase F digest, all E2-associated bands in both NAP-DNJ treated and untreated cell lysates exhibited decreased molecular weights and migrated to the same molecular weight (Figure 3.4B). The apparent molecular weight of E2E2 homodimers and E1E2 heterodimers were reduced by approximately 16kDa and 12kDa respectively, following PNGase F digestion. Glycoproteins E1 and E2 have 2 and 4 potential N-glycosylation sites respectively (*27*), therefore E2E2 homodimers have a total of 8 potential N-glycosylation sites, whilst E1E2 heterodimers have 6. In a previous study using chimeric BVDV E2 and VSV G proteins, the BVDV E2 protein

was reported to contain only oligomannose side chains and to be free of complex N-glycans (*28*). Given that the molecular weight of a fully mannosylated N-linked glycan such as $Man_9GlcNAc_2$ (M_9N_2) is approximately 1.9kDa, the total molecular weight of the glycans on E1E2 would therefore be close to 12kDa and that on E2E2 would be about 16kDa if all the potential N-glycosylation sites were occupied. These data suggest that N-linked glycans of these viral glycoproteins are oligomannose and that most or all of the sites are occupied. To confirm that the intracellular viral glycoproteins were not complex-type N-linked oligosaccharides, lysates of BVDV-infected cells treated with or without 75μM NAP-DNJ were digested with Endo-H_f, followed by western blot analysis using MAb214. The electrophoretic mobilities of the BVDV glycoproteins increased significantly following Endo-H_f digestion (Figure 3.4C), confirming that the glycans on the surface of the E2-associated proteins were not complex-type oligosaccharides but oligomannose-type. The molecular weight change was consistent with the PNGase F digest.

To find out whether the N-linked glycans of intra-cellular BVDV glycoproteins contain glucosylated species (*29*), (*30*), was incubated with the lysates from NAP-DNJ treated BVDV-infected cells were incubated with recombinant human endo-alpha-1,2-mannosidase (EM). Following EM digestion, the intra-cellular viral proteins in 75μM NAP-DNJ treated cells migrated with the same molecular weight as the untreated control (Figure 3.4D), thus indicating the presence of glucosylated oligosaccharides on intra-cellular BVDV glycoproteins following treatment with 75μM NAP-DNJ. However, E1E2 heterodimers and E2E2 homodimers on the surface of secreted virions in the culture supernatant of NAP-DNJ treated and untreated samples migrated with the same relative molecular weight before and

after EM treatment (Figure 3.4E). These data indicate that secreted virions detected in the culture supernatant of NAP-DNJ treated BVDV-infected cells had escaped α-glucosidase inhibition and had therefore retained an unmodified N-linked oligomannose composition.

3.3.7 Anti-viral efficacy of *N*-9-methoxynonyl-DNJ (UV4)

UV4 is a DNJ-derived compound in which an oxygen atom is present at the terminus of the alkyl side chain, previously shown to exhibit excellent, low micromolar (IC_{50} of 3μM) anti-viral activity against BVDV and HBV (*31*). In order to compare the α-glucosidase inhibitory potency and anti-viral efficacy between UV4 and NAP-DNJ, FOS analyses and infectivity assays were similarly carried out on UV4 treated BVDV-infected cells.

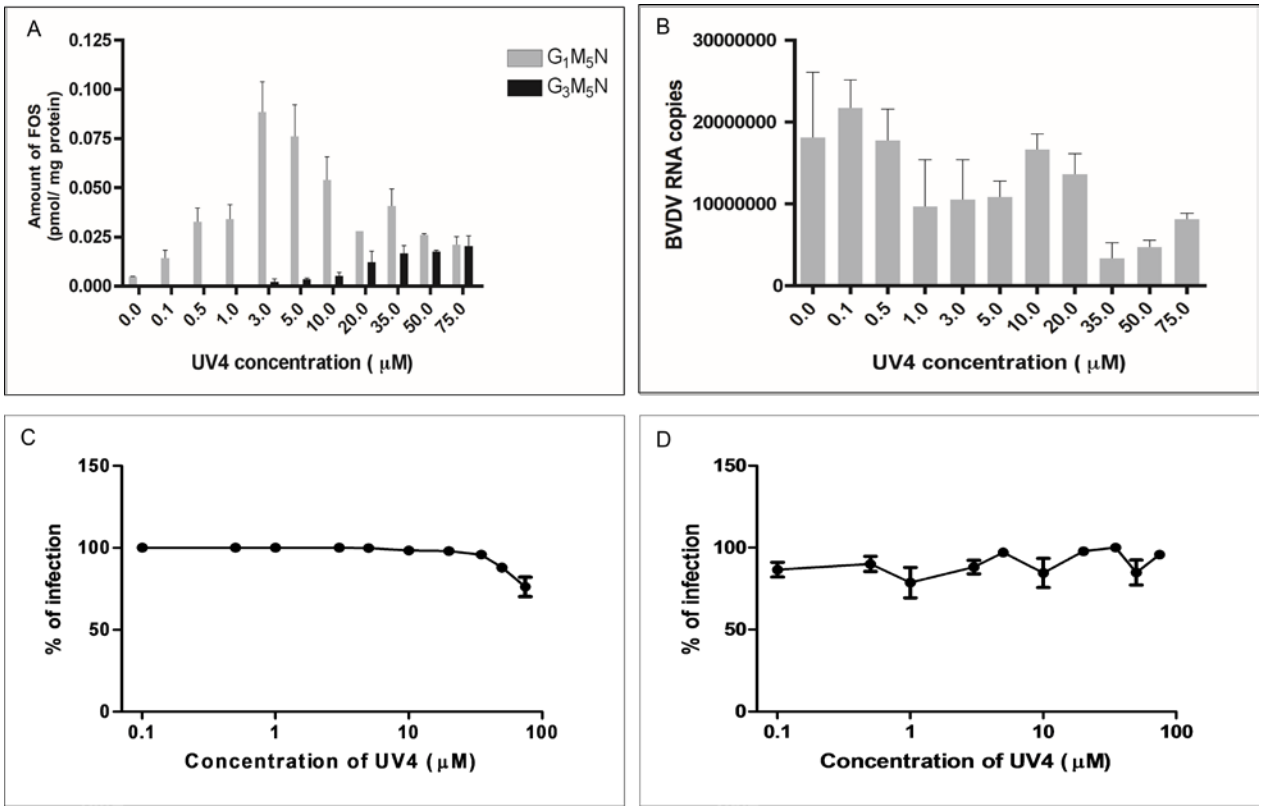

Figure 3.5 UV4 is a less potent anti-viral compound against BVDV compared to NAP-DNJ.

MDBK cells infected with BVDV at MOI 1 were incubated with different concentrations of UV4 for 24h. Cell lysates harvested were subjected to FOS analysis (A) and the culture supernatant subjected to RT-PCR (B). Culture supernatant was either used to directly

inoculate naïve MDBK cells for 24h (C) or normalised to the same RNA copy number as the sample treated with 75μM UV4 before inoculating naïve MDBK cells for 24h (D). The cells were fixed and probed with a monoclonal antibody against the BVDV NS2 and NS3 proteins, followed by incubation with an anti-mouse FITC-conjugated secondary antibody whilst cell nuclei were stained with DAPI. The number of infected cells was expressed as a percentage of total number of cells.

Like NAP-DNJ, UV4 inhibits the activity of both α-glucosidases I and II, although the inhibition of α-glucosidase I occurs at a higher concentration of 3μM (Figure 3.5A), relative to 1μM with NAP-DNJ (Figure 3.2A). The FOS profiles obtained for both BVDV-infected and uninfected samples were identical (data not shown). There was a two-fold reduction of viral RNA copies at 1μM UV4 (Figure 3.5B) compared to a larger three-fold decrease at the same concentration with NAP-DNJ (Figure 3.2B). The drop in infectivity levels for UV4 begins at a much higher concentration of 35μM (Figure 3.5C) relative to 0.1μM NAP-DNJ, following first round of re-infection (Figure 3.2C). There was no detectable reduction in infectivity even at 75μM UV4 (Figure 3.5D), whilst infectivity dropped by ~50% at the same concentration with NAP-DNJ following second round re-infection (Figure 3.2D). Taken together, these data indicate that NAP-DNJ is a considerably more potent α-glucosidase inhibitor compared to UV4.

The decrease in viral RNA copies (Figure 3.5B) coincides with the inhibition of α-glucosidase II and continues to perpetuate when both α-glucosidases were inhibited at higher UV4 concentrations (>3μM) (Figure 3.5A), corroborating with earlier findings that the exclusive α-glucosidase II inhibition could be sufficient to hinder viral RNA secretion.

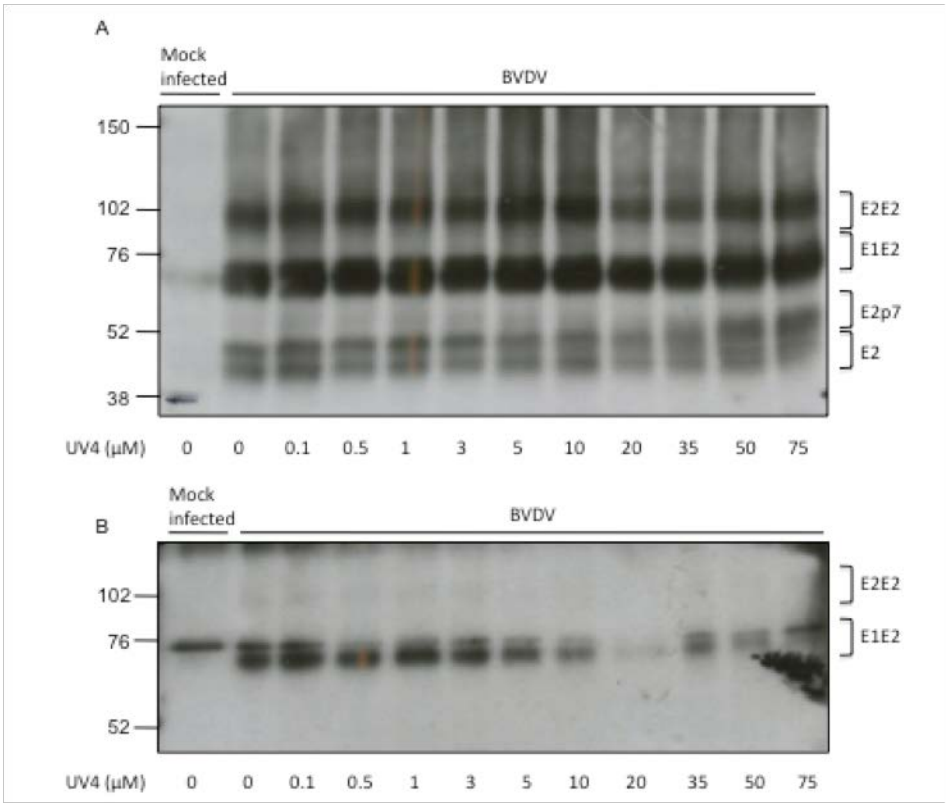

Figure 3.6 Anti-viral effect of UV4 against BVDV.

MDBK cells were either mock-infected or infected with BVDV at MOI 1, followed by incubation with different concentrations of UV4 for 24h. Cell lysates (A) and culture supernatant (B) harvested were subjected to western blotting using MAb214 to probe for BVDV E2 protein.

To find out whether the inhibition of ER α-glucosidases resulted in a decreased production of BVDV envelope glycoproteins, western blot analyses were performed on cell lysates and culture supernatant harvested from UV4-treated BVDV-infected cells. No significant concentration-dependent reduction in E2-associated proteins was detected (Figure 3.6A). However, a suitable loading control should have been carried out to further verify this. There was an upward band shift trend in all E2-associated proteins at UV4 concentrations ≥35μM (Figure 3.6A), which coincides with the drop in viral infectivity (Figure 3.5C). A concentration-dependent decrease in E1E2 heterodimer production was detected in the culture supernatant, and surprisingly, the E2E2 homodimers were barely detectable (Figure 3.6B).

3.4 DISCUSSION

DNJ and its derivatives have been shown to demonstrate anti-viral activity and hence therapeutic ability for treating several members of the Flaviviridae family including BVDV, an important veterinary pathogen that results in large annual losses in the cattle industry (*8*), (*11*). DNJ-based iminosugars reversibly compete with glucose substrates for the active sites of ER α-glucosidases I and II, arresting the morphogenesis of viral glycoproteins at various stages in the N-glycosylation pathway and hindering their assembly into pre-budding complexes (*34*), (*35*). The disruption to folding, maturation and assembly of viral envelope glycoproteins E1E2, primarily responsible for attachment to mammalian host cells, therefore leads to decreased virion release and infectivity (*36*). Perturbation of protein folding affects viruses to a larger extent than mammalian host proteins due to the critical reliance of the viruses on the glucosidase-mediated glycosylation process in the mammalian host (*11*). The emergence of glucosidase inhibitor-resistant mutants is therefore highly improbable.

NAP-DNJ is an iminosugar that demonstrates a more potent inhibitory activity against ER α-glucosidases I and II, both *in vitro* and in cells, relative to the previously reported anti-BVDV iminosugar, *N*B-DNJ (*17*), (*16*). In this study, <1μM NAP-DNJ was required to reduce virus titre by 50%, compared to 150 ± 50μM *N*B-DNJ to achieve the same anti-viral effect in BVDV-infected MDBK cells (*7*), confirming that NAP-DNJ is a more potent α-

glucosidase inhibitor and anti-viral compound compared to *N*B-DNJ.

The sharp decline in viral infectivity and RNA copies, and the decreased generation of BVDV glycoproteins following NAP-DNJ treatment showed that the compound was capable of breaching viral biogenesis and reducing the assembly of pre-budding complexes and packaging of viral proteins in infected host cells. However, the minor population (10-15% relative to untreated cells) of virus in the culture media of NAP-DNJ treated cells seem to have escaped the α-glucosidase block, since the progeny virus retained their infectious capability to establish entry, infection and replication in naïve mammalian cells, and continued to spread to neighbouring cells forming infectious foci in the absence of NAP-DNJ. Pre-treating the mammalian cells with NAP-DNJ before virus challenge was akin to prophylactic treatment and results have shown that the pre-treatment had conferred some form of protective effect against viral infection through α-glucosidase inhibition. Further to this, NAP-DNJ present at the time of infection conferred protective effect upon the 90% of cells that were not infected at MOI 0.1. These cells were therefore effectively pre-treated prior to infection. The >80% and close to 100% reduction in virus titre seen with pre-treatment at 1μM NAP-DNJ and 75μM NAP-DNJ respectively and sustained treatment during and after virus challenge was clearly the most effective anti-viral treatment amongst the four tested (Figure 3.3A). The anti-viral efficacy of NAP-DNJ against HCV, another member of the Flaviviridae known to share molecular and virological features with BVDV (*37*), (*38*), remains to be examined. Nevertheless, these findings have highlighted the promising utility of NAP-DNJ as a prophylactic treatment for BVDV and possibly also for HCV. Since recurrence of HCV infection post-liver transplantation is frequent,

compromising patient and graft survival, the promising utility of NAP-DNJ as a potent drug to protect transplant patients could be explored (*39*), (*40*), (*41*).

The sensitivity of BVDV to α-glucosidase inhibitors (*11*), together with improved potency by NAP-DNJ, where discrimination between α-glucosidase I and II activities can be followed with precision, allows further mechanistic studies of iminosugars and their anti-viral properties. Based on this unique α-glucosidase inhibitory property of NAP-DNJ, the findings in this study have demonstrated that the exclusive inhibition of α-glucosidase II significantly reduced amount of secreted virions, although this anti-viral response was even more pronounced with the inhibition of both α-glucosidases. These findings therefore highlight the importance of targeting the enzymatic activity of both α-glucosidases in order to impair viral biogenesis to a greater extent.

In order to further address the anti-viral effect of glucosidase II inhibition, an α-glucosidase inhibitor capable of exclusively inhibiting glucosidase II activity is required. To date, NAP-DNJ is the only α-glucosidase inhibitor that has been shown to discriminate between α-glucosidase I and II inhibition at the cellular level. Alternatively, siRNA designed against α-glucosidase II could be used to abrogate the expression of glucosidase II but achieving a complete knock-out of the enzyme will be challenging. The combined usage of low

concentrations of NAP-DNJ and siRNA against α-glucosidase II may facilitate a more complete inhibition of glucosidase II activity in cells.

Longer alkyl chain DNJ derivatives, such as *N*N-DNJ, have an additional p7 inhibitory effect in HCV other than ER α-glucosidase inhibition (*42*). It is not known whether NAP-DNJ exerts its anti-viral effects through p7 inhibition, in addition to ER α-glucosidase inhibition, given that it also has a relatively long alkyl linker comprising of a 6-carbon chain. Replacing the DNJ head group with a DGJ head group could be analysed for an anti-viral effect in addition to channel activity assays *in vitro* (*43*), (*44*). It was envisaged that the increased hydrophobicity of *N*N-DNJ, facilitates its uptake into intracellular membranes, providing prolonged retention within the intracellular environment (*11*) and improved potency for inhibition of ER α-glucosidases in cells (*23*). Increased hydrophobicity however, causes an increase in cytotoxicity (*25*), therefore highlighting the challenge in developing more potent and less toxic α-glucosidase inhibitors. Nonetheless the inhibitory potency of NAP-DNJ is not due to greater uptake or ER penetration. It has been hypothesized that the greater inhibitor binding energy contributed by the aryl nitro and azido moieties facilitates the formation of more stable inhibitor-enzyme complexes through stronger binding affinity at the auxiliary site of the enzyme, rendering the enzyme inactive (*23*), (*17*). This interaction is made more favourable by the slower hydrolysis of mono-glucosylated glycans by α-glucosidase II (*21*). Findings from this chapter have shown that NAP-DNJ is a more potent anti-viral compound against BVDV than UV4. The incorporation of an oxygen atom in the alkyl chain of UV4 most likely conferred a more hydrophilic nature to the compound relative to NAP-DNJ, most likely making the former less capable than the latter in targeting both α-

glucosidases in the ER. It will most likely require a higher concentration than 75μM of UV4 to inhibit both α-glucosidases. UV4 is therefore also capable of exhibiting anti-viral activity even though it is a weaker anti-viral compound than NAP-DNJ.

Our data also suggests that intra-cellular viral proteins consist of a mixed population of native and misfolded surface glycoproteins at higher concentrations of iminosugars, concurring with the observations made in an earlier study (*16*).

Based on our FOS results (Figure 3.2A), the following could be a likely scenario that requires further investigations. The binding sites on calnexin are saturated with bound mono-glucosylated proteins following exclusive glucosidase II inhibition at NAP-DNJ concentrations lower than 1μM, depriving the remaining pool circulating between the ER and Golgi of interaction with calnexin to assume their native conformations. However, a small proportion of properly folded calnexin-bound viral proteins eventually dissociate as a result of cleavage of the terminal glucose residue by any remaining α-glucosidase II that had escaped NAP-DNJ binding. As a result, the surface glycans of only this small population of properly folded viral proteins were trimmed further to an oligomannose structure and eventually packaged into complete viral particles to be secreted, explaining the sharp three-fold decrease in viral RNA copy numbers and reduced titre of progeny virus relative to untreated control. At higher NAP-DNJ concentrations, the prevalence of α-glucosidase I inhibition, in addition to α-glucosidase II inhibition, led to an increased number of viral glycoproteins assuming the tri-glucosylated glycoform (Figure 3.2A), reducing the amount of

mono-glucosylated proteins available to bind calnexin for proper folding. The perturbation of calnexin-glycoprotein interactions therefore curtailed the formation of disulphide bonds both within and between the viral envelope glycoproteins E1 and E2, interrupting the folding and biogenesis of pre-budding complexes available for virion assembly, reducing the overall production of mature virions.

Since anti-BVDV E1 antibodies are currently not commercially available, it is difficult to directly analyse changes to BVDV E1 glycoprotein following treatment with NAP-DNJ. The isolation and purification of BVDV envelope glycoproteins would allow the direct analysis of glycan compositions on these viral proteins. The precise identities of all E2-associated bands in our western blots in this chapter corroborate with those in a previous study (*16*).

This study not only highlights the importance of NAP-DNJ as a potent anti-viral compound, but also presents itself as a powerful tool to elucidate the anti-viral mechanism employed by DNJ-derived compounds. The significant reduction of virus titre following exclusive α-glucosidase II inhibition highlights the demonstration of a sustained anti-viral response, without the exigency to subscribe to higher NAP-DNJ concentrations. In this regards, the direct administration or pre-treatment with sub-micromolar concentrations of host factor-targeting iminosugars such as NAP-DNJ over an extensive period of time could therefore serve as an effective complementary therapeutic approach in targeting viral escape mutants following treatment with the current ensemble of anti-viral compounds that directly target viruses.

This comprehensive mechanistic study of NAP-DNJ has not only provided insight into the replicative cycle of flaviviruses but also established the groundwork for future developments of iminosugars with improved anti-viral capability and cytotoxicity profiles.

3.5 REFERENCES

1. Bergeron, J. J., Brenner, M. B., Thomas, D. Y., and Williams, D. B. (1994) Calnexin: a membrane-bound chaperone of the endoplasmic reticulum., *Trends in biochemical sciences 19*, 124-8.

2. Peterson, J. R., Ora, A., Van, P. N., and Helenius, A. (1995) Transient, lectin-like association of calreticulin with folding intermediates of cellular and viral glycoproteins., *Molecular biology of the cell 6*, 1173-84.

3. Miller, R. H., and Purcell, R. H. (1990) Hepatitis C virus shares amino acid sequence similarity with pestiviruses and flaviviruses as well as members of two plant virus supergroups., *Proceedings of the National Academy of Sciences of the United States of America 87*, 2057-61.

4. Houghton, P. J. (1996) Compounds with anti-HIV activity from plants., *Transactions of the Royal Society of Tropical Medicine and Hygiene 90*, 601-4.

5. Sessions, O. M., Barrows, N. J., Souza-Neto, J. a, Robinson, T. J., Hershey, C. L., Rodgers, M. a, Ramirez, J. L., Dimopoulos, G., Yang, P. L., Pearson, J. L., and Garcia-Blanco, M. a. (2009) Discovery of insect and human dengue virus host factors., *Nature*, Nature Publishing Group *458*, 1047-50.

6. Jordan, R., Nikolaeva, O. V., Wang, L., Conyers, B., Mehta, A., Dwek, R. a, and Block, T. M. (2002) Inhibition of host ER glucosidase activity prevents Golgi processing of virion-associated bovine viral diarrhea virus E2 glycoproteins and reduces infectivity of secreted virions., *Virology 295*, 10-9.

7. Durantel, D., Branza-nichita, N., Carroue, S., Butters, T. D., Dwek, R. A., and Zitzmann, N. (2001) Study of the Mechanism of Antiviral Action of Iminosugar Derivatives against Bovine Viral Diarrhea Virus, *Journal of virology 75*, 8987-8998.

8. Block, T. M., Lu, X., Platt, F. M., Foster, G. R., Gerlich, W. H., Blumberg, B. S., and Dwek, R. a. (1994) Secretion of human hepatitis B virus is inhibited by the imino sugar N-butyldeoxynojirimycin., *Proceedings of the National Academy of Sciences of the United States of America 91*, 2235-9.

9. Dwek, R. a, Butters, T. D., Platt, F. M., and Zitzmann, N. (2002) Targeting Glycosylation As a Therapeutic Approach, *Nature Reviews Drug Discovery 1*, 65-75.

10. Block, T. M., Lu, X., Mehta, A. S., Blumberg, B. S., Tennant, B., Ebling, M., Korba, B., Lansky, D. M., Jacob, G. S., and Dwek, R. A. (1998) Treatment of chronic hepadnavirus infection in a woodchuck animal model with an inhibitor of protein folding and trafficking., *Nature medicine 4*, 610-4.

11. Zitzmann, N., Mehta, a S., Carrouée, S., Butters, T. D., Platt, F. M., McCauley, J., Blumberg, B. S., Dwek, R. a, and Block, T. M. (1999) Imino sugars inhibit the formation and secretion of bovine viral diarrhea virus, a pestivirus model of hepatitis C virus: implications for the development of broad spectrum anti-hepatitis virus agents., *Proceedings of the National Academy of Sciences of the United States of America 96*, 11878-82.

12. Durantel, D., Carroue, S., Branza-nichita, N., Dwek, R. A., and Zitzmann, N. (2004) Effects of Interferon , Ribavirin , and Iminosugar Derivatives on Cells Persistently Infected with Noncytopathic Bovine Viral Diarrhea Virus, *Journal of virology 48*, 497-504.

13. Rice, C. (1996) Flaviviridae: the viruses and their replication (B. N. Fields, D. M. Knipe, P. M. Howley, et al, Ed.) Fields vir., pp 931-959, Lippincott-Raven Publishers, Philadelphia, Pa.

14. Thiel, H. J., Stark, R., Weiland, E., Rümenapf, T., and Meyers, G. (1991) Hog cholera virus: molecular composition of virions from a pestivirus., *Journal of virology 65*, 4705-12.

15. Weiland, E., Stark, R., Haas, B., Rümenapf, T., Meyers, G., and Thiel, H. J. (1990) Pestivirus glycoprotein which induces neutralizing antibodies forms part of a disulfide-linked heterodimer., *Journal of virology 64*, 3563-9.

16. Branza-nichita, N., Durantel, D., Carroue, S., Dwek, R. A., and Zitzmann, N. (2001) Antiviral Effect of N-Butyldeoxynojirimycin against Bovine Viral Diarrhea Virus Correlates with Misfolding of E2 Envelope Proteins and Impairment of Their Association into, *Society 75*, 3527-3536.

17. Rawlings, A. J., Lomas, H., Pilling, A. W., Lee, M. J.-R., Alonzi, D. S., Rountree, J. S. S., Jenkinson, S. F., Fleet, G. W. J., Dwek, R. a, Jones, J. H., and Butters, T. D. (2009) Synthesis and biological characterisation of novel N-alkyl-deoxynojirimycin alpha-glucosidase inhibitors., *Chembiochem : a European journal of chemical biology 10*, 1101-5.

18. Butters, T. D., van den Broek, L. A. G. M., Fleet, G. W. J., Krulle, T. M., Wormald, M. R., Dwek, R. A., and Platt, F. M. (2000) Molecular requirements of imino sugars for the selective control of N-linked glycosylation and glycosphingolipid biosynthesis, *Tetrahedron:Asymmetry 11*, 113-124.

19. Karlsson, G. B., Butters, T. D., Dwek, R. a, and Platt, F. M. (1993) Effects of the imino sugar N-butyldeoxynojirimycin on the N-glycosylation of recombinant gp120., *The Journal of biological chemistry 268*, 570-6.

20. Olafson, R. W., Thomas, J. R., Ferguson, M. A., Dwek, R. A., Chaudhuri, M., Chang, K. P., and Rademacher, T. W. (1990) Structures of the N-linked oligosaccharides of Gp63, the major surface glycoprotein, from Leishmania mexicana amazonensis., *The Journal of biological chemistry 265*, 12240-7.

21. Alonzi, D. S., Neville, D. C. a, Lachmann, R. H., Dwek, R. a, and Butters, T. D. (2008) Glucosylated free oligosaccharides are biomarkers of endoplasmic- reticulum alpha-glucosidase inhibition., *The Biochemical journal 409*, 571-80.

22. Neville, D. C. A., Coquard, V., Priestman, D. A., Vruchte, D. J. M. te, Sillence, D. J., Dwek, R. A., Platt, F. M., and Butters, T. D. (2004) Analysis of fluorescently labeled glycosphingolipid-derived oligosaccharides following ceramide glycanase digestion and anthranilic acid labeling., *Analytical biochemistry 331*, 275-82.

23. Alonzi, D. S., Dwek, R. a, and Butters, T. D. (2009) Improved cellular inhibitors for glycoprotein processing α-glucosidases: biological characterisation of alkyl- and arylalkyl-N-substituted deoxynojirimycins, *Tetrahedron: Asymmetry*, Elsevier Ltd *20*, 897-901.

24. Kukushkin, N. V., Alonzi, D. S., Dwek, R. A., and D, T. (2011) Ac ce pte d Ac ce pte d Ma, *Water*.

25. Mellor, H. R., Neville, D. C. a, Harvey, D. J., Platt, F. M., Dwek, R. a, and Butters, T. D. (2004) Cellular effects of deoxynojirimycin analogues: inhibition of N-linked oligosaccharide processing and generation of free glucosylated oligosaccharides., *The Biochemical journal 381*, 867-75.

26. Payne, A. F., Binduga-Gajewska, I., Kauffman, E. B., and Kramer, L. D. (2006) Quantitation of flaviviruses by fluorescent focus assay., *Journal of virological methods 134*, 183-9.

27. Dubuisson, J., and Rice, C. M. (1996) Hepatitis C virus glycoprotein folding: disulfide bond formation and association with calnexin., *Journal of virology 70*, 778-86.

28. Köhl, W., Zimmer, G., Greiser-Wilke, I., Haas, L., Moennig, V., and Herrler, G. (2004) The surface glycoprotein E2 of bovine viral diarrhoea virus contains an intracellular localization signal., *The Journal of general virology 85*, 1101-11.

29. Lubas, W. A., and Spiro, R. G. (1987) Golgi endo-alpha-D-mannosidase from rat liver, a novel N-linked carbohydrate unit processing enzyme., *The Journal of biological chemistry 262*, 3775-81.

30. Lubas, W. A., and Spiro, R. G. (1988) Evaluation of the role of rat liver Golgi endo-alpha-D-mannosidase in processing N-linked oligosaccharides., *The Journal of biological chemistry 263*, 3990-8.

31. Mehta, A., Ouzounov, S., Jordan, R., Simsek, E., Lu, X., Moriarty, R. M., Jacob, G., Dwek, R. a, and Block, T. M. (2002) Imino sugars that are less toxic but more potent as antivirals, in vitro, compared with N-n-nonyl DNJ., *Antiviral chemistry & chemotherapy 13*, 299-304.

32. Choukhi, a, Ung, S., Wychowski, C., and Dubuisson, J. (1998) Involvement of endoplasmic reticulum chaperones in the folding of hepatitis C virus glycoproteins., *Journal of virology 72*, 3851-8.

33. Ora, A., and Helenius, A. (1995) Calnexin fails to associate with substrate proteins in glucosidase-deficient cell lines., *The Journal of biological chemistry 270*, 26060-2.

34. Parodi, A. J. (2000) Role of N-oligosaccharide endoplasmic reticulum processing reactions in glycoprotein folding and degradation., *The Biochemical journal 348 Pt 1*, 1-13.

35. Parodi, A. J. (2000) Protein glucosylation and its role in protein folding., *Annual review of biochemistry 69*, 69-93.

36. Chapel, C., Garcia, C., Bartosch, B., Roingeard, P., Zitzmann, N., Cosset, F.-L., Dubuisson, J., Dwek, R. a, Trépo, C., Zoulim, F., and Durantel, D. (2007) Reduction of the infectivity of hepatitis C virus pseudoparticles by incorporation of misfolded

glycoproteins induced by glucosidase inhibitors., *The Journal of general virology 88*, 1133-43.

37. Buckwold, V. E., Beer, B. E., and Donis, R. O. (2003) Bovine viral diarrhea virus as a surrogate model of hepatitis C virus for the evaluation of antiviral agents., *Antiviral research 60*, 1-15.

38. Buckwold, V. E., Wei, J., Wenzel-Mathers, M., and Russell, J. (2003) Synergistic in vitro interactions between alpha interferon and ribavirin against bovine viral diarrhea virus and yellow fever virus as surrogate models of hepatitis C virus replication., *Antimicrobial agents and chemotherapy 47*, 2293-8.

39. Arjal, R. R., Burton, J. R., Villamil, F., and Rosen, H. R. (2007) Review article: the treatment of hepatitis C virus recurrence after liver transplantation., *Alimentary pharmacology & therapeutics 26*, 127-40.

40. Fabrizi, F., Lunghi, G., Dixit, V., and Martin, P. (2006) Meta-analysis: anti-viral therapy of hepatitis C virus-related liver disease in renal transplant patients., *Alimentary pharmacology & therapeutics 24*, 1413-22.

41. Guillouche, P., and Féray, C. (2011) Systematic review: anti-viral therapy of recurrent hepatitis C after liver transplantation., *Alimentary pharmacology & therapeutics 33*, 163-74.

42. Steinmann, E., Whitfield, T., Kallis, S., Dwek, R. a, Zitzmann, N., Pietschmann, T., and Bartenschlager, R. (2007) Antiviral effects of amantadine and iminosugar derivatives against hepatitis C virus., *Hepatology (Baltimore, Md.) 46*, 330-8.

43. Luik, P., Chew, C., Aittoniemi, J., Chang, J., Wentworth, P., Dwek, R. A., Biggin, P. C., Vénien-Bryan, C., and Zitzmann, N. (2009) The 3-dimensional structure of a hepatitis C virus p7 ion channel by electron microscopy., *Proceedings of the National Academy of Sciences of the United States of America 106*, 12712-6.

44. Pavlović, D., Neville, D. C. a, Argaud, O., Blumberg, B., Dwek, R. a, Fischer, W. B., and Zitzmann, N. (2003) The hepatitis C virus p7 protein forms an ion channel that is inhibited by long-alkyl-chain iminosugar derivatives., *Proceedings of the National Academy of Sciences of the United States of America 100*, 6104-8.

CHAPTER 4

GLYCAN ANALYSIS OF BVDV ENVELOPE GLYCOPROTEINS

4.1 INTRODUCTION

Enveloped viruses may contain one or more types of integral membrane proteins, and a majority of them are modified by the addition of *N*-linked glycans (*1*). *N*-linked glycosylation of viral glycoproteins contributes to a diverse set of functions such as receptor binding, mediation of membrane fusion and penetration into cells, directing virus morphogenesis at the budding site (*2*) and masking important functional domains from the immune system to attenuate viral immunogenicity. All *N*-linked oligosacchrides are essential for correct folding in some glycoproteins, for instance, the selective removal of *N*-linked glycosylation sites in the α heavy chain of immunoglobulin A results in degradation and reduced secretion (*3*). On the contrary, the elimination of the three *N*-linked glycosylation sites in the fusion protein of human respiratory syncytial virus did not affect the transport of the protein to the plasma membrane or proteolytic maturation, although fusion activity was affected (*4*).

BVDV NADL strain encodes three envelope glycoproteins, Erns, E1, and E2, which carry eight, two, and four potential N-glycosylation sites, respectively (*5*). E^{rns} has been reported to be dispensable for virus entry, whilst the formation of E1E2 heterodimers is essential (*6*). The BVDV E2 glycoprotein is a 53-kDa immunodominant protein of pestiviruses present on the surface of the mature virion (*7*), (*8*) and induces the production of neutralising antibodies in the host after infection or following immunization with live or killed vaccines (*9*), (*10*), (*11*), (*12*), (*13*). It forms a functional complex with the E1 glycoprotein via disulphide bonds, giving rise to E2E2 homodimers or E1E2 heterodimers (*14*), (*7*). Both E1 and E2 are membrane-anchored type I transmembrane proteins with an N-terminal ectodomain and a C-terminal hydrophobic anchor (*7*). BVDV entry into bovine cells is a multistep process involving attachment of

virions to cellular receptors, internalization, and membrane fusion. The E1E2 heterodimer has also been found to be the functional complex responsible for viral binding and entry (*15*), (*16*) and mutations at the N-linked glycosylation site of BVDV E2 affect this viral infection process (*17*).

In spite of the abundant studies reporting the anti-viral capability of α-glucosidase inhibitors such as iminosugars against BVDV infection, little is known about the effects of these inhibitors on their surface glycan structures of secreted progeny virions. For some viruses, virions secreted from infected cells that were treated with glucosidase inhibitors carried unprocessed or altered glycans on their envelope glycoproteins and exhibited reduced infectivity (*18*), (*19*). Intra-cellular BVDV E2 has previously been reported to contain only high-mannose oligosaccharide side-chains but no *N*-glycans of the complex type (*20*). The findings in the previous chapter corroborates with this. Based on the *in vitro* enzymatic digests on culture supernatant of NAP-DNJ treated BVDV-infected cells in the previous chapter, it was also found that the glycans on the surface of secreted virions are non-glucosylated whether or not α-glucosidase inhibition has been imposed in the mammalian host cells.

In this chapter, the isolation and purification of BVDV NADL E2 glycoprotein was attempted and changes to glycan composition on the surface of this protein was examined following NAP-DNJ treatment.

4.2 MATERIALS AND METHODS

4.2.1 Materials

AnalaR and HPLC grade solvents were from VWR International. PNGase F was purchased from New England Biolabs, UK. All other reagents were from Sigma.

4.2.2 Cells, virus and inhibitors

MDBK cells (European Collection of Animal Cell Cultures, Porton Down, United Kingdom) were grown in RPMI 1640 medium (GIBCO/BRL) supplemented with 10% BVDV-free fetal calf serum (PAA Laboratories, Teddington, United Kingdom), 2 mM L-glutamine, 50 units/ml penicillin and 50 μg/ml streptomycin (GIBCO) at 37°C in a humidified 5% CO_2 atmosphere. Cells were confirmed to be free of BVDV by reverse transcriptase-PCR (RT-PCR). Cytopathic BVDV-1-NADL (National Animal Disease Laboratory; American Type Culture Collection, Manassas, Va.) virus was provided by N. Zitzmann (University of Oxford). NAP-DNJ was synthesised as described in Chapter 2.

4.2.3 Antibodies

Monoclonal antibodies MAb214 raised against BVDV E2 glycoprotein was purchased from the Veterinary Laboratories Agency, Weybridge, United Kingdom.

4.2.4 Virus glycan analysis

MDBK cells were grown in T225 tissue culture flasks at 5.6 X 10^7 cells/ flask. For the immunopurification experiments, the cells were grown in IgG-depleted FCS supplemented RPMI medium. The cells were infected with cytopathic BVDV at a multiplicity of infection (MOI) of 1 FFU/cell, for 4h at 37ºC, 5% CO_2 atmosphere in RPMI medium supplemented with penicillin and streptomycin, but not with FCS. After the viral inoculum was removed, the cells were washed twice with phosphate-buffered saline (PBS) and treated with different concentrations of NAP-DNJ in FCS supplemented RPMI 1640 medium. At 24h p.i., the culture medium was harvested and clarified at 1300g for 10mins. The clarified supernatant was passed through a 0.22µm filter unit to remove cell debris.

4.2.4.1 Immunoprecipitation

Clarified culture supernatant harvested from NAP-DNJ treated, BVDV-infected MDBK cells was subjected to ultracentrifugation at 100 000g for 4h at 4ºC and the viral pellets obtained were resuspended in 100µl of 0.5% CHAPS in HSE buffer with a mixture of protease inhibitor cocktail (Sigma). To pre-clear the lysates, 200µl of protein G-Sepharose beads were added for 1h at 4°C. The lysates were then briefly centrifuged and the supernatants were incubated with MAb214 antibodies (diluted 1:50) overnight at 4°C. Protein G-Sepharose (200µl) was then added to the supernatants, and the incubation continued for 1h at 4°C. The slurry was washed six times with 0.5% CHAPS in HSE buffer. The final wash was discarded and the immunoprecipitated complexes were eluted by boiling the samples at 100ºC for 10min in SDS-PAGE sample buffer under non-reducing conditions. Samples were loaded onto a 12% non-reducing SDS gel and separated by SDS-PAGE and the gel was stained with Coomassie Blue.

4.2.4.2 Concentration using polyethylene glycol (PEG) followed by discontinuous sucrose gradient separation

MDBK cells were grown and infected as described above. Infected cells were either left untreated or treated with 5μM or 75μM NAP-DNJ. Culture supernatant was harvested as described above. A solution of 24% (w/v) PEG 8000 in 2M NaCl was added to the clarified virus until a 6% (v/v) PEG final concentration was obtained. The solution was kept at 4°C overnight with gentle stirring and then centrifuged at 2600g for 15mins. The PEG concentrated pellets were resuspended in 3ml PBS. To release virus from the PEG pellets, they were subjected to sonication for 30 bursts at 50% duty cycle using the Branson Sonifier 250. The PEG concentrated virus was subjected to two successive ultracentrifugations. The sonicated sample was layered onto 30% and 60% (w/v) discontinuous sucrose cushions prepared in PBS and centrifuged to equilibrium (81 250g) for 1h at 4°C. Single white bands seen in the sucrose cushions in each sample were isolated and diluted 20 times with PBS spun down at 100 000g for 4h at 4°C to obtain a pellet and resuspended in 2ml of PBS. The pellet was resuspended in 1ml PBS and further centrifuged at 135 240g for 30mins at 4°C. PNGase F digestion was carried out overnight at 37°C on the eventual pellet as described in the preceding chapter in the presence of 40mM DTT. The PNGase F digested samples were dried and resuspended in 30μl milliQ water. Anthranilic acid was used to label the released glycans, as published (*21*). The glycan structure of the virions was analysed by NP-HPLC as described in chapter 3.

4.2.4.3 Concentration using PEG followed by both discontinuous and continuous sucrose gradient separations

Samples were prepared as described above and culture supernatant was harvested, PEG concentrated, sonicated and loaded onto a 30%/ 60% (w/v) discontinuous sucrose gradient column as described above. Fractions (1ml) were collected and the viral RNA copies in each fraction were quantified as described in the previous chapter. The fraction containing the greatest amount of viral RNA was isolated for each sample, diluted 20 times with PBS and passed through a 0.22μm filter unit to remove cellular aggregates. The fraction was further spun down at 100 000g for 4h at 4°C to obtain a pellet and resuspended in 2ml of PBS. The resuspended pellet was layered onto a 10-40% (w/w) continuous sucrose gradient in PBS and subjected to centrifugation at 81 250g for 1h at 4°C. Fractions (0.5ml) were collected and the viral RNA copies in each fraction were quantified. The fractions containing the greatest amount of viral RNA were isolated and pooled for each sample, and subjected to centrifugation at 100 000g for 4h at 4°C. The pellet was resuspended in 1ml PBS and further spun down at 135 240g for 30mins at 4°C. PNGase F digestion was carried out overnight at 37°C on the pellet as described in the preceding chapter in the presence of 40mM DTT. The PNGase F digested samples were dried and resuspended in 30μl milliQ water. Anthranilic acid was used to label the released glycans, as published (*21*). The glycan structure of the virions was analysed by NP-HPLC as described in the preceding chapter.

4.2.4.4 Immunopurification using antibodies immobilised to cyanogen-bromide (CN-Br) activated sepharose 4B beads

MDBK cells were grown in 5 X T225 tissue culture flasks at 5.6 X 10^7 cells/ flask. The cells were infected with cytopathic BVDV at a multiplicity of infection (MOI) of 1 FFU/cell in FCS depleted RPMI, for 4h at 37ºC, 5% CO_2 atmosphere in FCS depleted medium. PBS was used to wash the cells twice. Infected cells were left to grow for 24h in FCS supplemented medium. The spent medium was harvested, spun down at 1300g for 10mins to remove cell debris. The supernatant was subjected to ultracentrifugation at 100 000g, for 4h at 4ºC, and the viral pellets were resuspended in 1ml of 2% SDS with 10µl of protease inhibitor cocktail, subsequently incubated at 37ºC for 30mins. To the resuspended pellet, binding/ wash buffer (50mM Tris-Cl, 0.5% Triton X-100, pH 7.5) was added to solubilise the viral membrane proteins and to raise the pH to 7-8. Protein G beads (200µl), previously washed thrice with binding buffer, were incubated with the viral proteins at 4ºC overnight. Aliquots of 10µl were taken at various stages throughout this protocol for western blotting to probe for BVDV E2 proteins using MAb214.

The CN-Br activated sepharose 4B beads (0.3g) from GE Healthcare Life Sciences was washed thrice and swollen with 60ml of 1mM HCl for 5mins. MAb214 (2mg) was dissolved in 2ml of coupling buffer (0.2M $NaHCO_3$, 0.5M NaCl, pH 8.5), added to the swollen beads and mixed end-to-end at 4ºC overnight. Excess unbound antibodies were removed and the beads were subjected to blocking in 1M ethanolamine, pH 9 for 2h at room temperature. The beads were then washed alternately with coupling buffer thrice and 0.1M acetate buffer, 0.5M NaCl, pH 4 twice.

The prepared virus was then added the antibody-immobilised beads and mixed end-to-end at 4ºC overnight. Unbound virus was removed and the beads were washed with wash

buffer once, and incubated with elution buffer (0.1M glycine, 0.5% Triton X-100, pH 2.5) at 4^{o}C for 10mins. The beads were then spun down at 530g for 5mins and binding buffer was added to the eluted proteins until the pH was raised to 7-8.

Protein G beads (200µl) was added to the eluted proteins and mixed end-to-end at 4^{o}C overnight. After spinning down at 530g for 5mins, 100mg/ml bovine serum albumin (BSA) and ice cold ethanol were added to the supernatant, incubated at -20^{o}C overnight and subsequently spun down at 25 704g for 30mins at 2^{o}C to precipitate viral proteins.

PNGase F digestion was carried out overnight at 37°C on the viral pellet as described in the preceding chapter in the presence of 40mM DTT. The PNGase F digested samples were dried and resuspended in 30µl milliQ water. Anthranilic acid was used to label the released glycans, as published (*21*). The glycan structure of the virions was analysed by NP-HPLC as described above.

4.2.4.5 Immunopurification using antibodies cross-linked to protein G beads

MDBK cells were grown in 5 X T225 tissue culture flasks at 5.6 X 10^7 cells/ flask in immunoglobulin G (IgG)-depleted FCS supplemented RPMI medium. The cells were infected with cytopathic BVDV at a multiplicity of infection (MOI) of 1 FFU/cell in FCS depleted RPMI, for 4h at 37^{o}C, 5% CO_2 atmosphere. PBS was used to wash the cells twice. Infected cells were left to grow overnight. The spent medium was harvested, spun down at 2krpm for 10mins using GS-6R Beckman centrifuge, GH-3.8 rotor and the supernatant was further passed through a 0.22μm filter unit to remove cell debris. The filtrate was subjected to ultracentrifugation at 100 000g for 4h at 4^{o}C, and the viral pellets were resuspended in 1ml of binding buffer (50mM Tris-Cl, 150mM NaCl, pH 7.5) with 0.5% Triton X-100 and 10μl of protease inhibitor cocktail. To solubilize membrane viral proteins, the resuspended virus was subjected to 30mins incubation at 4^{o}C. The viral proteins were further spun down at 135 240g for 15mins and the supernatant was added to the MAb214 (1mg)-immobilised Protein G HP SpinTrap columns (GE Healthcare) according to manufacturer's protocol. The immobilised antibodies, unbound and bound virus, consecutive wash and eluted fractions were collected according to manufacturer's protocol. Aliquots of 10μl of each fraction were subjected to SDS-PAGE under reducing and non-reducing conditions, followed by silver staining and western blot analyses using MAb214 to probe for BVDV E2. The ends of gel loading tips were cut to load the protein G beads onto the gels.

4.3 RESULTS

4.3.1 BVDV glycan analysis

4.3.1.1 Immunoprecipitation

In a previous study using chimeric BVDV E2 and VSV G proteins, the BVDV E2 protein was reported to contain only oligomannose side chains and to be free of complex N-glycans (*20*). The endomannosidase digest of BVDV glycoproteins following NAP-DNJ treatment from the previous chapter also indicated the presence of glucosylated oligosaccharides on intra-cellular BVDV glycoproteins following treatment with 75µM *NAP-DNJ* but secreted virions did not have glucosylated glycans. To confirm this, the culture medium harvested from NAP-DNJ treated or untreated BVDV-infected cells was subjected to immunoprecipitation to isolate the BVDV E2 glycoproteins. The precise Coomassie stained bands corresponding to BVDV E1E2 or E2E2 were not detected in Figure 4.1 and all the bands detected in the gel were present in all the samples, including the uninfected control.

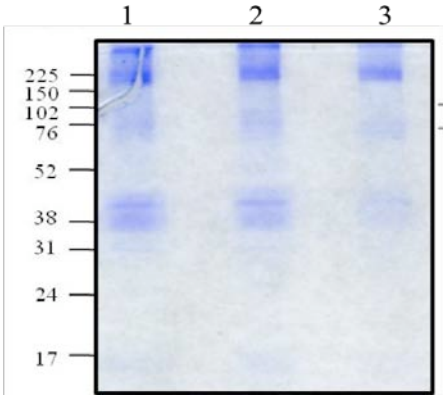

Figure 4.1 BVDV E2 glycan analysis using immunoprecipitation.

MDBK cells were subjected to the following treatment: (1) Uninfected, untreated, (2) infected with BVDV at MOI 1, untreated and (3) infected with BVDV at MOI 1, treated

with 75μM NAP-DNJ. Culture supernatant harvested was subjected to immunoprecipitation using MAb214 to isolate BVDV E2, followed by SDS-PAGE and Coomassie stain.

4.3.1.2 Concentration using PEG followed by discontinuous sucrose gradient separation

Since MAb214 was not able to successfully immunoprecipitate BVDV E2, another approach was sought out to isolate the viral glycoprotein. Concentration of the NADL strain using PEG has previously been reported to support optimal recovery of infectivity (*22*) and has therefore been used in this study to isolate BVDV E2-associated proteins in the culture supernatant of NAP-DNJ treated cells. There was no significant difference in the glycan profiles between the uninfected and infected samples as shown in Figure 4.2, suggesting that either sufficient amount of E2-associated proteins have not been successfully isolated from the sucrose cushions or the proteins have not been accurately isolated at all.

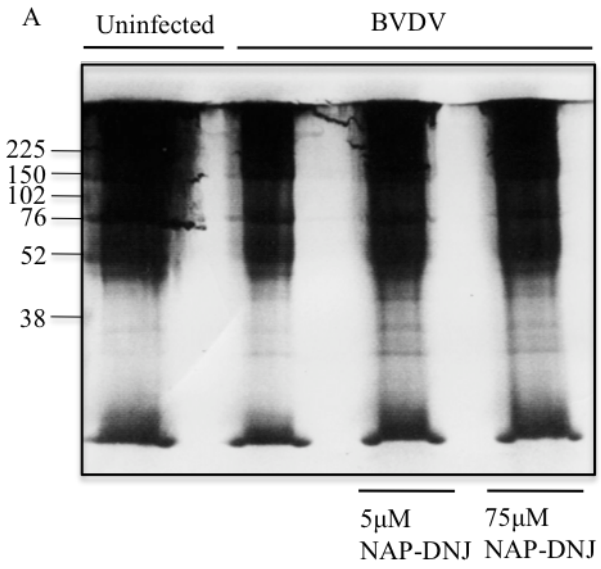

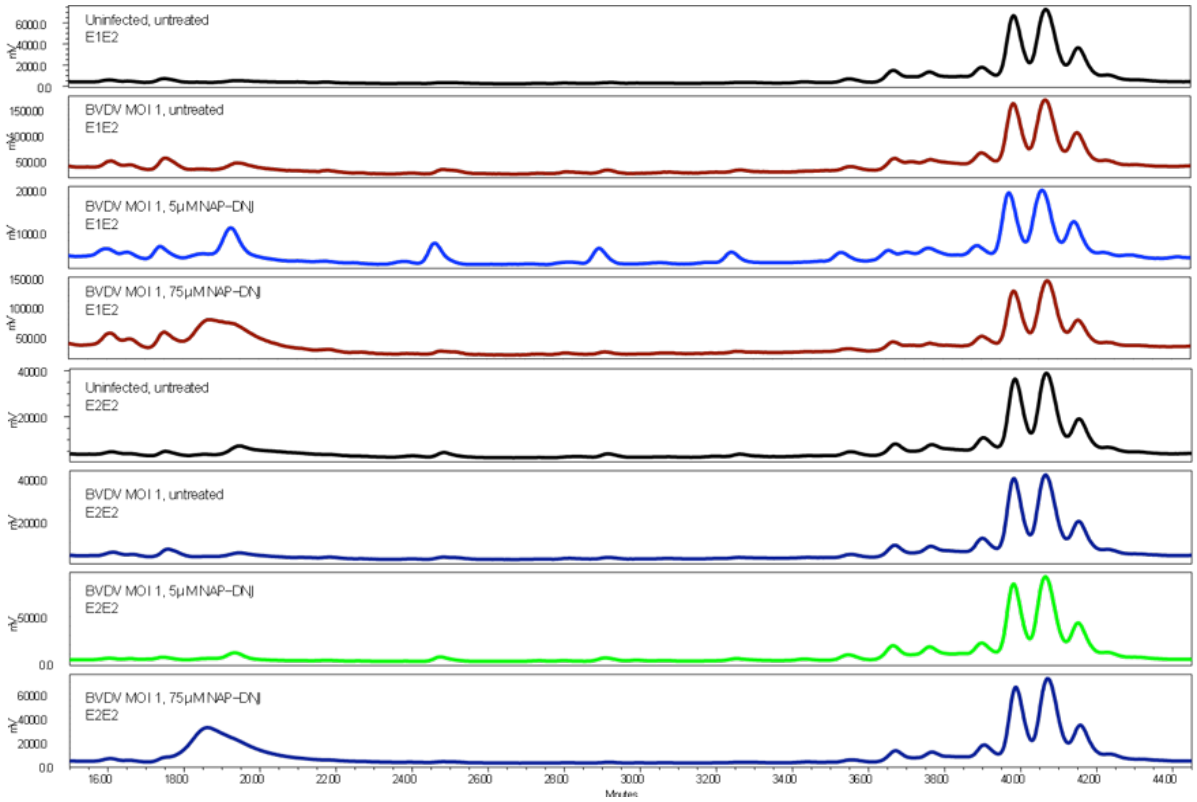

Figure 4.2 Glycan analysis of BVDV envelope glycoproteins.

Culture supernatant harvested from NAP-DNJ treated BVDV-infected MDBK cells was subjected to 30%/ 60% (w/v) discontinuous sucrose gradient separation. The isolated fraction from each sample was subjected to SDS-PAGE in a 12% SDS gel and stained with Coomassie blue (A). Bands corresponding to the molecular weights of E1E2 and E2E2 were excised and treated with PNGase F before the samples were 2AA-labeled and subjected to NP-HPLC analysis (B).

4.3.1.3 Concentration using PEG followed by both continuous and discontinuous sucrose gradient separations

In order to ensure that only BVDV E2-associated proteins were isolated from the sucrose cushions, the RNA copy number of each sample before and after PEG precipitation, as well as before and after sonication were quantified using RT-PCR. Figure 4.3 shows that the BVDV RNA copies were the highest after 10 bursts of sonication post-PEG precipitation, which was performed to release the viral particles from the virus-cell aggregates in the PEG precipitated pellets.

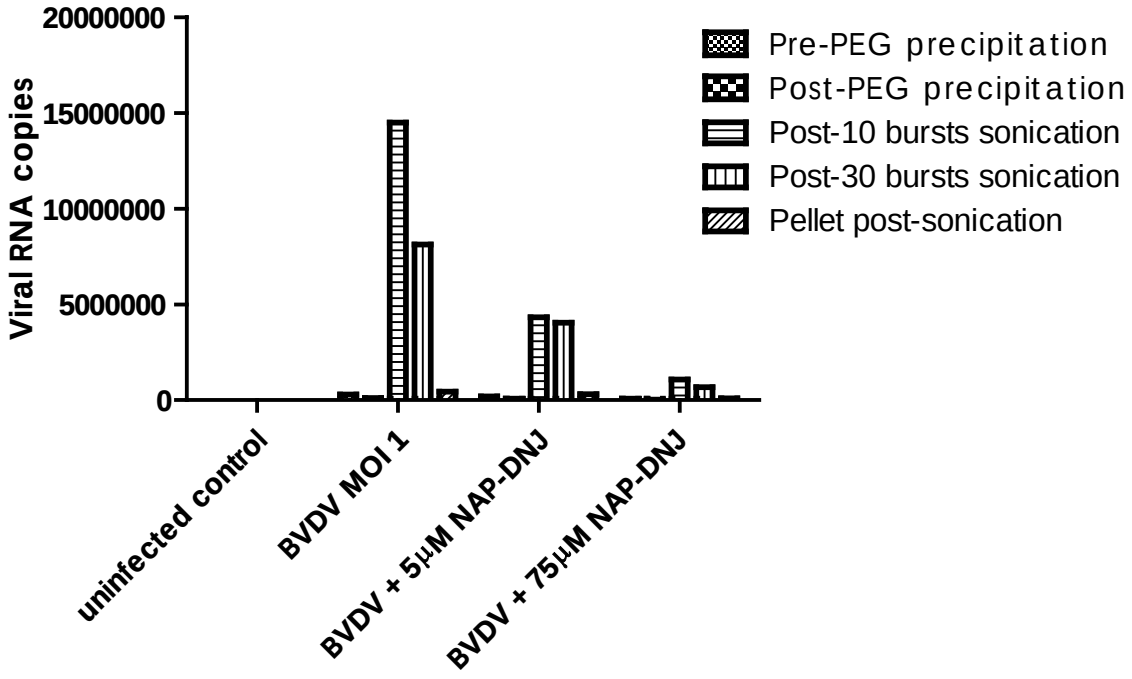

Figure 4.3 Viral RNA copy changes following concentration of BVDV using PEG.

Aliquots of 140μl were taken from the samples at various stages [pre-PEG precipitation, post-PEG precipitation, post-10 bursts sonication, post-30 bursts sonication (loaded onto sucrose cushion) and remaining pellet harvested post-sonication] and subjected to RNA extraction and RT-PCR described in Materials and Methods.

Post-separation on a 30%/ 60% (w/v) discontinuous sucrose gradient column, 1ml fractions of the sucrose column of each sample were isolated and the RNA copy numbers quantified. The highest amounts of BVDV RNAs were detected in fractions 7 of each sample as shown in Figure 4.4, which corresponded with a thick white band observed in each of the sucrose column after the separation.

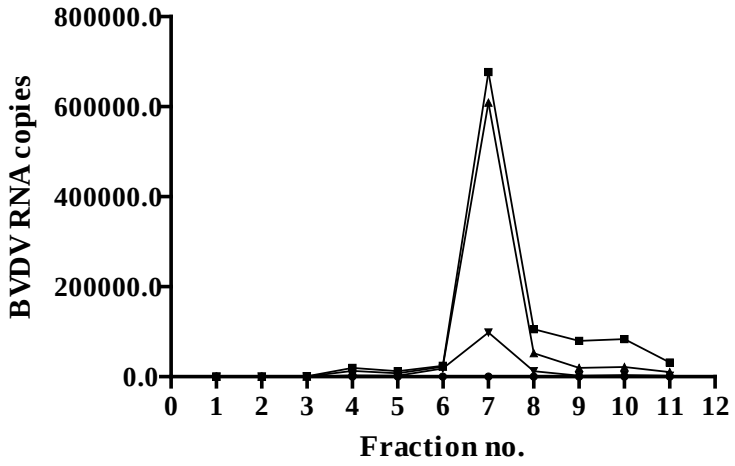

Figure 4.4 Comparison of viral RNA copies per 1ml fraction of discontinuous sucrose gradient column.

The PEG precipitated viral pellets from uninfected MDBK cells (●), MDBK cells infected with BVDV at MOI 1 (■), treated with 5μM NAP-DNJ (▲) or 75μM NAP-DNJ (▼) were sonicated and layered on to a 30% and 60% (w/v) discontinuous sucrose cushions prepared in PBS and centrifuged to equilibrium (81 250g) for 1h at 4°C. Subsequently, 1ml fractions were collected from each tube, diluted 20 times with PBS and aliquots of 140μl were taken from the samples, subjected to RNA extraction and RT-PCR described in Materials and Methods.

These fractions were passed through a 0.22μm filters to remove any remaining cellular debris and Figure 4.5 shows that there was no significant difference in viral RNA copies before and after filtration in each sample.

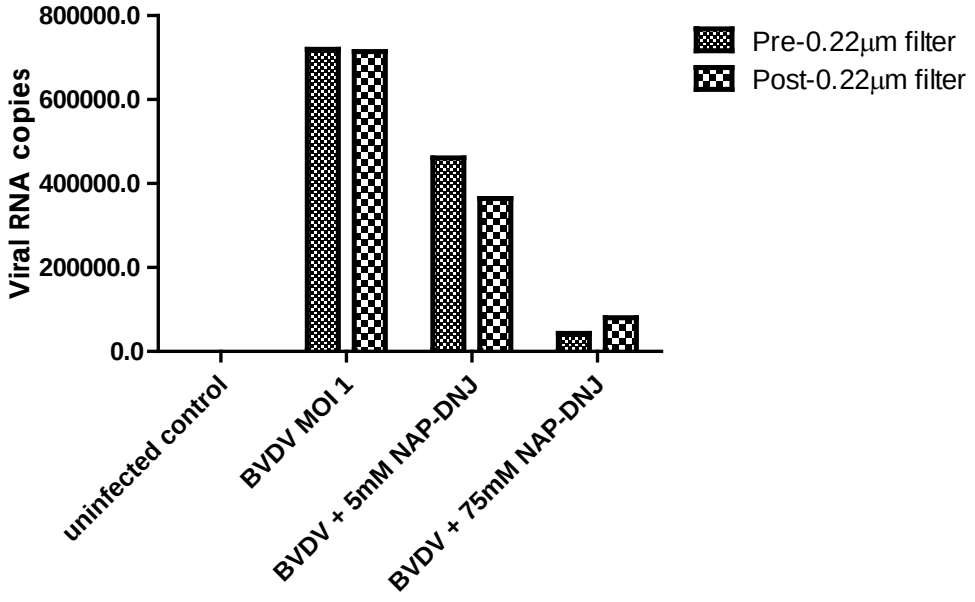

Figure 4.5 Changes in BVDV RNA copies following removal of cellular debris

Aliquots of 140μl were taken from the samples before and after filtration through 0.22μm filter, and subsequently subjected to RNA extraction and RT-PCR described in Materials and Methods.

The samples were subjected to further separations on a 10-40% (w/w) continuous sucrose gradient column in order to exclude any remaining cellular materials. Fractions (0.5ml) of the sucrose column of each sample were isolated and Figure 4.6 shows the different range in isolated fractions from each sample where significant amounts of viral RNA copies were detected. Fractions 7 and 8 from the infected untreated sample, fractions 6, 7 and 8 from the infected sample treated with 5μM NAP-DNJ and fractions 7, 8 and 9 from the

infected sample treated with 75μM NAP-DNJ showed relatively higher levels of viral RNA compared to the other fractions, and therefore together with fractions 7, 8 and 9 from the uninfected control, were pooled accordingly and concentrated to a smaller volume before PNGase F digest.

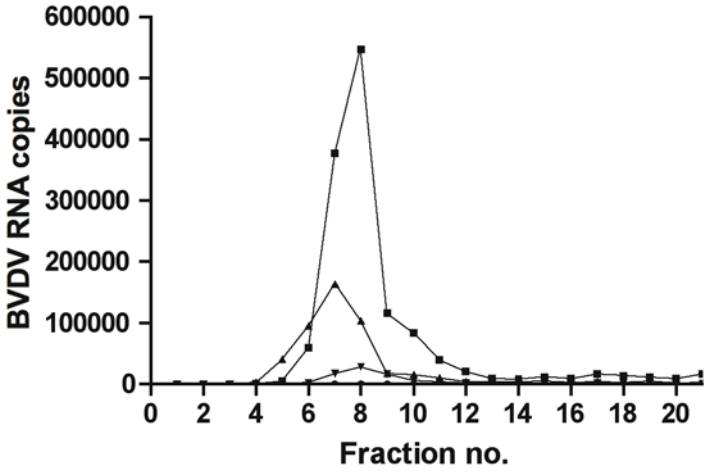

Figure 4.6 Comparison of viral RNA copies per 0.5ml fraction of continuous sucrose gradient column.

Fraction 7 harvested from uninfected MDBK cells (●), MDBK cells infected with BVDV at MOI 1 (■), treated with 5μM NAP-DNJ (▲) or 75μM NAP-DNJ (▼) in Figure 3.3 was layered on to a 10-40% (w/w) continuous sucrose gradient in PBS and subjected to centrifugation at 81 250g for 1h at 4°C in a SW 41Ti rotor with no brakes applied. Subsequently, 0.5ml fractions were collected from each tube, diluted 20 times with PBS and aliquots of 140μl were taken from the samples, subjected to RNA extraction and RT-PCR described in Materials and Methods.

Figure 4.7 showed that there was no difference in the glycan profile between the uninfected and infected samples, suggesting that either the amounts of viral glycoproteins isolated were not sufficient to allow for detection by NP-HPLC or the E2-associated proteins were lost in the sucrose gradient separations. The PNGase F treated α-1-antitrypsin sample showed that the overnight PNGase F digestion at 37°C worked effectively. No glycans were detected from the PNGase F digested samples of the BVDV-infected control.

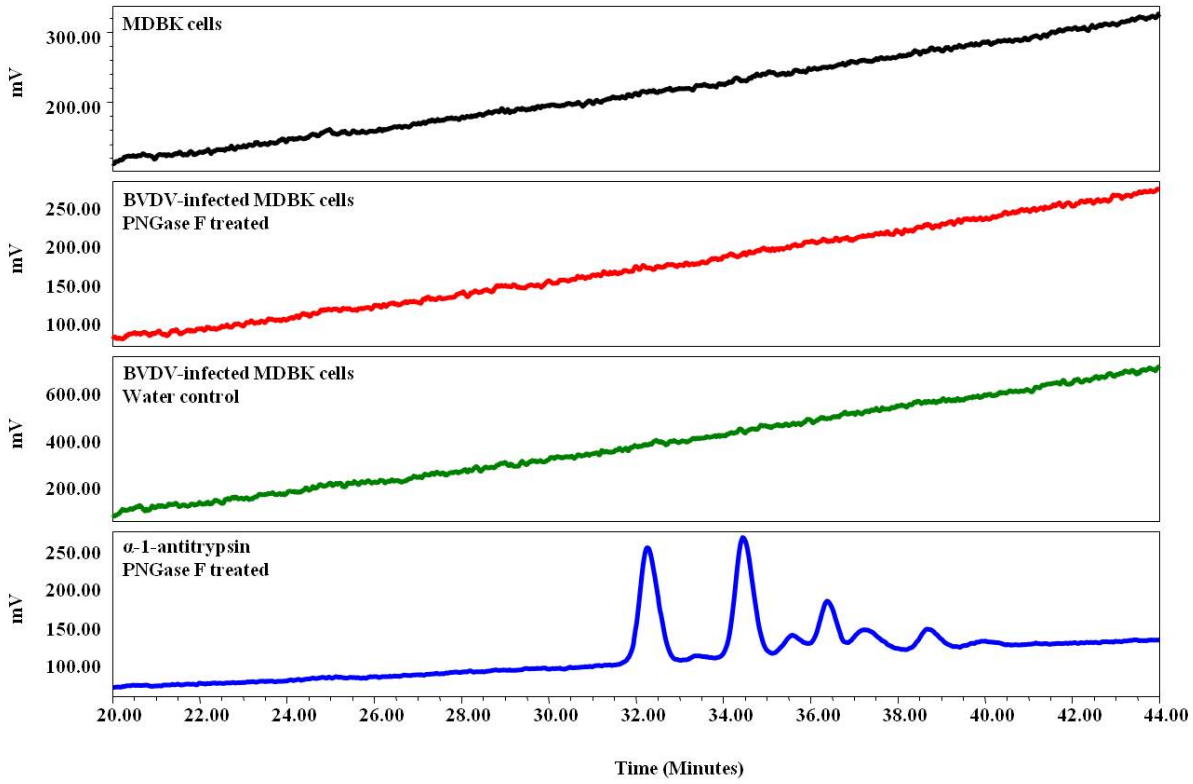

Figure 4.7 Glycan analysis of BVDV envelope glycoproteins.

N-linked oligosaccharides of secreted mature BVD virions from MDBK cells infected with BVDV at MOI 1 for 24h. Harvested culture medium was purified through sucrose gradient separations and isolated fractions were concentrated and subjected to PNGase F digest, followed by 2AA-labeling and NP-HPLC analysis.

Following this, in order to find out whether there was any BVDV proteins in the virus-infected samples, a 50µl aliquot of each of the samples were used to run an SDS-PAGE and subsequently a western blot analysis, using MAb214 to probe for BVDV E2. BVDV E1E2 heterodimers were detected in the untreated virus-infected control, but not in the NAP-DNJ treated samples (Figure 4.8). However, the amount of glycans on the heterodimers in the untreated virus-infected sample was probably too low to generate detectable peaks on the glycan profile after NP-HPLC.

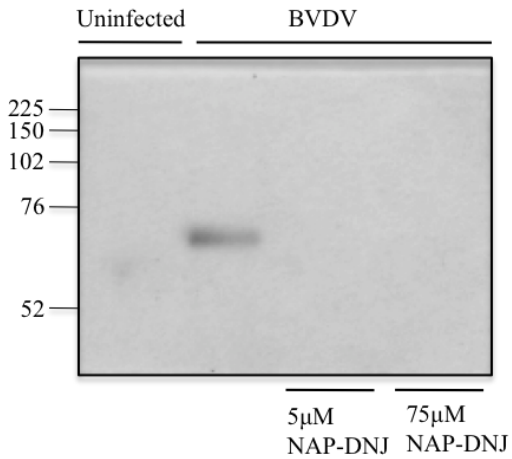

Figure 4.8 BVDV E1E2 detected in untreated control using western blot.

Prior to PNGase F digest, a 50µl aliquot of each sample was subjected to SDS-PAGE in a 12% gel followed by western blot analysis using MAb214.

4.3.1.4 Immunopurification using antibodies immobilised to CN-Br activated sepharose 4B beads

In order to isolate a greater amount of secreted BVDV E2-associated proteins, MAb214 was immobilised onto a CN-Br activated sepharose 4B beads column and harvested culture supernatant from BVDV-infected cells was passed through the column. Figure 4.9A confirms that MAb214 successfully bound to the CN-Br activated sepharose 4B beads column (Lane 3), with no unbound antibodies in the wash through (Lane 2). Figure 4.9B shows that majority of the viral proteins resided in the unbound flow-through in lane 3. Any viral proteins that were bound to the antibody column were removed with the wash in lane 4. No BVDV glycoproteins were detected in the eluted fraction in lane 5. However, Figure 4.9C shows that the MAb214 antibodies previously immobilised onto the CN-Br activated sepharose 4B beads were no longer intact following protein elution.

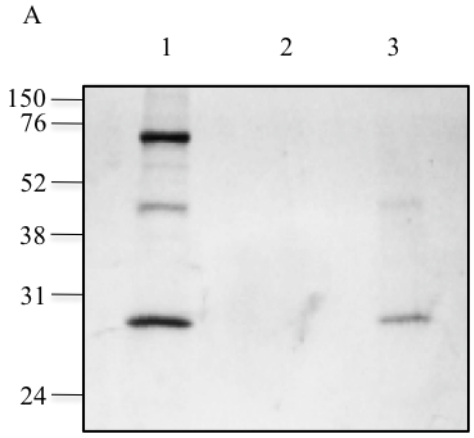

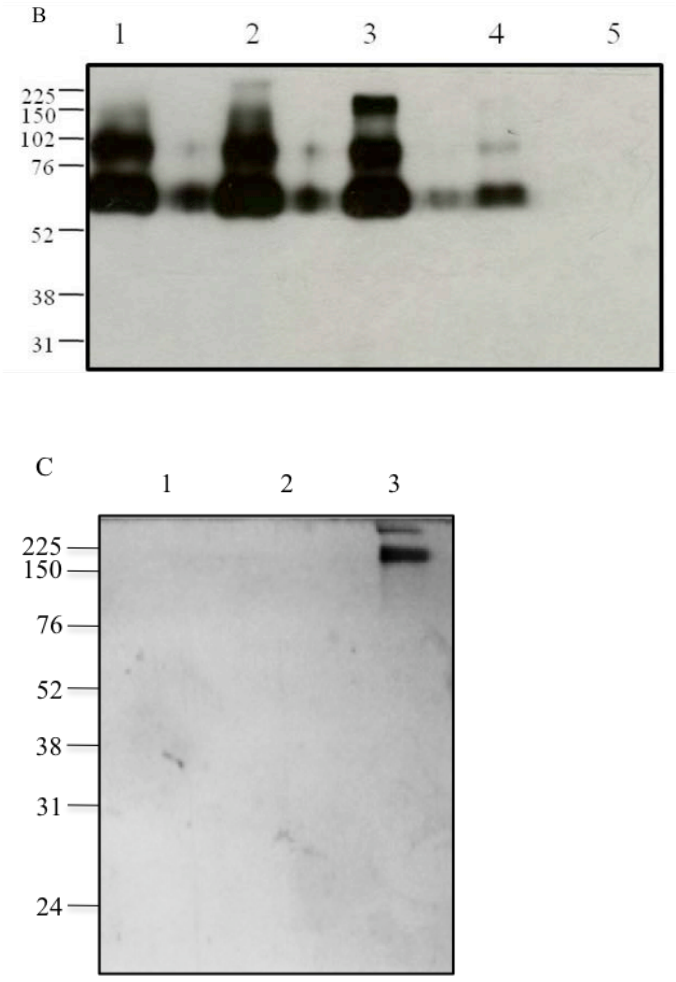

Figure 4.9 Immunopurification of BVDV E2 envelope glycoprotein using antibodies immobilised to CN-Br activated sepharose 4B beads

(A) 5µl MAb214 NEAT (Lane 1), unbound MAb214 (Lane 2) and a 5µl aliquot resin following antibody immobilisation (Lane 3) were subjected to SDS-PAGE on a 12% gel, followed by Coomassie staining. (B) Aliquots of 10µl were taken from solubilised viral proteins (Lane 1), solubilised viral proteins after IgG removal using protein G beads (Lane 2), unbound viral proteins after passing through antibody column (Lane 3), wash fraction (Lanes 4) and eluted fraction (Lane 5) and loaded onto a 12% gel, then subjected to SDS-PAGE under non-reducing condition, followed by western blotting using MAb214 to probe for BVDV E2. (C) A 5µl aliquot of CN-Br activated sepharose 4B

beads (Lane 1), 5µl aliquot of CN-Br activated sepharose 4B beads with previously immobilised MAb214 (Lane 2) and 5µl aliquot of NEAT MAb214 from stock (Lane 3) were subjected to SDS-PAGE in a 12% gel under non-reducing condition and stained with Coomassie blue.

4.3.1.5 Immunopurification using antibodies cross-linked to protein G beads

To ensure that the antibody used in this immunopurification study remained bound to the resin column, MAb214 was covalently bound to protein G beads using a cross-linking agent. No trace of the antibody was detected after silver staining in the unbound fraction (Lane 3), suggesting that majority of MAb214 antibodies were successfully bound to the protein G beads as shown in Lane 2 in Figure 4.10.

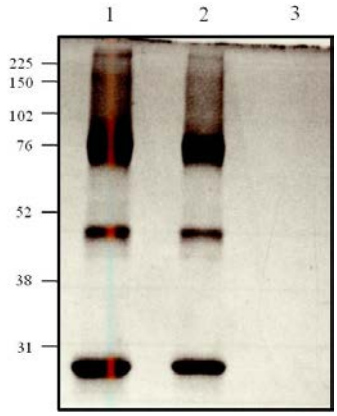

Figure 4.10 Anti-BVDV E2 antibodies were properly cross-linked to protein G beads.

MAb214 was allowed to bind to protein G beads overnight at 4°C, and subsequently cross-linked using 50mM dimethyl pimelimidate dihydrochloride in 200mM triethanolamine, pH 8.9. (1) 10µg antibody in binding buffer, (2) 10µl aliquot of bound antibody in protein G beads, (3) 10µl aliquot of wash fraction.

However, most of the virus was not able to bind efficiently to the MAb214 antibodies immobilised onto the protein G beads. Majority of the virus was detected in the unbound

flow-through (Lane 2 of Figure 4.11A and B) and a lesser amount in the first wash fraction (Lane 3 of Figure 4.11A and B), suggesting that only a small amount of virus introduced into the protein G columns were bound to the immobilised antibodies, and some of these bound virus were gradually washed off the column in the consecutive washes (Lanes 4-7 of Figure 4.11A and B), leaving very little or no bound virus remaining for elution. Some traces of BVDV E1E2 (Lanes 9 and 10) and E2E2 (Lanes 8, 9 and 10) were detected in the western blot analysis in Figure 4.11B.

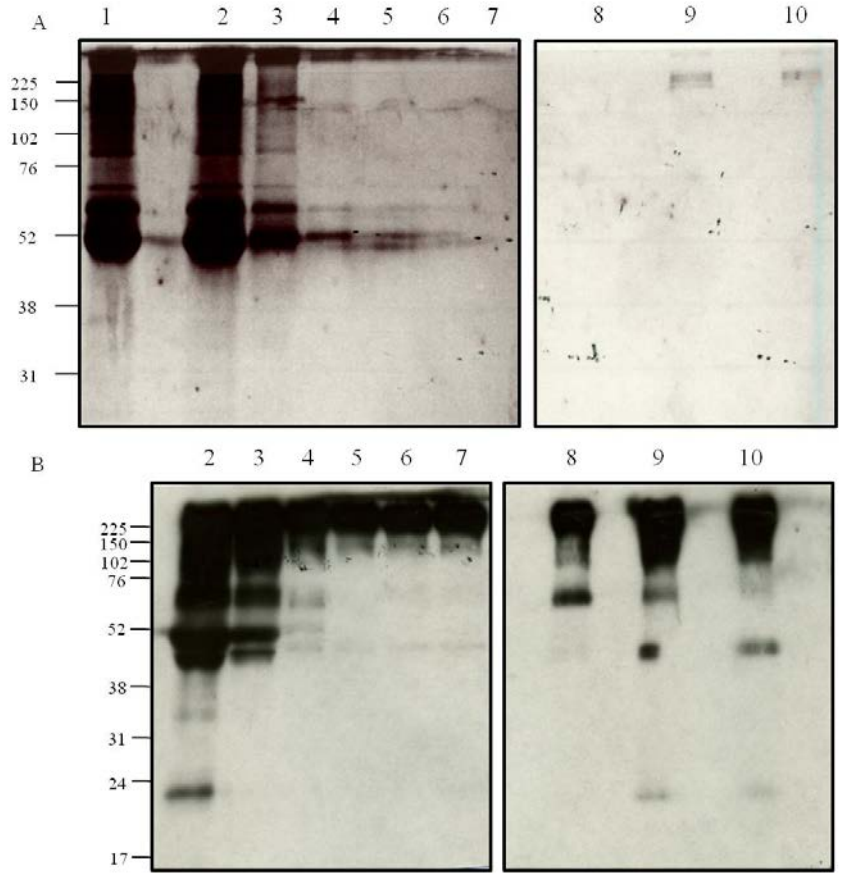

Figure 4.11 Immunopurification of BVDV E2 envelope glycoprotein using antibodies cross-linked to protein G beads

Spent medium harvested from MDBK cells infected with BVDV at MOI 1 for 24h was solubilised in 50mM Tris, 150mM NaCl, 0.5% Triton X-100, pH 7.5 and subsequently allowed to bind with MAb214 immobilised onto protein G sepharose beads. Aliquots of

10µl were taken from the BVDV before binding to MAb214 on protein G beads (Lane 1), unbound viral proteins (Lane 2), wash fractions (Lanes 3-7) and eluted fractions (Lanes 8-10) and loaded onto two sets of 12% gels, then subjected to SDS-PAGE under non-reducing condition. One gel was stained with coomassie blue for 1h and destained overnight at room temperature (A) and the other was subjected to western blotting using MAb214 to probe for BVDV E2 (B).

4.4 DISCUSSION

The monoclonal antibody against BVDV E2 protein, MAb214, used in this study was most likely too weak in its binding affinity to capture sufficient amounts of the viral protein for its isolation. The absence of commercially available anti-BVDV E1 antibody also makes the isolation of the E1 glycoprotein challenging. The glycan profiles detected by NP-HPLC following immunoprecipitation most likely originated from either the fetal calf serum used to grow MDBK cells or cellular proteins.

The disease caused by BVDV was first described in 1946 (*23*), (*24*) but much about the morphology and structure of the virus remains unresolved, largely due to the fragility and the ubiquity of the virus, the low titres in tissue cultures and the intimate association of its lipids, carbohydrates and proteins with the host cell membranes, making the purification with high recovery of infectivity challenging (*25*). The production and concentration of large volumes of tissue culture fluid are necessary in order to obtain enough material to purify virions and isolate their glycan structures for analysis. PEG precipitation has been reported to be successful in concentrating virus, including BVDV (*26*). In a previous study that compared the ultrafiltration teachnique and PEG concentration of crude BVDV culture supernatant, it was found that the latter allowed for 100% infectivity recoveries and unaltered virus morphology (*22*). The same observations were made in other viruses such as cytomegalovirus (*27*) and the human respiratory syncytial virus (*28*). Concentration by PEG followed by purification by ultracentrifugation through sucrose gradients therefore was reported to be satisfactory on the basis of higher recovery of infectivity, protein content and intact viral particles (*22*). Sucrose gradient separations

have also been used to successfully isolate HCV envelope glycoproteins and were found to be associated with fractions containing the most infectious viral particles (*29*).

Based on the results in 4.3.1.3, it appears that the RT-PCR technique was more sensitive than western blot in detecting the presence of BVDV since western blot did not pick up any signals in the NAP-DNJ treated samples but RT-PCR demonstrated the presence of viral RNA in these samples. BVDV virions were successfully isolated following the sucrose gradient column separations since BVDV E1E2 heterodimers were detected in the western blot analysis of the untreated sample. However, the glycans on the surface of the E1E2 heterodimers in the untreated control were most likely not sufficient to register a reading on the NP-HPLC profile. The amounts of E1E2 heterodimers in the treated samples were most probably even lower than the untreated control, therefore did not show up in the western blot analysis and there is an even lower chance that their surface glycans could be detectable by NP-HPLC. Hence, even though western blot might have been more suitable than RT-PCR to quantify for presence of BVDV at various steps in the protocol, the successful detection of BVDV E2 using western blots does not necessarily mean that there is sufficient glycans on the viral proteins for further analysis.

A more cumbersome approach to pursue the glycosylation changes on BVDV E2 following treatment with iminosugars is to create an efficient expression vector that produces the viral glycoprotein. Previous studies have reported the successful expression of BVDV E2 protein in insect cells (*30*).

4.5 REFERENCES

1. Doms, R. W., Lamb, R. A., Rose, J. K., and Helenius, A. (1993) Folding and assembly of viral membrane proteins., *Virology 193*, 545-62.
2. Braakman, I., and Anken, E. van. (2000) Folding of viral envelope glycoproteins in the endoplasmic reticulum., *Traffic (Copenhagen, Denmark) 1*, 533-9.
3. Taylor, A. K., and Wall, R. (1988) Selective removal of alpha heavy-chain glycosylation sites causes immunoglobulin A degradation and reduced secretion., *Molecular and cellular biology 8*, 4197-203.
4. Zimmer, G., Trotz, I., and Herrler, G. (2001) N-glycans of F protein differentially affect fusion activity of human respiratory syncytial virus., *Journal of virology 75*, 4744-51.
5. Rice, C. (1996) Flaviviridae: the viruses and their replication (B. N. Fields, D. M. Knipe, P. M. Howley, et al, Ed.) Fields vir., pp 931-959, Lippincott-Raven Publishers, Philadelphia, Pa.
6. Ronecker, S., Zimmer, G., Herrler, G., Greiser-Wilke, I., and Grummer, B. (2008) Formation of bovine viral diarrhea virus E1-E2 heterodimers is essential for virus entry and depends on charged residues in the transmembrane domains., *The Journal of general virology 89*, 2114-21.
7. Thiel, H. J., Stark, R., Weiland, E., Rümenapf, T., and Meyers, G. (1991) Hog cholera virus: molecular composition of virions from a pestivirus., *Journal of virology 65*, 4705-12.
8. Weiland, F., Weiland, E., Unger, G., Saalmüller, A., and Thiel, H. J. (1999) Localization of pestiviral envelope proteins E(rns) and E2 at the cell surface and on isolated particles., *The Journal of general virology 80 (Pt 5)*, 1157-65.
9. Baxi, M. K., Deregt, D., Robertson, J., Babiuk, L. A., Schlapp, T., and Tikoo, S. K. (2000) Recombinant bovine adenovirus type 3 expressing bovine viral diarrhea virus glycoprotein E2 induces an immune response in cotton rats., *Virology 278*, 234-43.

10. Donis, R. O., and Dubovi, E. J. (1987) Molecular specificity of the antibody responses of cattle naturally and experimentally infected with cytopathic and noncytopathic bovine viral diarrhea virus biotypes., *American journal of veterinary research 48*, 1549-54.
11. Elahi, S. M., Shen, S. H., Talbot, B. G., Massie, B., Harpin, S., and Elazhary, Y. (1999) Recombinant adenoviruses expressing the E2 protein of bovine viral diarrhea virus induce humoral and cellular immune responses., *FEMS microbiology letters 177*, 159-66.
12. Grigera, P. R., Marzocca, M. P., Capozzo, A. V., Buonocore, L., Donis, R. O., and Rose, J. K. (2000) Presence of bovine viral diarrhea virus (BVDV) E2 glycoprotein in VSV recombinant particles and induction of neutralizing BVDV antibodies in mice., *Virus research 69*, 3-15.
13. Wensvoort, G., Terpstra, C., Kluijver, E. P. de, Kragten, C., and Warnaar, J. C. (1989) Antigenic differentiation of pestivirus strains with monoclonal antibodies against hog cholera virus., *Veterinary microbiology 21*, 9-20.
14. Donis, R. O., and Dubovi, E. J. (1987) Differences in virus-induced polypeptides in cells infected by cytopathic and noncytopathic biotypes of bovine virus diarrhea-mucosal disease virus., *Virology 158*, 168-73.
15. Maurer, K., Krey, T., Moennig, V., Thiel, H.-J., and Rümenapf, T. (2004) CD46 is a cellular receptor for bovine viral diarrhea virus., *Journal of virology 78*, 1792-9.
16. Wang, Z., Nie, Y., Wang, P., Ding, M., and Deng, H. (2004) Characterization of classical swine fever virus entry by using pseudotyped viruses: E1 and E2 are sufficient to mediate viral entry., *Virology 330*, 332-41.
17. Pande, A., Carr, B. V., Wong, S. Y. C., Dalton, K., Jones, I. M., McCauley, J. W., and Charleston, B. (2005) The glycosylation pattern of baculovirus expressed envelope protein E2 affects its ability to prevent infection with bovine viral diarrhoea virus., *Virus research 114*, 54-62.
18. Jordan, R., Nikolaeva, O. V., Wang, L., Conyers, B., Mehta, A., Dwek, R. a, and Block, T. M. (2002) Inhibition of host ER glucosidase activity prevents Golgi processing of virion-associated bovine viral diarrhea virus E2 glycoproteins and reduces infectivity of secreted virions., *Virology 295*, 10-9.
19. Repp, R., Tamura, T., Boschek, C. B., Wege, H., Schwarz, R. T., and Niemann, H. (1985) The effects of processing inhibitors of N-linked oligosaccharides on the intracellular migration of glycoprotein E2 of mouse hepatitis virus and the

maturation of coronavirus particles., *The Journal of biological chemistry 260*, 15873-9.

20. Köhl, W., Zimmer, G., Greiser-Wilke, I., Haas, L., Moennig, V., and Herrler, G. (2004) The surface glycoprotein E2 of bovine viral diarrhoea virus contains an intracellular localization signal., *The Journal of general virology 85*, 1101-11.
21. Neville, D. C. A., Coquard, V., Priestman, D. A., Vruchte, D. J. M. te, Sillence, D. J., Dwek, R. A., Platt, F. M., and Butters, T. D. (2004) Analysis of fluorescently labeled glycosphingolipid-derived oligosaccharides following ceramide glycanase digestion and anthranilic acid labeling., *Analytical biochemistry 331*, 275-82.
22. Magar, R., and Lecomte, J. (1987) Comparison of methods for concentration and purification of bovine viral diarrhea virus., *Journal of virological methods 16*, 271-9.
23. Olafson, P., MacCallum, A. D., and Fox, F. H. (1946) An apparently new transmissible disease of cattle., *The Cornell veterinarian 36*, 205-13.
24. Childs, T. (1946) X Disease of Cattle - Saskatchewan., *Canadian journal of comparative medicine and veterinary science 10*, 316-9.
25. Horzinek, M. C. (1981) Non-arthropod-borne Togaviruses, Academic Press, London.
26. Chu, H. J., Zee, Y. C., Ardans, A. A., and Dai, K. (1985) Enzyme-linked immunosorbent assay for the detection of antibodies to bovine viral diarrhea virus in bovine sera., *Veterinary microbiology 10*, 325-33.
27. Hamelin, C., and Lussier, G. (1979) Concentration of human cytomegalovirus from large volumes of tissue culture fluids., *The Journal of general virology 42*, 193-7.
28. Trépanier, P., Payment, P., and Trudel, M. (1981) Concentration of human respiratory syncytial virus using ammonium sulfate, polyethylene glycol or hollow fiber ultrafiltration., *Journal of virological methods 3*, 201-11.
29. Vieyres, G., Thomas, X., Descamps, V., Duverlie, G., Patel, A. H., and Dubuisson, J. (2010) Characterization of the envelope glycoproteins associated with infectious hepatitis C virus., *Journal of virology 84*, 10159-68.
30. Bolin, S. R., and Ridpath, J. F. (1996) Glycoprotein E2 of bovine viral diarrhea virus expressed in insect cells provides calves limited protection from systemic infection and disease., *Archives of virology 141*, 1463-77.

CHAPTER 5

IN VIVO EFFECTS OF DNJ-DERIVED COMPOUNDS

5.1 INTRODUCTION

Even though iminosugars have been shown to demonstrate excellent broad-spectrum *in cellulo* anti-viral capability (*1*), (*2*), (*3*), (*4*), (*1*), (*5*), the preclinical and clinical development of α-glucosidase inhibitors as anti-viral drugs is hampered by their poor efficacy *in vivo* (*6*). *N*B-DNJ, for instance, did not achieve a sufficient anti-viral concentration in the circulation of treated individuals in a phase II clinical trial for evaluation as an anti-HIV agent, therefore did not demonstrate any anti-viral efficacy (*7*). Only modest anti-viral effects of glucosidase inhibitors such as *N*N-DNJ against DV (*8*) and Japanese encephalitis virus (*9*) in mice as well as woodchuck hepatitis virus in woodchuck (*10*) were reported in preclinical studies. In addition, only modest viremia reduction was detected in a previous study that tested the anti-viral efficacy of imino sugar derivatives, CM-9-78 and CM-10-18 (Table 5), against DV infection in mice, even though α-glucosidase activity was successfully inhibited (*6*). The relatively higher EC_{50} value and/or lower level of plasma drug concentration or low concentration of iminosugars in the virus-replicating cells as a result of low uptake or plasma protein binding are possible explanations for the modest anti-viral efficacy of these compounds (*6*).

Compound	Structure
CM-9-78	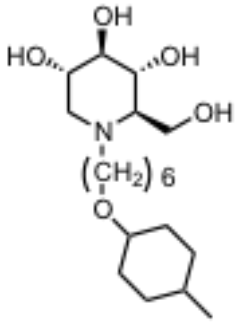
CM-10-18	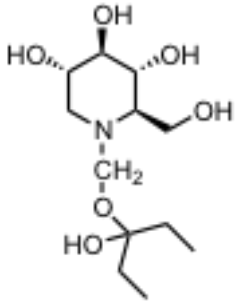

Table 5. Structure of CM-9-78 and CM-10-18.

A previous *in vivo* study that involved the investigation of ceramide-specific glucosyltransferase inhibition using *N*B-DNJ has shown that the pharmacokinetics of *N*B-DNJ are 2 orders of magnitude poorer in mice relative to humans based on comparison of steady state serum levels (*11*), (*12*), (*13*). Steady state trough level of approximately 20μM was detected in humans following administration with 43 mg/kg/day of the compound as an anti-viral agent, which is equivalent to steady state serum levels of 18.2μM in mice dosed with *N*B-DNJ at 600mg/kg/day (*14*). A separate study reported steady-state plasma concentrations with a maximum concentration of 0·86 g/mL 4–6 weeks after the first dose of 100 mg of *N*B-DNJ t.i.d. in humans (*15*).

Platt *et. al.* also found that at the serum levels of *N*B-DNJ achieved, there was no α-glucosidase inhibition occurring in the splenocytes, even though the Ki values for *N*B-DNJ against ceramide-specific glucosyltransferase and α-glucosidase I are 7.4 and 0.22μM, respectively (*14*). Since the α-glucosidases are localized within the ER, *N*B-DNJ has to cross the ER membrane to access and inhibit these enzymes, which explains why it takes a higher concentration of the compound to inhibit α-glucosidases relative to ceramide glucosyltransferase (*14*).

Normal glycoprotein trafficking and processing through the N-linked glycosylation pathway is hindered following *N*B-DNJ treatment and glycoproteins are subsequently directed to undergo ERAD generating FOS, as described in Chapter 1. Analysis of fluorescently labeled FOS by NP-HPLC provides unique and quantifiable biomarkers of ER α-glucosidase inhibition and was found to be a rapid and sensitive method that enabled the detection of all FOS species *in vitro*, in cells as well as *in vivo* (*16*). FOS analysis would therefore be a useful diagnostic tool to account for the amount of α-glucosidase inhibition in humans.

The combined administration of iminosugars with exisiting anti-viral compounds could also be a plausible therapeutic approach to enhance anti-viral efficacy *in vivo* (*6*). Increased dosing frequency, development of more potent glucosidase inhibitors or targeted delivery of iminosugars are some of the other alternative strategies.

The targeted liposome-mediated delivery of iminosugars, such as *N*B-DNJ, to host-encoded α-glucosidases in the ER provided an attractive therapeutic option against all clades of HIV, including drug-resistant strains, and also facilitated the efficient

prolonged delivery of encapsulated lipophilic drugs to their intracellular site of action across membrane barriers (*17*), (*18*), overcoming problems associated with high drug dosage necessary to decrease viral titers and increase CD4+ cell counts.

Liposomes alone were capable of reducing viral copy numbers (*19*). In fact, pre-treatment of naïve cells with polyunsaturated ER liposomes (PERLs) hampered the ability of both HCV and HIV to establish infections and present themselves as attractive delivery vessels for drug mixtures to treat an extensive range of cholesterol-dependent viral infections and co-infections (*20*). Cellular cholesterol reduction by PERLs has been reported to reduce viral infectivity of mature HCV virions (*21*), (*22*) since HCV assembly was found to occur within cholesterol-enriched ER membrane (*23*). However, it remains unclear the precise anti-viral mechanism of PERLs. The anti-viral response could be the result of reduced viral replication and egress or the release of non-infectious particles following treatment with PERLs. Relative to the high $\mu molL^{-1}$ of free *N*B-DNJ, CD4 linked liposomes encapsulating *N*B-DNJ induced 100 000-fold reduction in IC_{50} values to the low $nmolL^{-1}$ range when targeted to the gp120/gp41 complex of HIV-1 and HIV-2 (*19*). However, the costly procedure of producing iminosugars encapsulated in ER-targeting liposomes is a potential limitation. There is also the apparent risk of demyelination induced by these cholesterol-lowering PERLs in the event that they pass through the blood brain barrier. One of the major oxidation products of *cholesterol, 7-ketocholesterol*, was reported to induce neuronal damage in living brain tissue through the activation and migration of microglial cells (*24*). The route of delivery of these liposome-encapsulated drugs also results in differing anti-viral efficacies (*25*), (*26*), (*27*), (*28*), (*26*), (*29*).

NAP-DNJ has been shown to be a significantly more potent α-glucosidase inhibitor than *N*B-DNJ (*30*). Balb/c mice infected with Ebola Zaire virus (EBOV) receiving 100 mg/kg and 10 mg/kg BID showed a 71% survival rate relative to no survival in control mice, suggesting that NAP-DNJ presents itself as an anti-viral compound to treat EBOV infections (*31*). NAP-DNJ also gave EC_{50} values that were 3-fold and 5-fold better than UV4 when Vero cells were challenged with EBOV and Marburg virus (MARV) respectively (*31*).

This chapter assesses at the inhibitory potency of NAP-DNJ against α-glucosidases I and II in different tissues in C57BL/6 mice and preliminary results were compared to other DNJ-derived compounds such as *N*B-DNJ and UV4.

5.2 MATERIALS AND METHODS

5.2.1 Dose escalation studies

All animal experiments were conducted in accordance with the UK Home Office Animals (Scientific Procedures) Act 1986. C57Bl/6 mice were maintained on a diet of powdered chow. Lyophilised NAP-DNJ was dissolved in 32% HCl in milliQ water, freeze-dried and reconstituted in milliQ water to make up the appropriate concentrations. *N*B-DNJ, NAP-DNJ and UV4 were dosed at escalating concentrations twice a day over 10 days via oral gavage. Five mice were included in each dosing group. Each mouse was weighed before body fluids and tissues were collected 10 days post-administration. Harvested samples were stored at -20^{o}C prior to extraction.

5.2.2 Detection of FOS in tissues and body fluids from treated mice

FOS was isolated from 25µl of sera samples, 25mg (wet weight) from tissue samples or ≤20µl from urine samples from mice treated with indicated compounds, using a procedure described previously (*16*). The labelled oligosaccharides were further purified by chromatography using ConA-Sepharose 4B columns (100 ml packed resin) as described previously (*16*). ConA-Sepharose purified 2-AA-labelled oligosaccharides were separated by NP-HPLC (Waters) using a 4.6 X 250 mm TSKgel Amide-80 column (Anachem) with slight modifications to the published method (*32*), as described previously (*33*).

5.2.3 Sera FOS concentration

ConA-Sepharose purified 2-AA-labelled oligosaccharides from sera samples were passed through 200μl QAE sephadex columns pre-washed with 2ml milliQ water. The same volume of milliQ water was passed through the column following sample application. The concentrated oligosaccharides were then eluted with 2ml 0.5M acetic acid and separated by NP-HPLC (Waters) using a 4.6 X 250 mm TSKgel Amide-80 column (Anachem) with slight modifications to the published method (*32*), as described previously (*33*).

5.3 RESULTS

5.3.1 Concentration-dependent increase of $G_1M_4N_1$ and $G_3M_5N_1$

The *in cellulo* production of mono-glucosylated and tri-glucosylated oligosaccharides have previously been reported to be indicative of α-glucosidase II and I inhibition respectively (*16*). To determine and compare the *in vivo* inhibitory potency of NAP-DNJ, *N*B-DNJ and UV4, the peak areas of $G_1M_4N_1$ and $G_3M_5N_1$ were determined from the NP-HPLC chromatograms and normalized to the amount of proteins in each sample. Only the production of $G_1M_4N_1$ and $G_3M_5N_1$ showed an appreciable dose-dependent trend amongst the FOS detected in each of the 7 types of tissues, urine and sera (Appendix 2). NAP-DNJ has also been found to demonstrate considerable *in vivo* inhibitory potency against both α-glucosidases compared to *N*B-DNJ and UV4 seen in sera, urine and all tissues, except in brain tissues (Appendix 2). Figure 5.1 shows an overview of the amounts of $G_1M_4N_1$ and $G_3M_5N_1$ detected in selected tissues, sera and urine following NAP-DNJ treatment in mice. There were higher levels of $G_1M_4N_1$ relative to $G_3M_5N_1$ in these tissues, except for brain tissues, where no FOS was detected at the indicated NAP-DNJ doses.

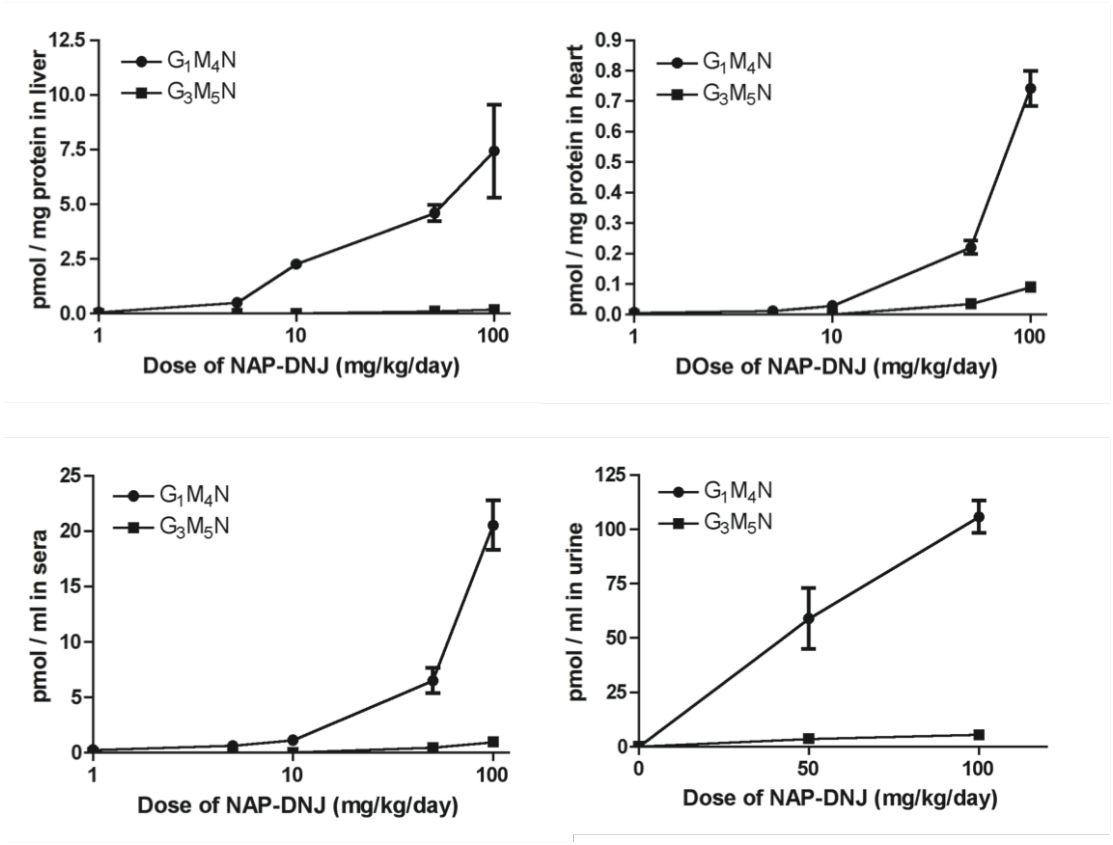

Figure 5.1 FOS analyses of selected mouse tissues, sera and urine following treatment with escalating NAP-DNJ concentrations for 10 days.

Liver, heart and brain tissues, as well as sera and urine were subjected to FOS analysis as described and peak areas obtained from NP-HPLC were normalized to either protein content or sample volume. The values corresponding to $G_1M_4N_1$ (●) and $G_3M_5N_1$ (■) were plotted against NAP-DNJ concentration.

5.3.2 NAP-DNJ and UV4 have limited capability in traversing the blood-brain barrier

A small but significant amount of $G_1M_5N_1$ and a small increase in $G_1M_5N_1$ were detected in brain tissues following *N*B-DNJ treatment in a previous study (*16*). To find out whether NAP-DNJ and UV4 were also able to traverse the blood-brain-barrier, FOS analyses were carried out on the brain tissues harvested and no $G_1M_4N_1$ or $G_3M_5N_1$ was detected in NAP-DNJ and UV4 treated tissues (data not shown), but significant amounts of these FOS were found in *N*B-DNJ treated tissues (Figure 5.2).

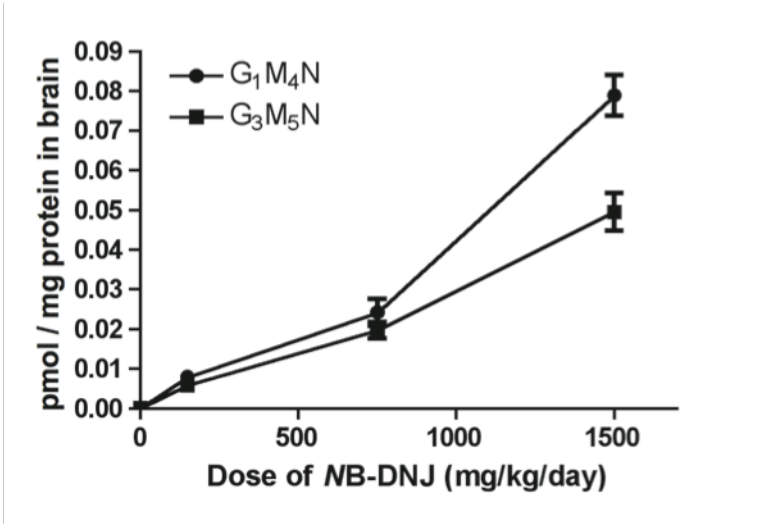

Figure 5.2 FOS analyses of mouse brain tissues following treatment with *N*B-DNJ for 10 days.

Brain tissues were subjected to FOS analysis as described and peak areas obtained from NP-HPLC were normalized to protein content. The values corresponding to $G_1M_4N_1$ (●) and $G_3M_5N_1$ (■) were plotted against compound concentration.

5.3.3 Poor retention of UV4 in the heart

The tri-glucosylated glycan was reported to be the major glycan detected in the heart following *N*B-DNJ treatment in a previous study (*16*). Even though more $G_3M_5N_1$ than $G_1M_4N_1$ was found in the heart tissues with UV4 treatment, the reverse trend was observed with NAP-DNJ and *N*B-DNJ treatment (Figure 5.3). The $G_3M_7N_2$ species was found only in *N*B-DNJ treated heart tissues. The overall production of both $G_1M_4N_1$ and $G_3M_5N_1$ in the heart following UV4 treatment also appeared to be significantly lower than that following NAP-DNJ or *N*B-DNJ treatment as shown in Figure 5.3.

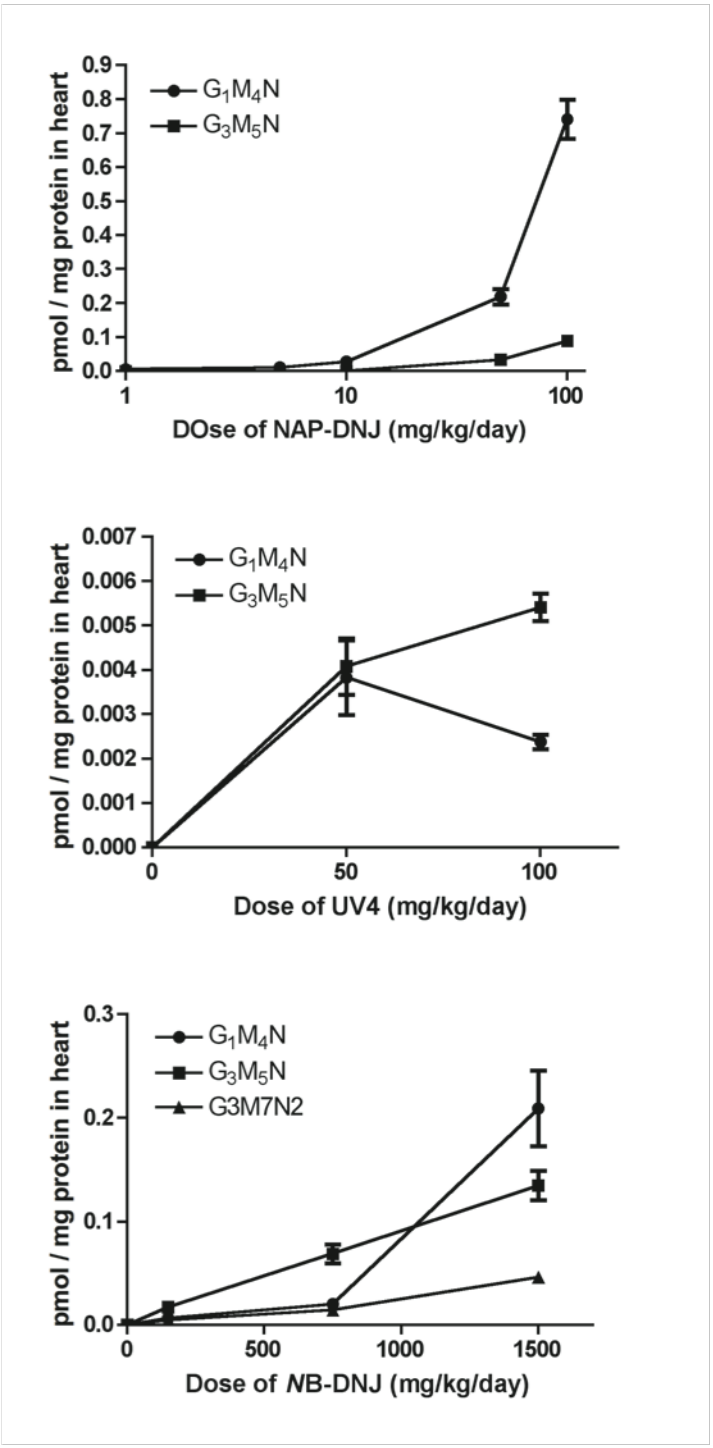

Figure 5.3 FOS analyses of mouse heart tissues following treatment with NAP-DNJ, UV4 and *N*B-DNJ for 10 days.

Heart tissues were subjected to FOS analysis as described and peak areas obtained from NP-HPLC were normalized to protein content. The values corresponding to $G_1M_4N_1$ (●) and $G_3M_5N_1$ (■) were plotted against compound concentration.

5.4 DISCUSSION

The production of G1 species was consistently higher than G3 species across all concentrations of drugs, indicating that there was a higher level of glucosidase II inhibition relative to glucosidase I inhibition, corroborating with the trend identified in *in cellulo* studies in Chapter 3. As observed in cultured cells, this is the more inhibitor-sensitive step in the glycosylation pathway. This observation is true even in the heart, contrary to what was previously reported (Alonzi et. al., 2008), likely due to longer retention time of NAP-DNJ and *N*B-DNJ in the heart. UV4 does not retain in the heart as well, likely due to its more hydrophilic nature. This explains the considerably lower levels of both $G_1M_4N_1$ and $G_3M_5N_1$, as well as the greater production of $G_3M_5N_1$ over $G_1M_4N_1$ in the heart following UV4 treatment. Concentration-dependent increases of linear M_3N and linear M_4N species in heart, kidney, lung, liver, thymus and spleen tissues and sera were also detected (Appendix 2). These smaller FOS species were most likely derived from the breakdown of high levels of G_1M_4N species at higher concentrations of the compounds. Unlike NAP-DNJ and UV4, *N*B-DNJ was found to be able to traverse the blood-brain barrier, corroborating with findings from a previous study where *N*B-DNJ demonstrated GSL biosynthesis inhibition in the brains of *N*B-DNJ treated mice inflicted with Tay-Sachs disease (*34*).

G_1M_4N was found to be the major glucosylated FOS produced in murine tissues following treatment with all three compounds. It therefore suggests that the catabolic endpoint for the clearance of glucosylated FOS from murine tissues is a M_4N species and not an M_5N species. Given a longer treatment period, the tri-glucosylated species detected, G_3M_5N, could also be broken down to G_3M_4N. This remains to be proven.

All three compounds resulted in an increase in glucosylated FOS in tissues, sera and urine, similar to the effects previously demonstrated in cultured cells in Chapter 3, highlighting the efficient *in vivo* delivery of DNJ-derived compounds to target organs.

Further analyses, including pharmacokinetics study and drug reversal study to test the bioavailability of these compounds, remained to be performed following these preliminary results from the FOS analyses. Blood samples should also be collected following each dosing to monitor systemic compound concentration using an optimized compound detection protocol. NAP-DNJ and UV4 have previously been shown to exhibit anti-viral efficacy against EBOV and MARV (*31*). The anti-viral efficiency of these compounds could also be tested against other viruses such as HIV and influenza, to explore its capacity as a broad-spectrum anti-viral compound like *N*B-DNJ and to find out whether NAP-DNJ, for instance, is better than *N*B-DNJ as an effective anti-viral drug.

5.5 REFERENCES

1. Block, T. M., Lu, X., Platt, F. M., Foster, G. R., Gerlich, W. H., Blumberg, B. S., and Dwek, R. a. (1994) Secretion of human hepatitis B virus is inhibited by the imino sugar N-butyldeoxynojirimycin., *Proceedings of the National Academy of Sciences of the United States of America 91*, 2235-9.

2. Bridges, C. G., Taylor, D. L., Kang, M. S., Brennan, T. M., and Tyms, a S. (1995) Treatment with the alpha-glucosidase 1 inhibitor 6-O-butanoyl castanospermine reduces the detection of LFA-1 (CD18/CD11a) by monoclonal antibodies., *Glycobiology 5*, 243-7.

3. Datema, R., Romero, P. A., Rott, R., and Schwarz, R. T. (1984) On the role of oligosaccharide trimming in the maturation of Sindbis and influenza virus., *Archives of virology 81*, 25-39.

4. Malvoisin, E., and Wild, F. (1994) The role of N-glycosylation in cell fusion induced by a vaccinia recombinant virus expressing both measles virus glycoproteins, *Virology*, Virology 11-20.

5. Zitzmann, N., Mehta, a S., Carrouée, S., Butters, T. D., Platt, F. M., McCauley, J., Blumberg, B. S., Dwek, R. a, and Block, T. M. (1999) Imino sugars inhibit the formation and secretion of bovine viral diarrhea virus, a pestivirus model of hepatitis C virus: implications for the development of broad spectrum anti-hepatitis virus agents., *Proceedings of the National Academy of Sciences of the United States of America 96*, 11878-82.

6. Chang, J., Schul, W., Butters, T. D., Yip, A., Liu, B., Goh, A., Lakshminarayana, S. B., Alonzi, D., Reinkensmeier, G., Pan, X., Qu, X., Weidner, J. M., Wang, L., Yu, W., Borune, N., Kinch, M. a, Rayahin, J. E., Moriarty, R., Xu, X., Shi, P.-Y., Guo, J.-T., and Block, T. M. (2011) Combination of α-glucosidase inhibitor and ribavirin for the treatment of dengue virus infection in vitro and in vivo., *Antiviral research*, Elsevier B.V. *89*, 26-34.

7. Fischl, M. A., Resnick, L., Coombs, R., Kremer, A. B., Pottage, J. C., Fass, R. J., Fife, K. H., Powderly, W. G., Collier, A. C., and Aspinall, R. L. (1994) The safety and efficacy of combination N-butyl-deoxynojirimycin (SC-48334) and zidovudine in patients with HIV-1 infection and 200-500 CD4 cells/mm3., *Journal of acquired immune deficiency syndromes 7*, 139-47.

8. Schul, W., Liu, W., Xu, H.-Y., Flamand, M., and Vasudevan, S. G. (2007) A dengue fever viremia model in mice shows reduction in viral replication and suppression of the inflammatory response after treatment with antiviral drugs., *The Journal of infectious diseases 195*, 665-74.

9. Wu, S.-fen, Lee, C.-jang, Liao, C.-len, Dwek, R. A., Zitzmann, N., and Lin, Y.-ling. (2002) Antiviral Effects of an Iminosugar Derivative on Flavivirus Infections, *Journal of virology 76*, 3596-3604.

10. Block, T. M., Lu, X., Mehta, A. S., Blumberg, B. S., Tennant, B., Ebling, M., Korba, B., Lansky, D. M., Jacob, G. S., and Dwek, R. A. (1998) Treatment of chronic hepadnavirus infection in a woodchuck animal model with an inhibitor of protein folding and trafficking., *Nature medicine 4*, 610-4.

11. Platt, F. M., Neises, G. R., Dwek, R. A., and Butters, T. D. (1994) N-butyldeoxynojirimycin is a novel inhibitor of glycolipid biosynthesis., *The Journal of biological chemistry 269*, 8362-5.

12. Platt, F. M., Neises, G. R., Karlsson, G. B., Dwek, R. A., and Butters, T. D. (1994) N-butyldeoxygalactonojirimycin inhibits glycolipid biosynthesis but does not affect N-linked oligosaccharide processing., *The Journal of biological chemistry 269*, 27108-14.

13. Platt, F.M., and Butters, T. D. (1995) Inhibitors of Glycosphingolipid Biosynthesis, *Trends in Glycoscience and Glycotechnology 7*, 495-511.

14. Platt, F. M., Reinkensmeier, G., Dwek, R. a, and Butters, T. D. (1997) Extensive glycosphingolipid depletion in the liver and lymphoid organs of mice treated with N-butyldeoxynojirimycin., *The Journal of biological chemistry 272*, 19365-72.

15. Cox, T., Lachmann, R., Hollak, C., Aerts, J., Weely, S. van, Hrebícek, M., Platt, F., Butters, T., Dwek, R., Moyses, C., Gow, I., Elstein, D., and Zimran, A. (2000) Novel oral treatment of Gaucher's disease with N-butyldeoxynojirimycin (OGT 918) to decrease substrate biosynthesis., *Lancet 355*, 1481-5.

16. Alonzi, D. S., Neville, D. C. a, Lachmann, R. H., Dwek, R. a, and Butters, T. D. (2008) Glucosylated free oligosaccharides are biomarkers of endoplasmic-reticulum alpha-glucosidase inhibition., *The Biochemical journal 409*, 571-80.

17. Block, T. M., and Jordan, R. (2001) Iminosugars as possible broad spectrum anti hepatitis virus agents: the glucovirs and alkovirs., *Antiviral chemistry & chemotherapy 12*, 317-25.

18. Costin, G.-E., Trif, M., Nichita, N., Dwek, R. A., and Petrescu, S. M. (2002) pH-sensitive liposomes are efficient carriers for endoplasmic reticulum-targeted drugs in mouse melanoma cells., *Biochemical and biophysical research communications 293*, 918-23.

19. Pollock, S., Dwek, R. a, Burton, D. R., and Zitzmann, N. (2008) N-Butyldeoxynojirimycin is a broadly effective anti-HIV therapy significantly enhanced by targeted liposome delivery., *AIDS (London, England) 22*, 1961-9.

20. Pollock, S., Antrobus, R., Newton, L., Kampa, B., Rossa, J., Latham, S., Nichita, N. B., Dwek, R. a, and Zitzmann, N. (2010) Uptake and trafficking of liposomes to the endoplasmic reticulum., *The FASEB journal : official publication of the Federation of American Societies for Experimental Biology*.

21. Pollock, S., Nichita, N. B., Böhmer, A., Radulescu, C., Dwek, R. a, and Zitzmann, N. (2010) Polyunsaturated liposomes are antiviral against hepatitis B and C viruses and HIV by decreasing cholesterol levels in infected cells., *Proceedings of the National Academy of Sciences of the United States of America*.

22. Aizaki, H., Morikawa, K., Fukasawa, M., Hara, H., Inoue, Y., Tani, H., Saito, K., Nishijima, M., Hanada, K., Matsuura, Y., Lai, M. M. C., Miyamura, T.,

Wakita, T., and Suzuki, T. (2008) Critical role of virion-associated cholesterol and sphingolipid in hepatitis C virus infection., *Journal of virology 82*, 5715-24.

23. Miyanari, Y., Atsuzawa, K., Usuda, N., Watashi, K., Hishiki, T., Zayas, M., Bartenschlager, R., Wakita, T., Hijikata, M., and Shimotohno, K. (2007) The lipid droplet is an important organelle for hepatitis C virus production., *Nature cell biology 9*, 1089-97.

24. Diestel, A., Aktas, O., Hackel, D., Hake, I., Meier, S., Raine, C. S., Nitsch, R., Zipp, F., and Ullrich, O. (2003) Activation of microglial poly(ADP-ribose)-polymerase-1 by cholesterol breakdown products during neuroinflammation: a link between demyelination and neuronal damage., *The Journal of experimental medicine 198*, 1729-40.

25. Kirby, C., Clarke, J., and Gregoriadis, G. (1980) Effect of the cholesterol content of small unilamellar liposomes on their stability in vivo and in vitro., *The Biochemical journal 186*, 591-8.

26. Scherphof G, Roerdink F, Hoekstra D, Z. J. and W. E. (1980) Liposomes in biological systems (Gregoriadis G, A. H., Ed.), p 179, Wiley, New York.

27. G, G. (1980) Liposomes in biological systems (Gregoriadis G, A. H., Ed.), p 377, Wiley, New York.

28. Gregoriadis, G. (1979) Drug Carriers in Biology and Medicine (Gregoriadis, G., Ed.), p 287, Academic, London.

29. Mauk, M. R., Gamble, R. C., and Baldeschwieler, J. D. (1980) Vesicle targeting: timed release and specificity for leukocytes in mice by subcutaneous injection., *Science (New York, N.Y.) 207*, 309-11.

30. Rawlings, A. J., Lomas, H., Pilling, A. W., Lee, M. J.-R., Alonzi, D. S., Rountree, J. S. S., Jenkinson, S. F., Fleet, G. W. J., Dwek, R. a, Jones, J. H., and Butters, T. D. (2009) Synthesis and biological characterisation of novel N-

alkyl-deoxynojirimycin alpha-glucosidase inhibitors., *Chembiochem : a European journal of chemical biology 10*, 1101-5.

31. Ramstedt U, Klose B, Zitzmann N, Dwek RA, B. T. (2011) Iminosugars and methods of treating foliviral diseases (Patent No. 12/873708).

32. Neville, D. C. A., Coquard, V., Priestman, D. A., Vruchte, D. J. M. te, Sillence, D. J., Dwek, R. A., Platt, F. M., and Butters, T. D. (2004) Analysis of fluorescently labeled glycosphingolipid-derived oligosaccharides following ceramide glycanase digestion and anthranilic acid labeling., *Analytical biochemistry 331*, 275-82.

33. Alonzi, D. S., Dwek, R. a, and Butters, T. D. (2009) Improved cellular inhibitors for glycoprotein processing α-glucosidases: biological characterisation of alkyl- and arylalkyl-N-substituted deoxynojirimycins, *Tetrahedron: Asymmetry*, Elsevier Ltd *20*, 897-901.

34. Platt, F. M., Neises, G. R., Reinkensmeier, G., Townsend, M. J., Perry, V. H., Proia, R. L., Winchester, B., Dwek, R. A., and Butters, T. D. (1997) Prevention of lysosomal storage in Tay-Sachs mice treated with N-butyldeoxynojirimycin., *Science (New York, N.Y.) 276*, 428-31.

CHAPTER 6
GENERAL DISCUSSION

6.1 FURTHER DISCUSSION

The intervention of α-glucosidase activity with iminosugars as a therapeutic approach in this project has shed light on the replication strategies that pestiviruses employ to perpetuate infection in their mammalian hosts, and more importantly, highlighted the potent anti-viral capability of targeting host-directed glycosylation using these DNJ-derived compounds. Based on the findings of this project, the exclusive inhibition of α-glucosidase II activity at low micro molar concentrations of NAP-DNJ was sufficient to impose a significant reduction in virus titre. Future developmental efforts could therefore focus on designing iminosugars capable of exhibiting more potent inhibitory activity against α-glucosidase II specifically. In fact, iminosugars such as JR2 and JR3 (see Chapter 2) were found to exclusively target ER α-glucosidase II at concentrations up to 100μM. These compounds could be use to further support the conclusions drawn. One other approach that could be taken into consideration includes designing siRNAs that targets the enzymatic activity of ER α-glucosidase II. However, achieving a 100% knockout could be a potential challenge. The synergistic approach of applying both gene knockout and inhibitors simultaneously could resolve this. No specific ER α-glucosidase II inhibitor has been identified thus far.

The increased potency of NAP-DNJ allowed concentration-dependent discrimination between α-glucosidase I and II activity to probe the dependency of BVDV envelope glycoproteins on the chaperone-mediated protein-folding pathway. Further analysis of secreted virions for the presence of homodimers and heterodimers will therefore provide further information regarding the nature of the viral envelope. However, due

to the weak antibody binding affinity to BVDV E2, it has not been possible to directly study the native glycan composition as well as the altered glycosylation pattern following NAP-DNJ treatment on the surface of these dimers. The lack of commercially available anti-BVDV E1 antibody has also made it challenging to obtain more information regarding the nature of this envelope glycoprotein. The construction of a reliable expression vector system capable of expressing high levels of the viral glycoproteins, E1 and E2, could be explored. This efficient expression vector could be transfected into a suitable cell line for the increased production of the viral glycoproteins E1, E2, E1E2 heterodimers or E2E2 homodimers, which could serve as a platform to improve the chances of elucidating the crystal structures of these viral proteins. This novel biophysical approach with BVDV helps to uncover the potential binding sites and interacting domains between the inhibitors and the enzymes and to understand the glycosylation of the virus better. This also brings us one step closer to identifying the glycoprotein domains that are specifically misfolded under the influence of the inhibitors, which then go down the ERAD pathway.

One other question that needs to be addressed is the influence of membrane lipid/protein ratios on virion formation. It would be useful to find out whether there are some virions that accumulate within the mammalian host cell and rendered incapable of being released. It would also be interesting to pursue the fate of the glycoproteins on the surface of these virions.

The ion channel molecule p7 has been reported to play an essential role for the infectivity of both BVDV and HCV. NAP-DNJ is a long alkyl-chained iminosugar that likely contains a sufficiently hydrophobic N-alkyl moiety to facilitate binding and

disruption of ion channel activity (*1*). To discriminate glucosidase inhibition from ion channel binding, NAP-DGJ, an imino sugar with galactose stereochemistry that is non-inhibitory for ER-glucosidases has been designed and synthesised. Both NAP-DNJ and NAP-DGJ could be administered to BVDV-infected MDBK cells and their anti-viral efficacy compared.

*N*B-DNJ blocks the ceramide-specific glucosyltransferase, which catalyses the formation of glucosyl ceramide (GlcCer), the precursor for GSLs (*2*). NAP-DNJ (IC50 = 0.057μM) was found to be a more potent inhibitor of ceramide glucosyltransferase, relative to UV4 (IC50 = 0.19μM) and *N*B-DNJ (IC50 = 20-50μM) in a study that involved the in vitro digestion of GSLs extracted from HL60 cells dosed with these compounds over three days (Unpublished data, DS Alonzi). Enveloped viruses are highly dependent on the repertoire of glycolipids on cellular membranes for the budding process (*3*), bearing important implications on the virus membrane architecture and this affects fusogenic activity. Since tetraspanin proteins form an essential component of lipid rafts (*4*), the administration of NAP-DNJ or NAP-DGJ might reduce viral entry efficiency by down regulating the expression of tetraspanin proteins in host cells. It would be interesting to find out whether viral replication and viral entry were altered following long-term (1-2 weeks) treatment of cells infected with the non-cytopathic BVDV strain with NAP-DNJ or NAP-DGJ.

The targeted liposome-mediated delivery of iminosugars, such as *N*B-DNJ, to host-encoded α-glucosidases in the ER provided an attractive therapeutic option against all clades of HIV, including drug-resistant strains, and also facilitated the efficient prolonged delivery of encapsulated lipophilic drugs to their intracellular site of action

across membrane barriers (*5*), (*6*), overcoming problems associated with high drug dosage necessary to decrease viral titers and increase CD4+ cell counts. However, the costly procedure of producing iminosugars encapsulated in ER-targeting liposomes is a potential limitation. Preliminary findings from our *in vivo* studies indicate that the delivery of DNJ-derived compounds to target organs is a highly efficient process. The development of more potent iminosugar derivatives with improved cytotoxicity profiles administered at low and tolerable concentrations could therefore be a more attractive therapeutic approach relative to using liposome-mediated delivery of drugs.

In addition to iminosugars, small molecule inhibitors with a high threshold for resistance, called thiazolides, also target host factors. Nitaxozanide (Romark Laboratories, Morristown, NJ, USA), for instance, is a thiazolide that activates the protein kinase R (PKR)-mediated anti-viral pathway and has shown an SVR of 80% and 79% when used in combination with pegylated IFN and/or ribavirin respectively to treat chronic HCV genotype 4 in a phase II clinical trial (*7*). No serious adverse effects have also been reported. Thiazolides have also been shown to selectively inhibit the assembly and egress of the haemagglutinin of the H1N1 swine influenza virus, responsible for establishing infection (*8*) and the development of new second generation and controlled release thiazolides are underway (*7*).

The administration of these host factor-targeting iminosugars and/or thiazolides could therefore serve as a complementary therapeutic approach in targeting escape mutants following treatment with DAAs. However, *in vivo* side effects such as off-target inhibition of host α-glucosidases necessitates the regular assessment of

pharmacological properties and *in vivo* toxicity of these iminosugars before the large-scale syntheses of reliable drug leads. Furthermore, the generation of iminosugars with more potent anti-viral activity and favourable cytotoxicity profiles relative to the existing ensemble of iminosugars is crucial since the concentrations required to achieve anti-viral response in man is currently unachievable with monotherapy (*9*).

In conclusion, the general water-soluble nature and tolerable cytotoxicity profile of iminosugars continue to make them attractive candidates for development as anti-viral compounds. Pharmaceutical companies can modify the sugar backbone by adding on or taking off functional groups to generate more complex and relevant drugs (*10*). More importantly, the delayed onset of viral resistance to iminosugars makes the development of α-glucosidase inhibitors a commensurate approach that complements the anti-viral efficacies demonstrated by the existing iminosugars.

6.2 REFERENCES

1. Pavlović, D., Neville, D. C. a, Argaud, O., Blumberg, B., Dwek, R. a, Fischer, W. B., and Zitzmann, N. (2003) The hepatitis C virus p7 protein forms an ion channel that is inhibited by long-alkyl-chain iminosugar derivatives., *Proceedings of the National Academy of Sciences of the United States of America 100*, 6104-8.
2. Svensson, M., Frendeus, B., Butters, T., Platt, F., Dwek, R., and Svanborg, C. (2003) Glycolipid depletion in antimicrobial therapy., *Molecular microbiology 47*, 453-61.
3. Genderen, I. L. van, Brandimarti, R., Torrisi, M. R., Campadelli, G., and Meer, G. van. (1994) The phospholipid composition of extracellular herpes simplex virions differs from that of host cell nuclei., *Virology 200*, 831-6.
4. Claas, C., Stipp, C. S., and Hemler, M. E. (2001) Evaluation of prototype transmembrane 4 superfamily protein complexes and their relation to lipid rafts., *The Journal of biological chemistry 276*, 7974-84.
5. Block, T. M., and Jordan, R. (2001) Iminosugars as possible broad spectrum anti hepatitis virus agents: the glucovirs and alkovirs., *Antiviral chemistry & chemotherapy 12*, 317-25.
6. Costin, G.-E., Trif, M., Nichita, N., Dwek, R. A., and Petrescu, S. M. (2002) pH-sensitive liposomes are efficient carriers for endoplasmic reticulum-targeted drugs in mouse melanoma cells., *Biochemical and biophysical research communications 293*, 918-23.
7. Keeffe, E. B., and Rossignol, J.-F. (2009) Treatment of chronic viral hepatitis with nitazoxanide and second generation thiazolides., *World journal of gastroenterology : WJG 15*, 1805-8.
8. Rossignol, J. F., La Frazia, S., Chiappa, L., Ciucci, A., and Santoro, M. G. (2009) Thiazolides, a new class of anti-influenza molecules targeting viral hemagglutinin at the post-translational level., *The Journal of biological chemistry 284*, 29798-808.
9. Tierney, M., Pottage, J., Kessler, H., Fischl, M., Richman, D., Merigan, T., Powderly, W., Smith, S., Karim, A., and Sherman, J. (1995) The tolerability

and pharmacokinetics of N-butyl-deoxynojirimycin in patients with advanced HIV disease (ACTG 100). The AIDS Clinical Trials Group (ACTG) of the National Institute of Allergy and Infectious Diseases., *Journal of acquired immune deficiency syndromes and human retrovirology : official publication of the International Retrovirology Association 10*, 549-53.

10. Spiro, R. G. (2004) Role of N-linked polymannose oligosaccharides in targeting glycoproteins for endoplasmic reticulum-associated degradation., *Cellular and molecular life sciences : CMLS 61*, 1025-41.

APPENDICES

Appendix 1

Structures and proportions of the major FOS produced naturally in MDBK cells

Structure	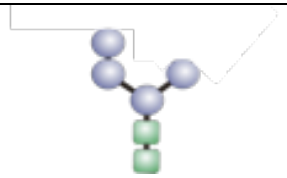	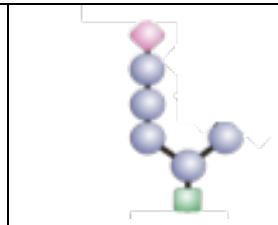	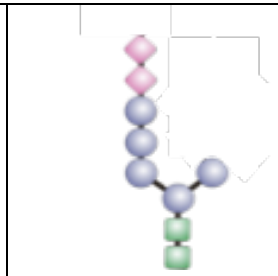	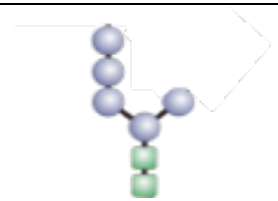	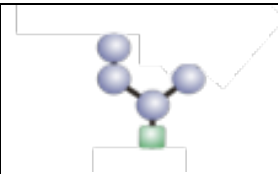
Name	$Man_4GlcNAc_2$	$Glc_1Man_5GlcNAc_1$	$Glc_2Man_5GlcNAc_1$	$Man_5GlcNAc_1$	$Man_4GlcNAc_1$
Abbreviation	M_4N_2	G_1M_5N	G_2M_5N	M_5N	M_4N
% of total FOS	11	5.09	0.04	16.93	13.56

Structures and proportions of FOS produced in MDBK cells upon treatment with 10μM NAP-DNJ for 24 hours

Structure	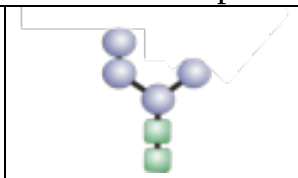	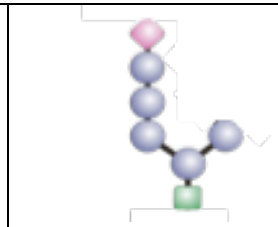	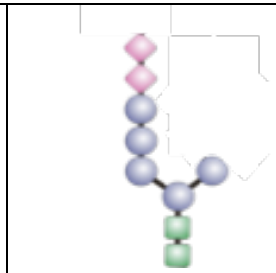	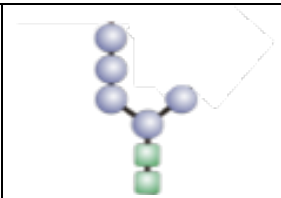	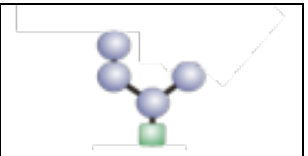
Name	$Man_4GlcNAc_2$	$Glc_1Man_5GlcNAc_1$	$Glc_2Man_5GlcNAc_1$	$Man_5GlcNAc_1$	$Man_4GlcNAc_1$
Abbreviation	M_4N_2	G_1M_5N	G_2M_5N	M_5N	M_4N
% of total FOS	3.24	20.33	4.74	3.14	3.72

Structures and proportions of FOS produced in MDBK cells upon treatment with 10μM NAP-DNJ for 24 hours (continued)

Structure	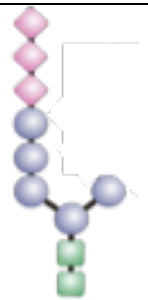	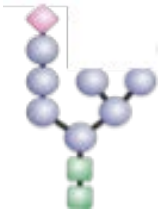	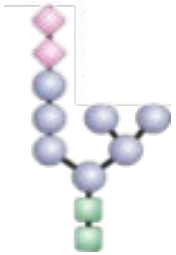	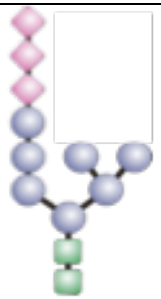
Name	$Glc_3Man_5GlcNAc_1$	$Glc_1Man_7GlcNAc_2$	$Glc_2Man_7GlcNAc_2$	$Glc_3Man_7GlcNAc_2$
Abbreviation	G_3M_5N	$G_1M_7N_2$	$G_2M_7N_2$	$G_3M_7N_2$
% of total FOS	8.43	7.85	11.23	17.08

Structures and proportions of the major FOS produced naturally in HL60 cells

Structure	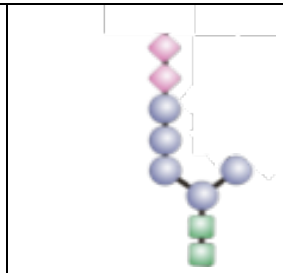	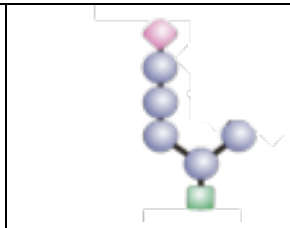	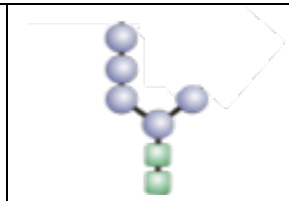	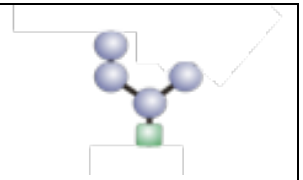
Name	$Glc_2Man_5GlcNAc_1$	$Glc_1Man_5GlcNAc_1$	$Man_5GlcNAc_1$	$Man_4GlcNAc_1$
Abbreviation	G_2M_5N	G_1M_5N	M_5N	M_4N
% of total FOS	3.17	21.42	58	17.58

Structures and proportions of FOS produced in HL60 cells upon treatment with 10μM NAP-DNJ for 24 hours

Structure	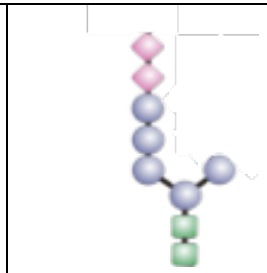	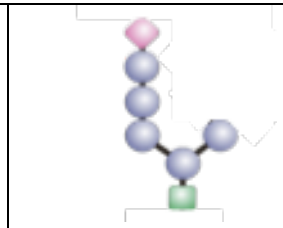	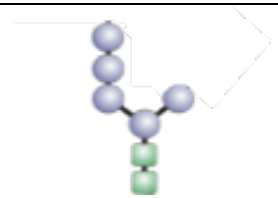	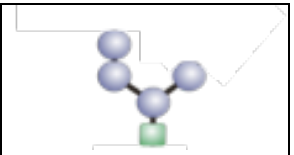
Name	$Glc_2Man_5GlcNAc_1$	$Glc_1Man_5GlcNAc_1$	$Man_5GlcNAc_1$	$Man_4GlcNAc_1$
Abbreviation	G_2M_5N	G_1M_5N	M_5N	M_4N
% of total FOS	17.04	21.49	9.38	5.56

Structures and proportions of FOS produced in HL60 cells upon treatment with 10μM NAP-DNJ for 24 hours (continued)

Structure	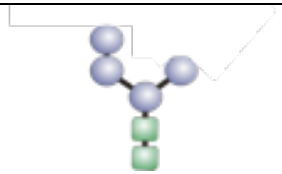		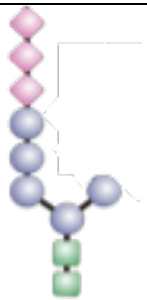
Name	$Man_4GlcNAc_2$	$Glc_3Man_4GlcNAc_1$	$Glc_3Man_5GlcNAc_1$
Abbreviation	M_4N_2	G_3M_4N	G_3M_5N
% of total FOS	20.10	4.62	15.71